Long Non-Coding RNA Antisense to Uchl1 Increases Its Protein Translation and Identifies a New Class of Protein Translation Activators

Thesis submitted for the degree of
"*Doctor Philosophiæ*"

SISSA – International School for Advanced Studies
Area of Neuroscience – Curriculum in Functional and Structural Genomics

CANDIDATE
Laura Cimatti

SUPERVISOR
Prof. Stefano Gustincich

29th October 2013

DECLARATION

The work described in this thesis was carried out at SISSA – International School for Advanced Studies in Trieste, Italy between November 2009 and October 2013 with the exception of:

- polysome fractionation and northern blot that were performed at the Laboratory of Molecular Histology and Cell Growth, DIBIT, San Raffaele, Milano, under the supervision of Prof. Stefano Biffo
- pulse labelling and immunoprecipitation that were performed at L.N.CIB - AREA Science Park in Trieste, Italy under the supervision of Prof. Licio Collavin

Part of the work described in this thesis is included in:

Long non-coding antisense RNA controls Uchl1 translation through an embedded SINEB2 repeat.

Carrieri C*, Cimatti L*, Biagioli M, Beugnet A, Zucchelli S, Fedele S, Pesce E, Ferrer I, Collavin L, Santoro C, Forrest AR, Carninci P, Biffo S, Stupka E, Gustincich S. *These authors contributed equally to this work.

Nature. 2012 Nov 15;491(7424):454-7. doi: 10.1038/nature11508. Epub 2012 Oct 14.

TABLE OF CONTENTS

Carrieri C, Cimatti L, Biagioli M, Beugnet A, Zucchelli S, Fedele S, Pesce E, Ferrer I, Collavin L, Santoro C, Forrest AR, Carninci P, Biffo S, Stupka E, Gustincich S. Long non-coding antisense RNA controls Uchl1 translation through an embedded SINEB2 repeat. Nature. 2012 Nov 15;491(7424):454-7. doi: 10.1038/nature11508. Epub 2012 Oct 14.

ABSTRACT

Thanks to continuous technical advances in the sequencing field nowadays we know that most of the mammalian genome is transcribed. This generates a vast repertoire of transcripts that includes protein-coding messenger RNAs (mRNAs), long non-coding RNAs (lncRNAs) and repetitive sequences, such as Short Interspersed Nuclear Elements (SINEs). A large percentage of ncRNAs is nuclear-enriched with unknown function. LncRNAs may be transcribed in antisense direction and may form sense/antisense pairs by pairing with an mRNA from the opposite strand to regulate chromatin conformation, transcription and mRNA stability.

We have identified a nuclear-enriched lncRNA antisense to mouse Ubiquitin Carboxyterminal Hydrolase L1 (Uchl1), a gene expressed in dopaminergic cells and involved in brain function and neurodegenerative diseases. Antisense Uchl1 (AS Uchl1) increases Uchl1 protein synthesis at a post-transcriptional level. AS Uchl1 function is under the control of stress signaling pathways, as mTORC1 inhibition by rapamycin causes an increase in Uchl1 protein that is associated to the shuttling of AS Uchl1 lncRNA from the nucleus to the cytoplasm of dopaminergic cells. AS Uchl1 RNA is then required for the association of the overlapping sense protein-coding mRNA to active polysomes for translation.

Moreover, AS Uchl1 activity depends on the presence of a 5' domain overlapping Uchl1 mRNA and an inverted SINEB2 element embedded along its 3' sequence. These features are shared by other natural antisense transcripts and among them a lncRNA antisense to Ubiquitously eXpressed Transcript (AS Uxt) increases Uxt protein expression in the presence of stable mRNA level similar to AS Uchl1. These data identified a new functional class of lncRNAs and reveal another layer of gene expression control at the post-transcriptional level.

Furthermore, through the replacement of AS Uchl1 5' overlapping region with an antisense sequence to Green Fluorescence Protein (GFP) we were able to redirect this upregulation of protein synthesis. In fact, the presence of a 5' overlapping sequence and an embedded inverted SINEB2 element confer to this artificial AS lncRNA to GFP (AS GFP) the capability to induce GFP protein with stable mRNA levels both in cells and *in vitro* translation assay. Further experiments are needed to set up the *in vitro* translation assay and to understand the translation enhancement of AS lncRNAs.

INTRODUCTION

From the beginning of the genetic age the relationship between DNA content and biological complexity has been an interesting subject of discussion. Defining biological complexity as a combination of metabolic and developmental complexity, in terms of number, types, and organization of cells in an organism, there is generally a close relationship between genome size and genetic capacity in the prokaryotes. In contrast, there are major incongruities between both cellular DNA content and the number of protein-coding genes in relation to developmental complexity in the eukaryotes, whose genomes contain large amounts of non-protein-coding sequences (Taft et al., 2007).

Evidence from numerous high-throughput genomic platforms suggests that the evolution of developmental processes regulating the complexity of the organism is mainly due to the expansion of regulatory potential of the noncoding portions of the genome (Mattick, 2004).

Moreover, genome sequence comparisons have shown that multicellular organisms exhibit significant conservation of non-protein-coding DNA, indicating that these sequences have genetic function (Dermitzakis, 2003).

These observations suggest that there may be a vast hidden layer of RNA regulatory information. Indeed, since the establishment of the concept of messenger RNAs (mRNAs), numerous regulatory RNAs which do not code for protein have been discovered.

Non-Coding RNAs

Insights into the transcriptional landscape of the human genome, based in part on the work of the international FANTOM Consortium, have revealed that more than 70% of the genome is transcribed (The FANTOM Consortium, 2005), whereas less than 2% is subsequently translated (Bertone et al., 2004; Cheng et al., 2005; Kapranov et al., 2005). In accordance with this observation, the more recent work of the ENCODE Consortium has indicated that at least 80% of the human genome is transcribed, resulting in the generation of a large number of non-coding RNA (ncRNA) transcripts (Derrien et al., 2012; Djebali et al., 2012).

Until recently, most of the known non-coding RNAs fulfilled the relative generic function of being ‘infrastructural’ RNAs, such as rRNAs and tRNAs involved in

translation, spliceosomal uRNAs and small nuclear RNAs (snRNAs) involved in splicing and small nucleolar RNAs (snoRNAs) involved in the modification of rRNAs.

Besides their structural role, some of these ncRNAs partecipate in regulatory processes. For examples, U1 RNA is an interactor of TFIIH and regulates RNA transcription (Kwek et al., 2002); small RNAs with similarity to box H/ACA sno RNA are components of telomerase and mutated in a genetic form of dyskeratosis congenital (Vulliamy et al., 2001); 7SL RNA is a component of the Signal Recognition Particle (SRP) that plays a key role in the delivery to the ER of proteins with a leader sequence (Nagai et al., 2003).

The world of ncRNA adds new members on almost a daily basis. Several types of classification have been proposed based on the length of the RNA species, their locations on the genome and their function. Classes of non-coding transcripts can be divided between housekeeping ncRNAs, which are constitutively expressed, and regulatory ncRNAs, which are further distinguished between long and short according to their length (Ponting et al., 2009). Representative examples for each class of regulatory ncRNAs follow.

Small Nucleolar RNAs

Small nucleolar RNAs (snoRNAs) generally range from 60 to 300 nucleotides and guide the site-specific modification of nucleotides in target RNAs via short region of base-pairing. There are two classes of snoRNAs: the box C/D snoRNAs that guide the O'-ribose-methylation, and the H/ACA box which drives the pseudouridylation of target RNA. Initially it was thought that snoRNAs functions were restricted to ribosomal RNA (rRNA) modification in ribosome biogenesis, given their specific nucleolar localization. Now it is evident that they can target other cellular RNAs, as evidenced by the snoRNA involved in the aberrant splicing of the serotonin receptor 5-HT-(2C)R gene in Prader-Willi syndrome patients (Kishore and Stamm, 2006).

Although the snoRNA involved in ribosome biogenesis are located in the nucleolus, a subset of C/D snoRNAs is located into Cajal bodies (Meier, 2005). Most of them come from intronic regions of protein-coding genes, but apparently some snoRNAs are independently transcribed as evidenced by the presence of methylated guanosine at their 5' end (Kiss, 2002).

Small Interfering RNAs and MicroRNAs

Small interfering (siRNAs) and microRNAs (miRNAs) are 22 bps nucleotides long RNAs that derives from stem-loop or double-stranded RNA precursors, respectively.

Sources of siRNAs precursors are both endogenous genomic loci and foreign nucleic acid introduced into the cytoplasm (Mello and Conte, 2004). Centromeres, transposons, repetitive sequences, and specific genomic transcripts are sources of endogenous siRNAs (Allen et al., 2005).

miRNA derive from introns or exons of numerous protein-coding and non-coding genes (Lee et al., 2004; Rodriguez et al., 2004) as well as from retrotransposon sequences (Smalheiser and Torvik, 2005). miRNAs are transcribed by RNA Polymerase II from introns of numerous protein-coding and non-coding genes (Lee et al., 2004; Rodriguez et al., 2004) as primary miRNA (pri-miRNA) transcripts. The hairpin structure formed in these pri-miRNA transcripts are processed by RNase III enzyme Drosha into pre-miRNA, then exported from the nucleus and processed by Dicer to form the mature miRNA. The double strand mature miRNA is then incorporated into RNA-induced silencing complex (RISC) and acts as an adaptor for miRISC to specifically recognize target mRNAs. The interaction of miRISC with the 3' Untranslated Region (UTR) of target mRNA results into either cleavage, or translational inhibition of the target mRNA (Bartel, 2004). The nature of miRNA-mRNA base pairing is thought to determine the regulatory mechanism of post-transcriptional repression: perfect complementarity allows cleavage of the mRNA strand via activation of the RISC endonucleolytic complex (RNA interfering), whereas central mismatches promote repression of mRNA translation.

The expression of miRNA is a process tightly regulated and has been estimated central in several processes including cell proliferation (Brennecke et al., 2003), left-right patterning, cell-fate, neuronal gene expression (Klein et al., 2005), brain morphogenesis (Giraldez et al., 2005), muscle differentiation (Naguibneva et al., 2006) and stem-cell division (Croce and Calin, 2005).

miRNA have also a unequivocal role in human diseases. For example sequence variants in the binding site for *miR-189* in the SLITRK1 mRNA have been linked to Tourette's syndrome (Abelson, 2005). miRNA expression is clearly deregulated in cancer cells (Iorio et al., 2005). As another example of involvement in cancer, the proto-oncogene *c-myc* drives the expression of a cluster of six miRNAs on human chromosome 13; this cluster contains two miRNA (*miR17-5p* and *miR-20a*) that act

as translational downregulator of the E2F1 factor, a cell-cycle progressor (O'Donnell et al., 2005). Deregulation of *miR17-5p* and *miR-20a* is observed in various cancer cell models.

Recent studies have shown that miRNA do not require evolutionary conservation and many newly discovered human RNA seem to be primate specific and drive 'higher-mammals' specific fine tuning in gene regulation (Bentwich et al., 2005).

Piwi-interacting RNAs

Piwi-interacting RNAs (piRNAs) were first identified from mouse testis as component murine Piwi homolog (Miwi or Mili) proteins, a large subclass of Argonaute proteins found in all multicellular organisms with a highly conserved expression pattern in germ cells indicating an important role in development (Aravin et al., 2006; Girard et al., 2006; Grivna et al., 2006; Watanabe et al., 2008). These RNAs are 24-30 nucleotides long and are generated by a Dicer independent mechanism; mature piRNAs have 5' uridine monophosphate and a 2-*O*-methylated 3'end.

PiRNAs are thought to be involved in gene silencing, specifically the silencing of transposons. In fact, the majority of piRNAs are antisense to transposon sequences, suggesting that transposons are piRNA targets (Malone and Hannon, 2009). In mammals it appears that the activity of piRNAs in transposon silencing is most important during the development of the embryo (Aravin and Bourc'his, 2008), and in both *C. elegans* and humans, piRNAs are necessary for spermatogenesis (Wang and Reinke, 2008). piRNAs direct the Piwi proteins to their transposon targets. A decrease or absence of PIWI protein expression is correlated with an increased expression of transposons. Transposons have a high potential to cause deleterious effect on their host (O'Donnell and Boeke, 2007), and, in fact, mutations in piRNA pathways are found to reduce fertility in *Drosophila melanogaster* (Brennecke et al., 2008). However, piRNA pathway mutations in mice do not demonstrate reduced fertility; this may indicate redundancies to the piRNA system (Klattenhoff and Theurkauf, 2007).

Promoter-Associated Small RNAs

Promoter-associated small RNAs (PASRs) are broadly defined as short transcripts transcribed within a few hundred bases of the transcription start site (TSS) of protein-coding and noncoding RNAs. They have been described in all major eukaryotic lineages. A hidden repertoire of TSS-proximal transcripts first emerged from gene expression studies after removal of specific exosome components in plants and human cells (Chekanova et al., 2007; Preker et al., 2008). Small RNAs of at least 70 nt long collinear with the 5' end of mRNAs have been then described in almost all genes in physiological conditions (Guenther et al., 2007).

At least three classes of these RNAs have been identified to date: (1) Promoter-associated small RNAs (PASRs) are generally 20–200 nt long, capped, with 5' ends that coincide with the TSSs (Kapranov et al., 2007a). They have been first detected using genome-wide tiling arrays of human cell lines and subsequently analyzed with high-throughput sequencing. Their biogenesis is not well understood, although it may result from transcription of independent, capped, short transcripts or from cleavage of larger capped mRNAs (Fejes-Toth et al., 2009); (2) Transcription Start Site associated RNAs (TSSa-RNAs) are 20–90 nucleotide long and localized within -250 to +50 of TSSs (Seila et al., 2008); (3) transcription initiation RNA (tiRNA) are predominantly 18 nts in length and found in human, mouse, chicken and *D.melanogaster*. Their highest density occurs downstream of TSSs with positional conservation across species (Taft et al., 2009). All three classes are strongly associated with highly expressed genes and with regions of RNA Polymerase II binding. They are weakly expressed, showing a bidirectional distribution that mirrors RNA Pol II (Fejes-Toth et al., 2009).

Interestingly, several studies have indicated that short 19-21 nucleotide RNAs directed to promoter regions can be regulators of gene expression. In some cases gene silencing has been induced (Morris et al., 2004), whereas in others examples gene activation was surprisingly triggered (Janowski et al., 2007). Analysis of PASRs mimetics (20-250 nts) directed *in trans* against MYC and CTGF genes indicates that their levels correlate with decreased expression of the corresponding mRNAs (Fejes-Toth et al., 2009). The manipulation of PASRs may thus be gene-specific and leading to positive or negative regulation of target gene expression (Janowski et al., 2007).

Long Non-Coding RNAs

Long non-coding RNAs (lncRNAs) are RNA molecules whose length range from 200 nucleotides to several kilobases. The GENCODE v7 catalog reports the annotation of 14,880 human lncRNAs (Derrien et al., 2012). In contrast to small RNAs, which are highly conserved, lncRNAs are poorly conserved at the primary sequence level but there are several similarities in their mode of action.

In contrast to most mRNAs, which ultimately localize to the cytoplasm after processing, most lncRNAs are localized in the nucleus at steady state. This is especially true for poly A- long ncRNAs that account for a large portion of the total transcribed sequences (Wu et al., 2008) and lncRNAs transcribed from intronic regions (Cheng et al., 2005). Just a small subset of lncRNAs is located in both nucleus and cytoplasm (Imamura et al., 2004; Kapranov et al., 2007b) while some lncRNAs seem to be selectively localized in cytoplasm (Louro et al., 2009).

Although only a small number of functional lncRNAs have been characterized to date, they have been shown to control every level of the gene expression program (Wapinski and Chang, 2011), from chromatin remodeling to translation. Together with the large number of lncRNAs whose function is still to be uncovered, a comprehensive annotation of lncRNAs is missing. Indeed, the simplest classification of lncRNAs could be based on their loci of origin. On the basis of such denomination lncRNAs could be grouped into five separate categories: (1) transcripts that arise from the antisense strand of protein-coding genes, (2) transcripts that represent the introns of protein-coding genes, (3) transcripts that correspond to the promoters and/or 5' untranslated or 3' untranslated regions of protein-coding genes, (4) Independent transcripts that initiate within the protein-coding genes, and finally (5) transcripts originating from regions outside of protein-coding genes.

Another proposed classification has been based on their ability to be "*cis*-acting" or "*trans*-acting" lncRNAs.

Wang and Chang (Wang and Chang, 2011) recently suggested a classification based on the molecular functions that lncRNAs execute. They identified 4 archetypes of basic molecular mechanisms – signal, decoy, guide, and scaffold – whose analysis from an evolutionary perspective highlights a simple process of incremental modifications conferring alteration in molecular utility.

In the first archetype lncRNAs function as signals. In fact, lncRNAs show cell type-specific expression and respond to diverse stimuli, suggesting that their expression is

under considerable transcriptional control. As such, lncRNAs can serve as molecular signals, because transcription of individual lncRNAs occurs at a very specific time and place to integrate diverse stimuli. Some lncRNAs in this archetype possess regulatory functions, while others are merely by-products of transcription. The advantage of using RNA as a medium suggests that potential regulatory functions can be performed quickly without protein translation. For example, in mouse placenta, lncRNAs such as Air and Kcnq1ot1, which map to the Kcnq1 and Igf2r imprinted gene clusters, accumulate at promoter chromatin of silenced alleles and mediate repressive histone modifications in an allele-specific manner (Mohammad et al., 2009). Interestingly, a new class of lncRNAs recently identified belongs to this archetypal group. Enhancer RNAs (eRNAs) are lncRNAs produced by activity-dependent RNA Polymerase II binding of specific DNA enhancers. The level of eRNA expression from these enhancers positively correlates with the level of mRNA synthesis at nearby genes, suggesting that enhancers have a more active ‘‘promoter-like’’ role in regulating gene expression (Kim et al., 2010; Wang et al., 2011a).

In the second archetype lncRNAs function as decoys. In this group an lncRNA is transcribed and then binds and titrates away a protein target, but does not exert any additional functions. LncRNAs that fit into this functional archetype would presumably act by negatively regulating an effector, that is an RNA-binding protein (RBP). Recently, the lncRNA Gas5 (growth arrest-specific 5) has been identified as a novel mechanism by which cells can create a state of glucocorticoid resistance (Kino et al., 2010). Gas5 represses the glucocorticoid receptor through formation of an RNA motif from one of its stem-loop structures, mimicking the DNA motif equivalent to that of hormone response elements found in the promoter regions of glucocorticoid-responsive genes. Therefore, Gas5 competes for binding to the DNA binding domain of the glucocorticoid receptor and effectively precludes its interaction with the chromosome. Interestingly, recent work on the tumor suppressor pseudogene PTENP1 has brought forth the idea that it may have biological function through sequestration of miRNAs to affect their regulation of expressed genes (Poliseno et al., 2010). Specifically, the 3’ UTR of PTENP1 RNA was found to bind the same set of regulatory miRNA sequences that normally target the tumor-suppressor gene PTEN, reducing the downregulation of PTEN mRNA and allowing its translation.

In the third archetype lncRNAs function as guides: the RNA transcript binds ribonucleoproteins (RNPs) to direct their localization to specific targets. lncRNAs can

guide changes in gene expression either in *cis* (on neighboring genes) or in *trans* (distantly located genes). The most studied and best understood *cis* mechanism of regulation by lncRNAs is the mammalian X inactivation center (Xic), a genetic locus that specifies a number of ncRNAs, including Xist (Plath et al., 2002). Xic controls the silencing of one of the two X chromosomes in female mammals, to achieve dosage compensation between the sexes. Initially the recruitment of polycomb repressive complex 2 (PRC2) is brought in *cis* by RepA RNA, a 1.6 kb ncRNA originating from the 5' end of Xist (Wutz et al., 2002). RepA-mediated PRC2 recruitment and H3K27 trimethylation of the Xist promoter result in the creation of a ''heterochromatic state'' (Sun et al., 2006) that is required for transcriptional induction of Xist. Spreading of Xist is accompanied by the recruitment of polycomb and their associated chromatin modifications to the inactive X chromosome (Xi). More recently, a matrix protein, hnRNP U, was shown to be required for the accumulation of Xist RNA on the Xi (Hasegawa et al., 2010). Xist RNA and hnRNP U interact, and depletion of hnRNP U causes Xist to detach from the Xi and to localize diffusely in the nucleoplasm. An example of lncRNA guides acting in *trans* is lincRNA-p21, one of the direct p53 targets in response to DNA damage which is located upstream of CDKN1A gene. LincRNA-p21 is able to exert its effects on chromatin structure and transcription across multiple sites in the genome (Huarte et al., 2010). Ectopic expression of lincRNA-p21 induces gene expression changes and apoptosis, bypassing the upstream regulator p53. It remains to be determined how the repressive complex associated with lincRNA-p21 recognizes targeted gene loci and how this complex silences transcription.

In the forth archetype lncRNAs function as scaffolds. LncRNAs can serve as central platforms upon which relevant molecular components are assembled. This is the most complex class where the lncRNA possesses different domains that bind distinct effector molecules. The lncRNA would bind its multiple effector partners at the same time and by doing so brings the effectors, which may have transcriptional activating or repressive activities, together in both time and space. The telomerase is a conserved reverse transcriptase specifically involved in maintenance of genome stability by adding back telomeric DNA repeats lost from chromosome ends. Telomerase catalytic activity requires the association of two telomerase subunits: an integral RNA subunit, the telomerase RNA (TERC) that provides the template for repeat synthesis, and a catalytic protein subunit, the TERT, as well as several species-

specific accessory proteins. RNA domains have been identified in TERC that affect template usage (Lai et al., 2003; Chen and Greider, 2004) as well as TERT association (Ly et al., 2003). Mutations that alter the equilibrium between different conformational states of TERC result in disease states such as dyskeratosis congenital (Chen and Greider, 2004), presumably through disruptions of the RNA flexible scaffold structure into which are plugged modular binding sites for telomeric regulatory proteins.

These archetypes are not meant to be mutually exclusive and an individual lncRNA may fulfill several groups. Rather, the combinatorial usage of archetypal molecular mechanisms has been proposed in order to illustrate how apparently complex functions can be constructed and developed through the evolution of molecular mechanisms.

It is becoming clear that lncRNAs can have numerous molecular functions and it will be likely possible that newly discovered lncRNAs may serve to other functional paradigms.

A major current issue is to understand how the molecular functions of these lncRNAs affect the organism. It is already known that lncRNAs are implicated in numerous developmental events (Amaral and Mattick, 2008), such as the formation of photoreceptors in the developing retina (Young et al., 2005) and the regulation of cell survival and cell cycle progression during mammary gland development (Ginger et al., 2006). The generation of specific knockout animal models will be a key tool to shed light on this issue and will likely definitively show that many lncRNAs are not transcriptional ‘‘noise,’’ but are instead required for normal development.

LncRNAs are also misregulated in various human diseases, especially cancer (Prasanth and Spector, 2007), and even thought the mechanisms by which these transcripts affect tumor initiation and/or progression are currently unknown, some are already used as specific markers of tumors (de Kok et al., 2002).

Considering all these information it is reasonable that lncRNAs can also allow us to identify new therapeutic pathways and may be themselves therapeutic targets of molecular medicine. Furthermore, lncRNAs represent a promising therapeutic strategy which can afford the upregulation of endogenous genes in a locus-specific manner (Wahlestedt, 2013).

Antisense Transcription

The initial description of genomes organization has consisted in the separation between regulatory and protein-coding DNA stretches. This simple model has supported the "one region-one function" theory: a genome is a linear arrangement of functional elements interspersed with non-functional regions. Advances in transcriptomics technologies have shown that a genomic region can be used for different purposes giving rise to several different RNA molecules and that functional elements can co-locate in the same region of the genome.

Given the extend of the transcriptional overlap in the same genomic region, a large portion of the non-coding transcripts can be located in antisense direction to protein-coding loci (**Fig. 1**).

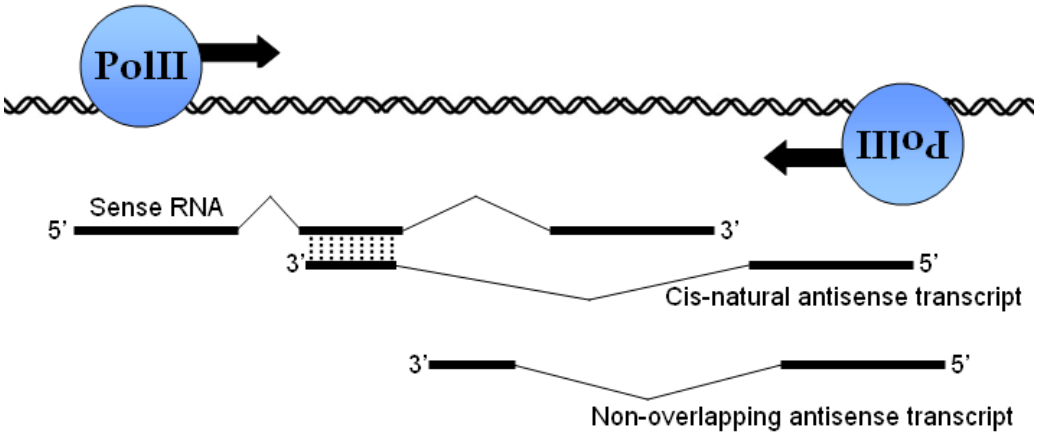

Figura 1. Definition of *cis*-NATs. *Cis*- NATs are transcribed at the same genomic loci of other genes, but from the opposite direction and off the opposite DNA strand. *Cis*- NATs share at least partial sequence complementarity with their sense strand partner. Similar to *cis*-NATs, non-overlapping antisense transcripts (NOT) are transcribed at the same genomic loci as another gene. However, NOTs do not share sequence complementarity with the sense RNA due to the effects of splicing.

It is estimated that 5,880 human transcription clusters (22% of those analyzed) form sense/antisense (S/AS) pairs with most antisense transcripts being ncRNA (Chen et al., 2004), an arrangement that exhibits considerable evolutionary conservation between the human and pufferfish genomes (Dahary et al., 2005). A detailed analysis of the mouse transcriptome indicated that 43,553 transcriptional units (72%) overlap with transcripts coming from opposite strand (Dahary et al., 2005).

S/AS pairs or Natural Antisense Transcripts (NATs) appear to be involved in different cellular pathways, although it remains unclear whether they present any

special sequence or structure-related feature, as well as what their protein partners are. As far as we know, NATs appear to be a heterogeneous group of regulatory RNAs with a variety of different biological roles and specific pattern of expression (tissues, cells, developmental stages).

Interestingly, a large fraction of NATs are expressed in specific regions of the brain, supporting the idea that they are involved in sophisticated regulatory brain functions and may be involved in complex neurological diseases (Qureshi et al., 2010).

Many well-characterized regulatory ncRNAs acts in *cis* as receivers of other *trans* acting signals by forming secondary structures. Several examples of *cis*–acting RNAs are provided by the regulatory sequences found in the UTRs of mammalian genes that are known to be target of different processes: RNA editing, control of mRNA stability and/or translatability (Gebauer and Hentze, 2004; Kuersten and Goodwin, 2003; Moore, 2005). Examples for *trans*-acting RNAs are the so-called riboswitches that are RNA molecules sensitive to several metabolic pathway, capable to bind to vitamins, lipids or small ligands and change their allosteric conformation in consequence of binding (Kubodera et al., 2003; Sudarsan et al., 2003).

Most NATs are *cis*-encoded antisense RNA (Kumar and Carmichael, 1998; Vanhée-Brossollet and Vaquero, 1998). By definition, *cis*-NATs are complementary RNA with an overlapping transcriptional unit (TU) at the same chromosomal locus. *Trans*-NATs are complementary RNA transcribed from different chromosomal locations (Sioud and Røsok, 2004; Makalowska et al., 2005; Li et al., 2008).

Characteristics of *Cis*-NATs

Cis-Antisense RNAs are widely distributed across the genome, althought they have a propensity for being located 5' and 3' to protein coding RNAs (Core et al., 2008).

According to their genomic anatomy *cis*-NAT are defined by their location relative to nearby protein-coding genes. The most common orientation for S/AS pairs is the tail-to-tail or convergent orientation, where the 3' ends of both transcripts align together. Divergent or head-to-head orientation and complete overlap *cis*-NAT are less frequent (**Fig. 2**).

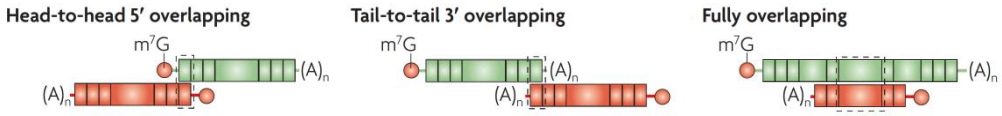

Figure 2. Genomic arrangement of *cis*-NATs. From left to right, divergent or head-to-head S/AS pairs share a 5' end overlap, whereas convergent or tail-to-tail *cis*-NAT overlap at their 3' end. The two transcripts are fully overlapping when one transcript is entirely contained within the second. Modified from Faghihi and Wahlestedt, 2009.

Antisense RNAs tend to undergo less splicing events and are often lower abundant than sense protein-coding partner.

Expression of the antisense transcript is not always linked to the expression of the sense protein-coding partner, thus suggesting the usage of alternative regulatory elements. Knocking down antisense genes results in multiple outcomes, with the corresponding sense gene being either increased or decreased.

These results indicate that antisense transcription can operate through a variety of different mechanisms and are a heterogeneous group of regulatory RNAs. Different models have been proposed for antisense–mediated regulation of sense gene.

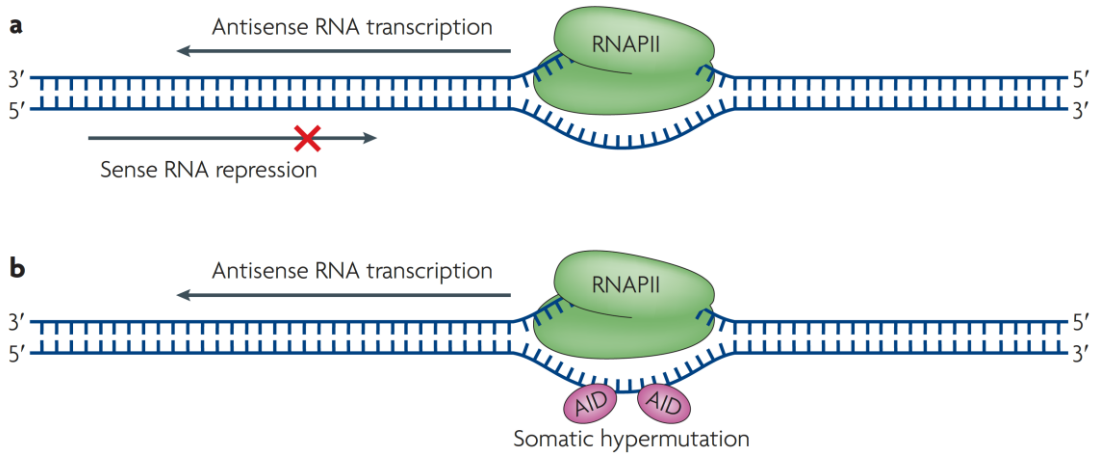

Figure 3. Transcription-related modulation a, In the collision model RNA transcription occurring in antisense direction halts sense transcription, thus transcription occurs in only one direction at any given time. **b**, During genomic rearrangements in hypervariable regions of B and T lymphocytes natural antisense transcription opens a transcriptional bubble that exposes ssDNA to AID. Modified from Faghihi and Wahlestedt, 2009.

The act of transcription itself in the antisense direction modulates the transcription of the sense RNA, either for transcriptional collision or genomic rearrangements. The first model is based on the assumption that RNA polymerase binds to the promoter of convergent genes on opposite strands and collides in the overlapping regions, blocking further transcription (Shearwin et al., 2005) (**Fig. 3a**). Genomic rearrangement occurs in lymphocyte B through a recombination process in the variable region of immunoglobulin genes (somatic hypermutation) and in lymphocyte T for T cell-receptor selection (class-switch recombination). RNA transcription from antisense direction creates a transcriptional bulge of 17 ± 1 melted bases in the target DNA, making it accessible to the activation-induced cytidine deaminase enzyme (AID). This is involved in somatic recombination and requires at least 5 nucleotides in ssDNA for optimal cytosine deamination (Sastry and Hoffman, 1995) (**Fig. 3b**).
NATs may also be involved in epigenetic regulation of transcription through DNA methylation, chromatin modification and monoallelic expression. Antisense RNA molecule itself can bind to complementary DNA target locus and triggers DNA methylation, DNA demethylation and chromatin modification of non-imprinted autosomal loci.

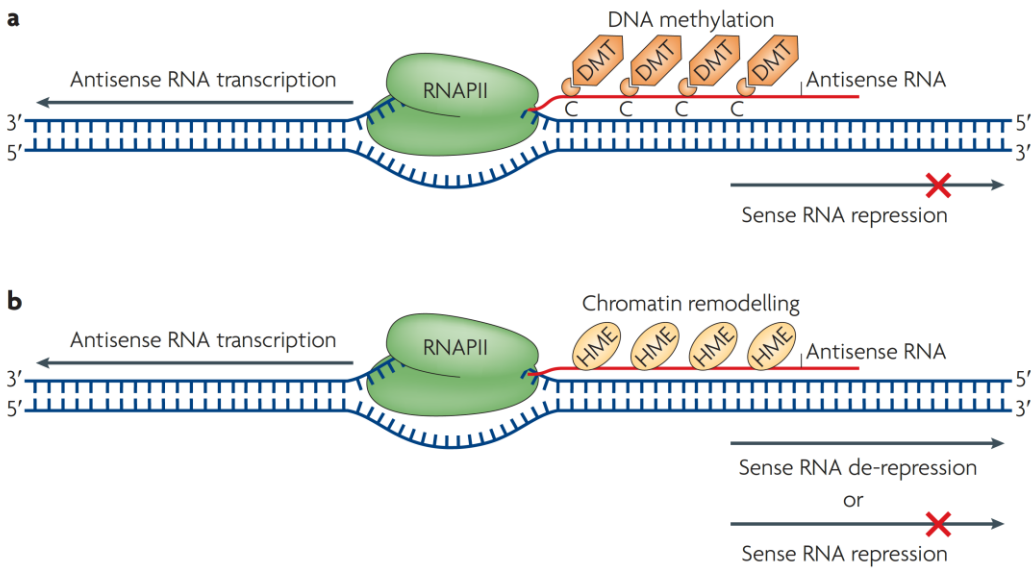

Figure 4. RNA-DNA interaction models. a, The newly formed AS RNA can induce directly or indirectly the DNA methyl tranferase (DMT) causing a repression of the sense RNA transcription. **b**, Newly formed antisense RNA transcripts can recruit histone-modifying enzymes (HMes) modulating chromatin architecture and epigenetic memory. Modified from Faghihi and Wahlestedt, 2009.

Some examples of antisense-mediated transcriptional silencing occurs at the promoter regions of α-globulin 2 (HBA2), p15, p21 and progesteron receptor (PR) gens by mean of methylation and heterochromatin formation (Morris et al., 2008; Schwartz et al., 2008; Tufarelli et al., 2003; Yu et al., 2008). The proposed mechanism can explain functionality even when abundance of antisense RNA molecules is very low (**Fig. 4a**).

Pervasive antisense RNA transcription at promoter and termination regions gives rise to promoter-associated small RNAs (PASRs) and termini associated RNAs (TASRs) or promoter-upstream transcripts (PROMPTs). The local accumulation of those small RNAs along transcribed regions overlaps with active chromatin domain marks such as trimethylation of Lys4 of histone3 (H3K4me3) (**Fig. 4b**).

Additionally some of the antisense-mediated epigenetic changes might spread to neighboring region not complementary to the antisense transcript causing either random monoallelic exclusion or including a whole cluster of genes, such as in genomic imprinting of the Kcnq1 locus. Finally, the expansion process occasionally involves the whole chromosome such as in the X chromosome inactivation in females.

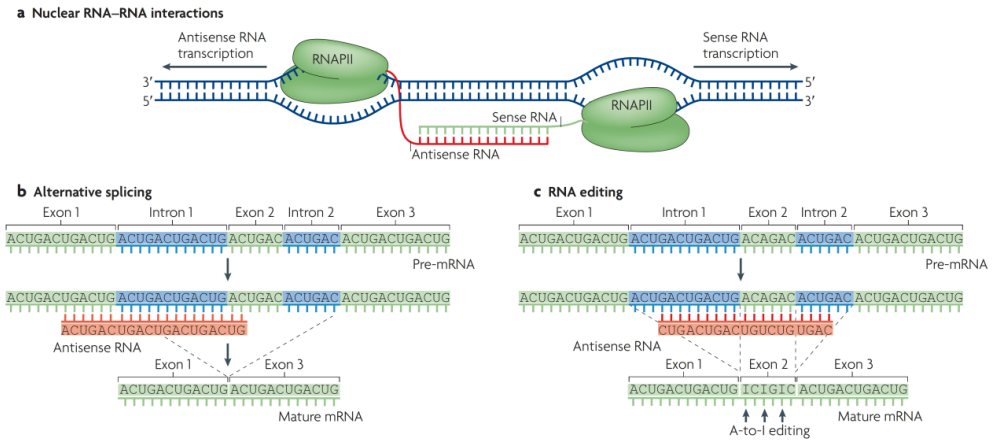

Figure 5. Nuclear S/AS pairing inhibiting senses RNA processing. a, Nuclear RNA pairing might occur locally after transcription interfering with sense RNA processing. **b**, RNA splicing Natural antisense transcript can cover acceptor or donor splice sites in the sense pre-mRNA. **c**, A-to-I editing by the ADAR enzyme induced by nuclear RNA duplex formation. Modified from Faghihi and Wahlestedt, 2009.

An alternative type of antisense-mediated gene regulation is based on the formation of hybrid RNA duplex in the nucleus that can be target of different enzymes.

An antisense RNA can bind the relative sense mRNA, tuning the balance between different splicing forms. This is the case of the thyroid hormone recptor-α gene where the antisense transcript RevErbAα influences the splicing of the two isoform variants (Hastings et al., 1997). In a similar manner it can potentially cause alternative termination and polyadenylation of sense RNA (**Fig. 5**).

Duplex formation between sense and antisense RNAs can modulate nuclear export. Nuclear retention is commonly observed for non-coding RNAs. Several cell stressors can mobilize antisense RNA molecules thus contributing to the nuclear shuffling of the protein-coding partner (**Fig. 5c**). In *D.melanogaster* antisense transcription is also been related to RNA editing. Duplex RNA formation in the nucleus can recruit ADAR (adenosine deaminase that act on the RNA) enzymes, which deaminates the target adenosine in inosine (Peters et al., 2003; Ohman, 2007).

Instead cytoplasmic RNA hairpins can affect both RNA stability/translation or cover miRNA binding sites on the sense mRNA.

The expression of the sense and antisense pair in the same cell can result in the activation of the endogenous siRNA processing machinery, which mediates sequence-specific knock-down of targeted genes. However, coexpression of NATs with their sense counterparts, together with the frequently observed concordant regulation of sense and antisense RNAs in many tissues and cell lines, provides evidences against endogenous siRNA being the sole mechanism of antisense-mediated gene regulation.

The overlapping RNA region might affect RNA stability by reducing mRNA decay, protecting the 5' end of the sense RNA from exonucleolytic degradation by various RNases. Antisense transcript for inducible nitric oxide synthase (*INOS*) interacts with the AU-rich element (ARE) binding antigen R (HuR) suppressing iNOS degradation. On the contrary, antisense RNA of hypoxia inducible factor 1 α (HIF1A) alters the secondary structure and exposes the ARE element in mRNA reducing its stability (Uchida et al., 2004). In the case of β-site APP-cleaving enzyme 1 (BACE1), the expression of its antisense RNAs BACE1-AS enhances the mRNA half-life by two mechanisms, increase of mRNA stability and masking of miRNA-binding sites along its sequence (Faghihi et al., 2008).

In the case of PU.1 mRNA, its non-coding counterpart is a polyadenilated transcript which has a longer half-life than the protein-coding RNA. The cytoplasmic binding of the processed AS RNA to its corresponding sense RNA stalls PU.1 translation between initiation and elongation steps (Ebralidze et al., 2008).

Characteristics of *Trans*-NATs

A recent study on *trans*-NAT showed that these regulatory elements are much more abundant than previously expected. Although the authors had applied very stringent criteria for selecting *trans*-NATs, eliminating all the NATs originating from repeat regions and pseudogenes, they reported that at least 4.13% of transcriptional units of various species are *trans*-NATs (Li et al., 2008).

Trans-NATs often originate from pseudogenes or repeat regions. Repetitive sequences in genome and pseudogenes have long been considered to be non-functional artifacts of transposition pathways. However, an increasing number of reports point to the functional role for repetitive elements in post-transcriptional events (Peaston et al., 2004).

Antisense transcription of pseudogenes may constitute a mechanism for controlling their cognate (parental) genes. Such a regulatory role has been demonstrated for topoisomerase I, neural nitric oxide synthase, inducible nitric oxide synthase and fibroblast growth factor receptor-3 pseudogenes (Zhou et al., 1992; Weil et al., 1997; Korneev et al., 1999, 2008). Importantly, recent reports proposed a role for a subset of mammalian pseudogenes in the production of endogenous siRNAs (endo-siRNA) through formation of double stranded RNA (Kawaji et al., 2008; Tam et al., 2008; Watanabe et al., 2008).

Chimerical NATs are antisense RNAs with sequence complementary to more than one region of the genome (Nigumann et al., 2002; Lavorgna et al., 2004). They offer partial complementarity to more than one target transcript (Li et al., 2000), being capable of regulating many sense mRNA at the same time.

Repetitive Elements

Most gene sequences are unique, found only once in the genome. In contrast, repetitive DNA elements are found in multiple copies, in some cases thousands of copies and most repetitive elements do not code for protein or RNA. Even thought about half of the human genome is comprised of repetitive sequences, what functions they serve, if any, are mainly unknown. The repeat content of the human genome is likely even higher, given that sequencing and assembly is less than perfect in repeat-rich regions. Their presence and spread causes several inherited diseases, and they have been linked to major events in evolution. Repetitive elements differ in their position in the genome, sequence, sizes, number of copies, and presence or absence of coding regions within them. The two major classes of repetitive elements are interspersed elements and tandem arrays.

Sequences that are "tandemly arrayed" are present as duplicates, either head-to-tail or head-to-head. So-called satellites, minisatellites, and microsatellites largely exist in the form of tandem arrays commonly localized at centromere and at or near telomeres. Because they are difficult to sequence, sequences repeated in tandem are underrepresented in the draft sequence of the human genome. This makes it difficult to estimate the copy number, but they certainly represent at least 10% of the genome.

Interspersed repeated elements are usually present as single copies and distributed widely throughout the genome. The interspersed repeats alone constitute about 45% percent of the genome. The best-characterized interspersed repeats are the transposable genetic elements (TEs), also called mobile elements or "jumping genes" and recently, TEs have been identified as the major contributors to the origin, diversification, and regulation of vertebrate lcnRNAs (Kapusta et al., 2013).

TEs may be categorized by their mobilization mechanism as either DNA transposons or retrotransposons. DNA transposons propagate via a cut-and-paste mechanism and unlike other TEs, they are found in both eukaryotes and prokaryotes. In contrast, retrotransposons use an RNA intermediate; are reverse transcribed; and move within the genome through a copy-and-paste mechanism. Retrotransposons are the most abundant class of TEs and they are further subdivided into two groups on the basis of presence or absence of Long Terminal Repeats (LTRs). The most prominent members of LTR-retrotransposons are endogenous retroviruses (ERVs). Essentially, such elements are endogenous retroviruses, which result from viral infections of germ cells. ERVs comprise about 8% of the human genome (Lander et al., 2001).

Two main families of non-LTR retrotransposons are actively mobilized. These are Long Interspersed Elements (LINEs), and Short Interspersed Elements (SINEs). Their success is evident through the fact that non-LTR retrotransposons occupy about one-third of the human genome, making them the most populous TE group in the human genome (Lander et al., 2001).

LINEs are the only currently known autonomous (providing its own enzymatic machinery for retrotransposition) retrotransposons that are currently mobilizing within the human genome. They comprise about 17% (~500,000 copies) of the human genome (Lander et al., 2001). LINEs are widespread among eukaryotes, but are less common among unicellular ones.

Among TEs SINEs are one of the most prolific mobile genomic elements in most of the higher eukaryotes, but their biology is still not thoroughly understood. SINEs length ranges from 100 to 600 bp (Kramerov and Vassetzky, 2005; Ohshima and Okada, 2005; Deragon and Zhang, 2006). The genomes can contain tens or hundreds of thousands of SINE copies. These copies are not identical and their sequence can vary by 5–35%. Altogether, these sequences constitute a SINE family. In contrast to all other TEs transcribed by RNA Polymerase II, SINEs are transcribed by RNA Polymerase III (Pol III) and contain a Pol III promoter in their sequence. SINEs encode no proteins and have to use LINE reverse transcriptase (RT) for their retrotransposition (Jurka, 1997; Kajikawa and Okada, 2002; Dewannieux et al., 2003). SINEs are widespread among eukaryotes but not as wide as other TEs. Apparently, they can be found in all mammals, reptiles, fishes, and some invertebrates. SINEs are also common in many flowering plants. At the same time, *D.melanogaster* species lack SINEs, and SINEs are missing in most unicellular eukaryotes.

The organism's interaction with SINEs (as well as with other mobile genetic elements) largely resembles the host–parasite coevolution. Essentially, SINEs are genomic parasites and can cause damage to the host genome through insertional mutagenesis or unequal crossover. At the same time, SINE copies can be beneficial for the host as sources of promoters, enhancers, silencers, insulators, and even genes encoding RNAs and proteins; they can underlie alternative splicing and polyadenylation; finally, SINE RNAs can act as trans factors of transcription, translation and mRNA stability (Makalowski, 2000; Ponicsan et al., 2010; Gong and Maquat, 2011).

Nevertheless, the organism tries to suppress SINE amplification using, for example, APOBEC3-mediated system (Chiu et al., 2006; Hulme et al., 2007) or SINE DNA methylation (Rubin et al., 1994). As LINE RT is required for SINE amplification, LINE repression also protects the genome from SINE expansion. LINEs can be repressed through RNA interference or the APOBEC3 system, and the repression can be fixed by DNA methylation. At the extremes, too aggressive SINEs (or LINEs) can destroy their host organism and are eliminated by selection; on the other hand, there are many examples of SINE family death (cessation of amplification). More commonly, ups and downs in the activity of particular SINEs or LINEs are observed.

Structure and Classification of SINEs

Most SINEs consist of two or more modules: 5' terminal 'head,' 'body' and 3' terminal 'tail.'

The head of all SINE families known to date demonstrate a clear similarity with one of the three types of RNA synthesized by Pol III: tRNA, 7SL RNA, or 5S rRNA (**Fig. 6**).

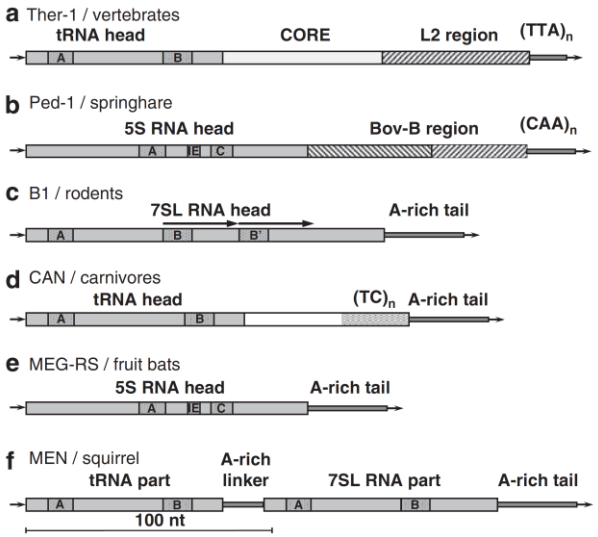

Figure 6. SINE structure examples. a, Ther-1 is a tRNA-derived CORE SINE of stringent recognition group. **b**, Ped-1, 5S rRNA-derived SINE of stringent recognition group with bipartite LINE region. **c**, B1, 7SL RNA-derived quasi-dimeric SINE of relaxed recognition group. **d**, CAN, tRNA-derived SINE of relaxed recognition group with a variable polypyrimidine region. **e**, MEG-RS, simple 5S rRNA-derived SINE of relaxed recognition group. **f**, MEN, dimeric tRNA/7SL RNA (heterodimeric) SINE of relaxed recognition group. Modified from Kramerov and Vassetzky, 2011.

The SINE head similarity with one of the cellular RNAs suggests its origin from this RNA. SINEs originating from tRNAs are particularly abundant. A particular tRNA species of origin can be confidently identified for many SINE families, although nucleotide substitutions in SINE evolution make it impossible in other ones. To date, 7SL RNA-derived SINEs have been identified only in rodents (Krayev et al., 1980; Veniaminova et al., 2007), primates (Deininger et al., 1981; Zietkiewicz et al., 1998) and tree shrews (Nishihara et al., 2002; Vassetzky et al., 2003). The 7SL RNA (B300 nt) is found in all eukaryotes as the RNA component of the Signal Recognition Particle (SRP), the ribonucleoprotein that targets secreted proteins to the endoplasmic reticulum. The number of SINE families originating from 5S rRNA is also not high; they have been found in some fishes (Kapitonov and Jurka, 2003; Nishihara et al., 2006) and in a few mammals: fruit bats (Gogolevsky et al., 2009) and springhare (Gogolevsky et al., 2008). The genes of all these RNAs (as well as the corresponding SINEs) have an internal Pol III promoter. The promoter in tRNA and 7SL RNA genes consists of two boxes (A and B) of about 11 nt spaced by 30–35 nt, while the 5S rRNA genes have three such boxes: A, IE and C (Schramm and Hernandez, 2002). The presence of the promoter within the transcribed sequence is critical for SINE amplification, as the promoter is preserved in new SINE copies.

The body of most SINE families (67%) consists of a central sequence of unknown origin. The central sequence is specific for each SINE family; however, it can contain domains common for distant families. Currently, four such domains are known: CORE domain in vertebrates (Gilbert and Labuda, 1999), V-domain in fishes (Ogiwara et al., 2002), Deu-domain in deuterostomes (Nishihara et al., 2006) and Ceph-domain in cephalopods (Akasaki et al., 2010). A substantial fraction of SINEs (20%) has a 30–100 bp region of similarity with the 3’ terminal sequence of LINE, whose RT is involved in SINE amplification (Ohshima and Okada, 2005). The LINE-derived regions of SINEs are required for the recognition of their RNA by the RT of some LINEs, while RTs of other LINEs require no specific recognition sequence. Accordingly, SINEs are divided into the stringent and relaxed recognition groups.

The tail is a sequence of variable length consisting of simple (often degenerate) repeats. All SINEs have the 3’ terminal tail composed of repeated mono-, di-, tri-, tetra- or pentanucleotides. The tail of many SINEs is a poly(A) or irregular A-rich sequence (A-tail), the amplification of all such SINEs in mammals depends on the RT of LINE1 family (L1). In some SINEs, the end of A-rich tails can contain the signals

of transcription termination and polyadenylation responsible for the synthesis of poly(A) at the 3' end of SINE RNA (Borodulina and Kramerov, 2008).

At the same time, not all SINEs have body (in particular, all known 7SL RNA-derived SINEs): 6% of SINE families consist of the head and tail only. Such elements resembling pseudogenes of cellular RNAs are called simple SINEs and can be distinguished from pseudogenes by specific nucleotide substitutions, which indicate their immediate origin from a SINE copy with such substitutions rather than from an RNA gene (Gogolevsky et al., 2009).

On the other hand, the structure of SINEs can be more complex. Two or more SINEs can combine into a dimeric (or a more complex) structure, which is further amplified as a dimer. Representatives of the same or different SINE families can combine. One of the first discovered SINEs, Alu in primates, consists of two similar parts derived from 7SL RNA (Deininger et al., 1981; Ullu and Tschudi, 1984). There are dimeric and trimeric SINEs derived from tRNAs (Schmitz and Zischler, 2003; Churakov et al., 2005). On the other part, complex elements composed of different SINE families or even types have been described. There are many such SINEs combining simple 7SL RNA- and tRNA-derived elements (**Fig. 6f**); most of them were described in rodents (Serdobova and Kramerov, 1998; Veniaminova et al., 2007; Churakov et al., 2010), but they also exist in primates (Daniels and Deininger, 1983). Hybrid 5S rRNA/tRNA SINEs have been described (Nishihara et al., 2006; Gogolevsky et al., 2009), while no SINEs combining 7SL RNA- and 5S rRNA-derived elements are known yet.

Origin and Evolution of SINEs

The origin of a new SINE family is a multistage process. SINE amplification relies on at least two processes, transcription and reverse transcription/integration, and a SINE genomic copy should be efficiently transcribed, while its RNA should be efficiently reverse transcribed within the period when active LINE RT is available.

SINEs originate from pseudogenes of tRNAs, 7SL RNA or 5S rRNA but the majority of 7SL RNA pseudogenes are not transcribed, as the transcription of 7SL RNA genes depend on the regulatory elements upstream of the gene in addition to the internal promoter (Ullu and Weiner, 1985). Accordingly, a 7SL RNA pseudogene transformation into a SINE requires modifications that allow its transcription

irrespective of the flanking sequences. It is possible that the deletion of the central region and/or smaller mutations in the 7SL RNA pseudogene in the genome of the common ancestor of primates and rodents have eventually led to the emergence human Alus and mouse SINE B1s. Apparently, most tRNA pseudogenes with intact internal promoter can be transcribed, and their conversion into SINEs requires no such radical modifications. Thus, SINEs emerged from tRNAs many times during evolution but, probably, only once from 7SL RNA.

Reverse transcription of foreign molecules by LINE RT is an extremely rare event compared with the reverse transcription of LINE RNA. Currently, we know two systems protecting LINE RTs from processing foreign templates: sequence recognition of the RNA encoding the enzyme and *cis*-preference, when the RNA molecule used for RT translation is used by the translated enzyme as the template for reverse transcription (Esnault et al., 2000; Wei et al., 2001; Kajikawa and Okada, 2002). Overcoming this protection is an essential step in SINE formation. In the first case, it is realized by the acquisition of the fragment(s) recognized by the RT. The mechanism of *cis*-preference violation remains unclear; the SINE RNA interaction with the factors of the RT complex can be proposed. For instance, B1 and Alu (as well as 7SL) RNAs form a complex with SRP proteins SRP9/14 (Weichenrieder et al., 2000), which can bind to polyribosomes. This way B1 and Alu transcripts can be presented to the synthesized L1 RT as the template for reverse transcription. A similar mechanism can be proposed for SINEs derived from tRNAs or 5S rRNA, components of the ribosomal complex. The *cis*-preference violation can be mediated by poly(A)-binding protein, which can bind proteins of the translational machinery (Roy-Engel et al., 2002); in this case, the acquisition of an A-tail should be an essential step in the evolution of SINEs mobilized by an RT with *cis*-preference. In some SINEs (for example, rodent B2), a polyadenylation signal at the 3' end provides for the A-tail synthesis (Borodulina and Kramerov, 2008).

Former evidences suggest that SINE RNA should not be involved in the gene processes of the cellular RNA from which it originates. This assumes accumulations of changes from the original structure. For instance, transcripts of simple tRNA-derived SINEs cannot form the clover leaf structure, and their nucleotides are not modified as in tRNAs (Rozhdestvensky et al., 2007; Sun et al., 2007). As a result of such changes, SINE transcripts lose the capacity to bind to at least some protein factors of tRNA processing or transport. This excludes SINE transcripts from tRNA

biochemical pathways and opens up a way for efficient retroposition. A similar pattern can be expected for the conversion of 7SL RNA and 5S rRNA pseudogenes into SINEs. For instance, B1 and Alu transcripts largely lose the similarity with the 7SL RNA secondary structure, although the structure of two domains is preserved (Labuda and Zietkiewicz, 1994).

In addition to transcription and reverse transcription, SINE replication involves other yet poorly known processes such as SINE RNA degradation or nuclear export (Kramerov and Vassetzky, 2005). The transport of SINE RNA is likely mediated by the interaction of its domains with cellular factors. For instance, Alu RNA transport is likely mediated by SRP9 and SRP14 (He et al., 1994). However, the absence of universal SINE structure responsible for its transport suggests different pathways of their RNA transport and, accordingly, different pathways for the acquisition of this function.

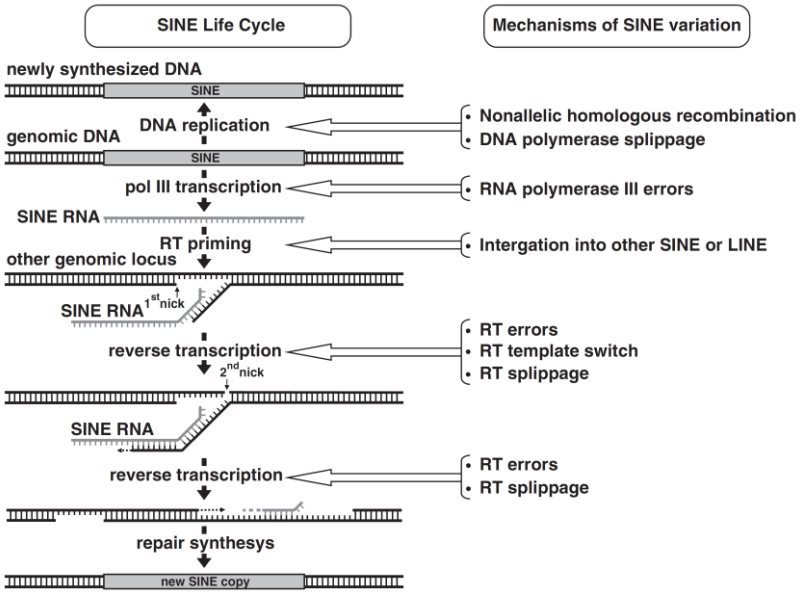

Figure 7. Mechanisms of SINE variation during their life cycle. Modified from Kramerov and Vassetzky, 2011.

The life cycle of SINEs includes DNA and RNA stages (**Fig. 7**). Little is known about the factors that determine their duration, but it can vary substantially. Clearly, a decline in LINE activity makes impossible further SINE amplification. Thus, correlation in activity is observed for many SINE/LINE partners.

In contrast to other mobile genetic elements, SINEs emerged in evolution many times. For instance, at least 23 primary SINE families independently appeared in the

evolution of placental mammals (currently, 51 mammalian SINE families have been described). This amazing property results, on the one hand, from their simple modular structure and the availability of the source modules (for example, tRNA or 3' end of LINE) in the cell. Moreover, high variation in SINE structures suggests that there are no stringent requirements for their nucleotide sequences excluding several short conserved regions. On the other hand, the emergence and replication of SINEs depend on LINE RT, which is not very secure from processing foreign sequences. Interestingly, some modules and RTs are particularly favorable for SINE emergence. According to the number of their genomic copies, dimerization is usually a progressive evolutionary event; however, dimeric SINEs are not necessarily more successful than the monomeric counterparts.

Non-mammals SINEs are unrelated to SRP RNA and believed to be derived from tRNA species. However, SINEs from mammals belong to either SRP- or tRNA-derived superfamilies. Rodents genomes contain both SRP RNAs (B1 elements) and tRNA superfamily (B2) SINEs, with SINEB1 basically resembling the left human Alu monomer. Prosimiam species have both SINEs, B1 and B2, and full-length dimeric Alus. This intermediate composition suggests a transition between rodents and human. Sequence database analysis and hybridization experiment excluded the presence of tRNA SINEs in human genome. The reason why Alus flourished in higher primate genome while tRNA SINEs are undetectable is still unknown. It can be either that Alus may have established a state of complete neutrality with the human host or more probably they have compensated their hosts with selective advantages. Several experimental evidences suggest that Alus may serve a variety of functions.

The human Alu is the most extensively studied SINE and it exemplifies most features of this unusual class of sequences.

There are at least 1 billion Alus per haploid genome (Schmid, 1996). Individual Alus share a common consensus sequence of 283 bps which is typically followed by a 3'A-rich region resembling poly(A) tail (**Fig. 8**). The Alu consensus sequence is a divergent tandem dimer in which the two monomers are separated by a short A-rich region that flanked the ancestral monomer. Except for 30 nucleotide insertion in the right monomer, Alu monomers are homologous to SRP RNA, also known as 7SL RNA. Most Alus are flanked by short direct repeats which represent the duplicated insertion sites.

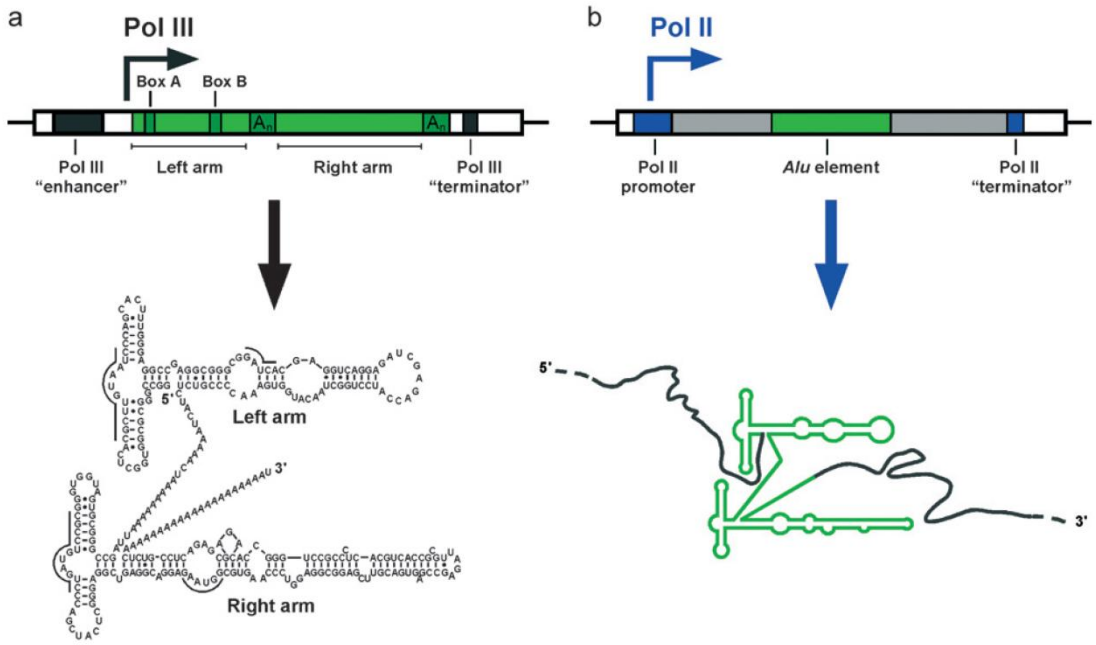

Figure 8. Transcription of Alu elements by Pol II and Pol III. a, Free Alu RNA. This hypothetical Alu element, shown in green, is transcribed by its internal Pol III promoter elements (Box A and Box B), which are helped by an upstream Pol III enhancer (or upstream promoter elements) for efficient transcription. A Pol III terminator (TTTT-3') is depicted downstream of the Alu element. Both Pol III enhancer and terminator are provided by the locus of integration of the Alu element. The secondary structure of the resulting Alu RNA was drawn based on the secondary structure determined by Sinnett et al., 1991 and adapted to the sequence of the Alu element of intron 4 of the *a*-Fetoprotein gene, which was shown to bind the SRP9/14 proteins. Underlined letters indicate the binding sites of SRP9/14 by analogy to SRP RNA. **b**, Embedded Alu RNA. This hypothetical Alu element, shown in green, is located inside of a protein-coding gene. It might be inserted into an intron, a UTR, and exceptionally into a coding region. This Alu element is then transcribed by Pol II, embedded inside a larger transcription unit. Depending on the sequence environment, as well as on its own sequence, the embedded Alu RNA might adopt a typical Alu fold. Modified from Häsler et al., 2007.

Alu elements inherited the two highly conserved sequences A and B boxes from the 7SL RNA promoter gene. However these elements are not sufficient to drive the transcription *in vivo* and Alus depend on flanking sequences for their expression. RNA Pol III-dependent transcripts of this class are referred to as "free" Alus.

Alus transcribed in the context of larger transcriptional units of both protein coding and non-coding RNAs are called "embedded" Alus. Katerina Straub and collegues screened the human transcriptome to identify Alu elements contained in the transcribed UTRs of human cDNA library. They identified 299 Alus embedded in the 5' UTRs of 244 transcripts and 2142 Alus embedded in the 3' UTRs of 1548

transcripts (http://cms.unige.ch/sciences/biologie/bicel/Strub/researchAlu.html). For Alu RNAs embedded in 5' UTRs of specific mRNAs, a role in inhibiting translation has been proved. BRCA1 presents a transcript isoform specifically expressed in cancer tissue that contains an Alu sequence in its 5' UTR forming a stable secondary structure and causing a translational defect (Sobczak and Krzyzosiak, 2002). Similarly, an antisense Alu element in the 5' UTR of the zinc finger protein ZNF177 (Landry et al., 2001), in the growth hormone receptor (Goodyer et al., 2001) and in the contactin mRNA isoform (Rome et al., 2006) decreased the translation efficiency of relative mRNAs. Concerning Alu elements in the 3' UTR, it has been proposed that inverted Alus could generate adenine and uracile rich element called AREs, as for the LDL receptor transcript (Wilson et al., 1998).

A function for Alu elements embedded in mRNA has also been identified. RNA editing is a very well characterized post-transcriptional RNA modification which consists in conversion of adenosine to inosine via the deaminase activity of a class of enzymes called ADARs (Adenosine Deaminase acting on RNA). Alus account for the 90% of editing events in nuclear RNA (Nishikura, 2006). ADAR enzymes preferentially edit adenosine present in double stranded RNA molecules and have no precise sequence specificity. Adenosine editing within an Alu sequence is favored when two Alus are present at a short distance in opposite orientation. This gives rise to intramolecular base pairing events as seen for NFkB1 and Cyclin M3 mRNAs editing (Kawahara and Nishikura, 2006). Furthermore, dsRNA formation has been related to nuclear retention and silencing of long non polyadenilated nuclear RNA (Chen et al., 2008).

Mouse SINE elements

Rodents genomes contain both SRP RNAs (B1) and tRNA superfamily (B2) SINEs with SINEB1 basically resembling the left human Alu monomer.

SINEs are the only transposable elements transcribed by RNA Polymerase III (Pol III). Cellular RNA Pol III can transcribe SINEs due to the presence of an internal promoter in their 5′ region, which is composed of A and B boxes spaced 30–40 nucleotides apart. SINE B1 family in mice originated from 7SL RNA, a component of SRP, involved in translation of secreted proteins in all eukaryotes. All these SINE families include sequences corresponding to the terminal regions of 7SL RNA with

the central 144–182 nucleotides deleted. In contrast to human Alu, murine or rat B1 (140 bp) is a monomer. However, it has an internal 29-bp duplication, which prompted Labuda et al. to consider B1 as a quasi-dimer (Labuda et al., 1991).

Mouse B2 RNA is encoded by short interspersed elements dispersed throughout the mouse genome with ~350,000 copies per cell. SINEB2s are transcribed by RNA Pol III to produce B2 RNAs that are ~180 nucleotides in length. The promoter elements (e.g., the A box and B box) that drive transcription are downstream from the transcription start site and therefore contained within the early transcribed region of SINEB2s. The 70 nucleotides at the 5′ end of B2 RNAs are evolutionary related to tRNAs, and the very 3′ end of B2 RNAs contain an A-rich sequence conserved among all SINEs (Kramerov and Vassetzky, 2005).

Examples of functional roles for mouse SINEB2 elements follow.

SINEB2 as Chromatin Boundary Element

During the development of the pituitary gland, in specific cells, the murine growth hormone (GH) becomes transcriptionally active. At embryonic stage 17.5 the promoter passes from a state in which H3 is trimethylated at K9 site (which is a mark for condensed heterochromatin) to a state in which H3 is dimethylated. The chromatin boundary where this transition starts has been localized to a region 10–14 Kb upstream of the GH transcription start site. Intriguingly, this region contained a SINEB2 element.

To test the hypothesis of the boundary element, a 1.1 Kb region containing the SINEB2 module has been tested for its enhancer blocking activity when placed between enhancer and the core promoter of a reporter gene and it resulted that the SINEB2 is necessary to block reporter gene expression. Strand specific PCR experiments showed that ongoing transcription through the RNA Pol III promoter (in sense direction) and through the RNA Pol II promoter (antisense direction) is important for enhancer blocking activity. These results suggest that a mouse SINEB2 serves as a boundary element and its bidirectional transcription causes a developmentally relevant change in chromatin structure (from heterochromatin to euchromatin), which establishes a permissive environment that allows transcription of the GH gene (Lunyak et al., 2007) (**Fig. 9**).

Interestingly, in human cells over 9,000 Alus are found within 1 Kb upstream of transcription initiation sites, raising the possibility that some Alu SINEs might also affect mRNA transcription by serving as boundary elements (Dagan et al., 2004).

tRNA genes have been found to serve as boundary elements in yeast, but the mechanism of function also appears to be somewhat different from that of the GH SINEB2 (Lunyak, 2008). Although ongoing RNA Pol III transcription of tRNA genes is required for boundary element function in yeast, there is no evidence of antisense RNA Pol II transcription through the tRNA genes.

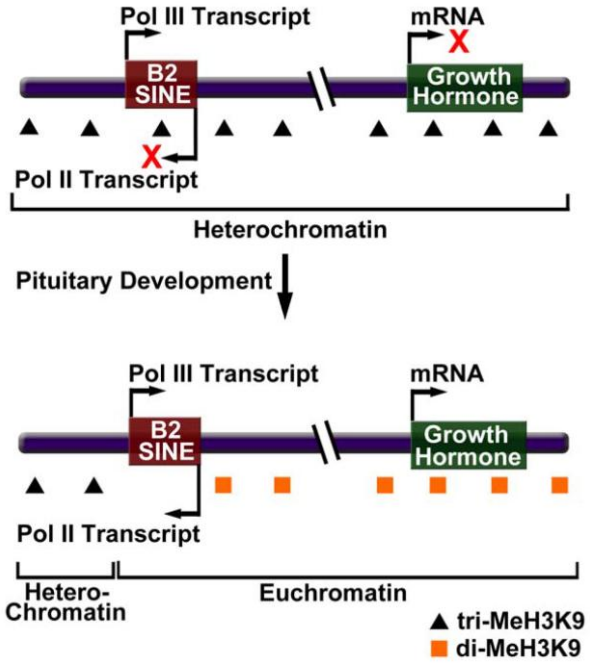

Figure 9. A B2 SINE serves as a boundary element to regulate transcription during pituitary development in mouse cells. Bidirectional transcription of a B2SINE upstream of the growth hormone locus facilitates a change in chromatin structure from a repressive heterochromatic state to a permissive euchromatic state. Modified from Ponicsan et al., 2010.

SINEB2 and Alus as *Trans*-Regulators of mRNA Transcription

SINEB2 and Alu RNAs may function as repressors of mRNA transcription during heat shock. As cells respond to heat shock, transcription of some genes is upregulated (e.g., hsp70), while transcription of others is repressed (e.g., β-actin, and hexokinase II) (Allen et al., 2004; Mariner et al., 2008). When Alu or SINEB2 RNAs are silenced, transcriptional repression at several genes upon heat shock is abrogated, indicating that SINEB2 and Alu RNAs act as inhibitor of transcription.

In an *in vitro* transcription system, Alu RNA and SINEB2 RNAs were potent repressors of RNA Pol II. Interestingly, physical binding of B2 RNA and Alu RNA to core Pol II has been demonstrated. Consistent with this finding, ChIP assays have proved that in heat shocked mouse or human cells, SINEB2 RNA or Alu RNA colocalize with Pol II at the promoters of transcriptionally repressed genes. These observations led to the model where Alu RNA and SINEB2 RNA are upregulated upon heat shock, bind RNA Pol II to enter complexes at promoters, and finally block transcription (**Fig. 10**).

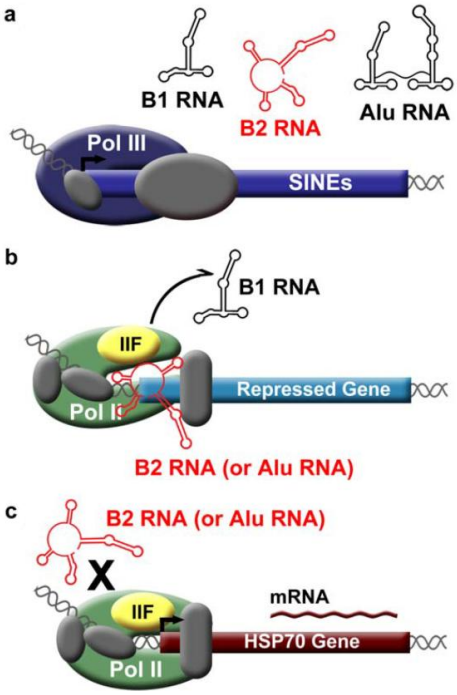

Figure 10. SINE RNAs control the heat shock response in mouse and human cells. a, Pol III transcribed SINE RNAs increase upon heat shock. **b**, During heat shock, mouse B2 RNA or human Alu RNA enters complexes at the promoters of repressed genes. TFIIF facilitates dissociation of B1 RNA from Pol II. **c**, Heat shock activated genes are resistant to repression by B2 RNA and Alu RNA. Modified from Ponicsan et al., 2010.

Deletion studies with SINEB2 RNA gave the first hints that these ncRNA share distinct functional domains. Nucleotides 81–130 of B2 RNA were fully functional for binding Pol II and repressing transcription *in vitro*; however, further truncation to 99–130 yielded an RNA domain capable of binding Pol II, but lacking the ability to repress transcription. Similarly, deletion analysis of Alu RNA demonstrated that it had two separable 'Pol II binding' domains and two different 'transcriptional repression' domains (Mariner et al., 2008).

A series of *in vitro* studies were performed to determine the molecular mechanism by which Alu RNA and B2 RNA repress transcription. Given that these ncRNAs co-occupy promoters with Pol II, they likely repress transcription after complexes bind to DNA but before initiation. They do so by preventing RNA Pol II from properly engaging the DNA after assembling into complexes with promoter-associated transcriptional factors (**Fig. 10**). B1 and B2 RNAs bind Pol II competitively and with similarly high affinity, which raised the intriguing question of whether B1 RNA could block B2 RNA from binding Pol II and repressing transcription. This possibility was investigated using an *in vitro* transcription system, and surprisingly, B2 RNA was found to repress transcription when B1 RNA had been pre-bound to Pol II (Wagner et al., 2009). Further experiments elucidated that TFIIF facilitates the dissociation of B1 RNA from Pol. II (**Fig. 10**). Moreover, fusing a transcriptional repression domain from Alu RNA onto B1 RNA created a chimerical ncRNA that remained stably bound to Pol II in the presence of TFIIF, showing that repression domains make RNA Pol II–ncRNA complexes resistant to the destabilizing effects of TFIIF.

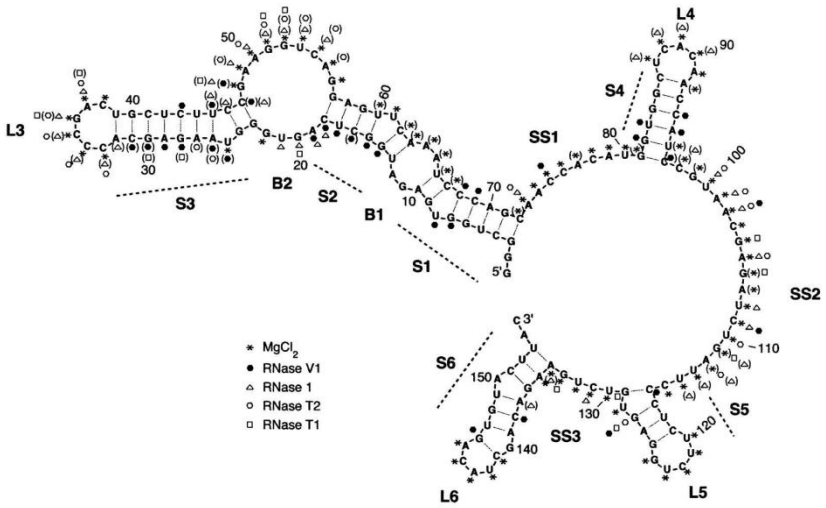

Figure 11. Model for the secondary structure of B2 RNA. Nucleotides 1–155 of B2 RNA are shown. Nucleotides 156–178, which constitute an A-rich single-stranded 39 tail, are not shown in the model. Symbols in parentheses indicate positions cleaved only weakly. Predominant features in the secondary structure are labeled as: stems 1–6 (S1–S6), bulges 1 and 2 (B1 and B2), loops 3–6 (L3–L6), and single-stranded regions 1–3 (SS1–SS3). Modified from Espinoza et al., 2007.

With the goal of understanding which regions of B2 RNA are important for high-affinity binding to RNA Polymerase II and repression of transcription, Espinoza et al. performed a structural and deletion analysis of a 178 nucleotide B2 RNA. (Espinoza et al., 2007). Deletion studies revealed that a 51-nucleotide region (from 81 to 131) of B2 RNA is sufficient for high-affinity binding to RNA Polymerase II, association with preinitiation complexes, and repression of transcription *in vitro*, the latter of which involves a large predominately single-stranded region within the RNA. In addition, this piece of B2 RNA blocked the polymerase from properly associating with template DNA during the assembly of elongation complexes. Further deletion revealed that a 33-nucleotide piece of B2 RNA (from 99 to 131) binds RNA Polymerase II, associates with preinitiation complexes, but cannot repress transcription. These results support a model in which RNA Polymerase II contains a high-affinity ncRNA docking site to which a distinct region of B2 RNA binds, thereby allowing another region of the RNA to repress transcription. Moreover, the mechanism of transcriptional repression by B2 RNA likely involves disrupting critical contacts between RNA Polymerase II and the promoter DNA (**Fig. 11**).

SINEB2 and Alu RNAs as *Trans*-Regulators of Translation

Cell stress dramatically increases the abundance of human full length Alu RNAs (fl Alu RNAs) and other mammalian SINE RNAs (Fornace and Mitchell, 1986; Liu et al., 1995). For example, heat shock causes a nearly 100-fold increase in mouse B1 RNA making this sparse transcript abundant (Fornace and Mitchell, 1986). Mouse B2 and rabbit C RNAs show similar increases, indicating that the heat shock response is conserved by the SRP RNA and tRNA SINE superfamilies. In addition to heat shock, other classic cell stress treatments increase full length Alu RNAs (flAlu RNA). Cell stress does not change the lifetime of flAlu RNA but probably increases Alu transcription (Liu et al., 1995). Viral infection or administering cycloheximide to cells also significantly increases the abundance of SINE RNA (Singh et al., 1985; Jang and Latchman, 1992; Jang et al., 1992; Panning and Smiley, 1993, 1995). The induction of Alu RNA by either cycloheximide or heat shock occurs <20 min after subjecting cells to these stresses (Liu et al., 1995).

The rapidity of these responses suggests that they arise from the modification of existing factors and do not involve either DNA demethylation or *de novo* synthesis. Do these increases in SINE RNA merely reflect an aberrant breakdown in regulation or are they a controlled response? Schmid and colleagues have shown that after viral infection, along with a global block in protein synthesis, the cytoplasmic concentration of flAlu RNAs dramatically increases. The halt of translation initiation that we observe after exposure to viral-stress is usually due to a change in the activity of PKR (double-stranded RNA activated kinase). The PKR is an intracellular protein kinase whose function is to sense cell stresses. Upon exposure to double stranded viral RNA PKR increases its autophosphorylation activity and hyperphosporylate the α subunit of eiF2 complex. eIF2 is responsible for the transport of the metionil-tRNA at the site of translation initiation. Phosphorylation of eIF2α on Ser-51 inhibits the formation of the ternary complex with the met-tRNA and impairs general translation levels. Small highly structured RNAs (like Alu RNAs) sequester PKR as bound monomers and inhibit its autophosphorylation, thereby potentially increasing protein synthesis. Since flAlu RNAs increase protein synthesis after viral infection, it has been proposed that this is mediated by PKR inhibition. However, translation stimulation is still present in knock-out cells (Rubin et al., 2002).

The absence of Alu RNAs in most mammals and tRNA SINEs in humans indicates that their sequence *per se* is not essential for function but their secondary structure is important. PKR binding primarily requires only a minimum number of base pairs within an RNA secondary structure so that several unrelated RNA sequences can functionally be Alu-substitutes as PKR inhibitors (Bhat and Thimmappaya, 1983; Clemens, 1987). As a classic example, when cells are infected and PKR activation blocks protein synthesis, the adenoviral VAI RNA gene inhibits virally induced PKR activation, restoring viral protein synthesis. Both protein synthesis and viral infectivity are impaired for VAI mutants. As another example of PKR binding element, the gene for an entirely unrelated RNA, EBER1, rescues both infectivity and protein synthesis for VAI mutants (Bhat and Thimmappaya, 1983).

According to this experiment, the cell stress-induced transcripts from the tRNA SINE superfamily could serve the same PKR regulatory role as Alu RNA. Yet a minimal RNA secondary structure alone cannot be sufficient to inhibit PKR *in vivo*. Otherwise, cellular RNAs, e.g. rRNA, would present an extraordinary number of PKR binding sites. Presumably, rRNA and other functional RNAs are unavailable for

PKR binding because of their subcellular location or organization into ribonucleoprotein (RNP) structures.

Similarly, short-lived flAlu RNA (Chu et al., 1995) could be rapidly reduced to basal levels when they are no longer required for PKR inhibition. As otherwise functionless RNAs, the RNP structure and subcellular location of SINE RNAs could promote their PKR accessibility. In support of the notion that Alu RNPs are accessible for PKR binding, the only other proteins known to form Alu RNPs are two small SRP 9/14 proteins and La, which transiently binds to the 3′ ends of nascent RNA Pol III transcripts.

Parkinson's Disease

Parkinson's Disease (PD) is the second most common progressive neurodegenerative disorder following Alzheimer's Disease (AD) and affects 1-2% of all individuals above the age of 65. The main pathological hallmark of PD is the progressive loss of neuromelanin-containing dopaminergic neurons in the Substantia Nigra pars compacta (SNc) of the ventral midbrain and the presence of eosinophilic intraneuronal inclusions, called Lewy bodies (LBs), composed of specific cytoplasmic proteins like alpha-synuclein, parkin, synphilin, ubiquitin, and oxidized neurofilaments (Goldman et al., 1983). This cell loss entails severe dopamine depletion in the striatum therefore causing the motor symptoms associated with PD, especially bradykinesia, tremor at rest, rigidity, and loss of postural control (Ehringer and Hornykiewicz, 1960; Bernheimer et al., 1973).

While the precise pathological mechanisms remain unclear, the identification of several genes associated with rare, heritable forms of PD have highlighted potential pathogenic causes, such as mitochondrial dysfunction, oxidative and nitrosative stress and aberrant protein degradation (**Table 1**).

Locus	Inheri-tance	Chromosome	Gene	Name of protein	Protein function	Pathology	Comments
PARK1	AD	4q21-23	*SNCA*	α-synuclein	Synaptic protein	LB+	Protein is major component of LB
PARK2	AR	6q25.2-q27	*PRKN*	Parkin	Ubiquitin-protein ligase	Pleomorphic (most LB-)	Most common cause of AR-JP
PARK3	AD	2q13	*SPR?*	Aldo-keto reductase?	Unknown	Unknown	Gene not known with certainty
PARK4	AD	4q21-23	*SNCA*	α-synuclein	Excess of α-synuclein protein		Multiplication of *SNCA* gene
PARK5	AD	4p14	*UCHL1*	UCHL-1	Hydrolyze small C-terminal adducts of ubiquitin	Unknown	Role uncertain
PARK6	AR	1p36-p35	*PINK1*	PINK1	Mitochondrial kinase	Unknown	Second most common cause of AR-JP
PARK7	AR	1p36	*DJ-1*	DJ-1	Oxidative stress protection	Unknown	Rare
PARK8	AD	12p11-q13	*LRRK2*	LRRK2	Muliple functions by several domains	Pleomorphic (LB+, tau+, ub+)	Most common cause of dominant Parkinson disease
PARK9	AR	1p36	*ATP13A2*	ATPase type 13A2	Lysosomal protein	Unknown	Complex phenotype (Parkinsonism, spasticity, and dementia)
PARK11	AD	2q37.1	*GIGYF2?*	GRB10 interacting GYF protein 2	Unknown	Unknown	Role uncertain
PARK13	AD?	2p12	*OMI/ HTRA2*	HtrA serine peptidase 2	Serine protease+	Unknown	No cosegregation shown to support pathogenicity
PARK14	AR	22q13.1	*PLA2G6*	A2 phospholipase	Phospholipid remodelling+	Unknown	Allelic to neuroaxonal dystrophy: adult-onset dystonia-parkinsonism in two patients
PARK15	AR	22q12-q13	*FBXO7*	F-box protein 7	Phosphorylation-dependent ubiquitination	Unknown	Early-onset, severe phenotype with spasticity and dementia

Table 1. List of PD-associated loci.

About 5-10% of all cases of PD are familial. Two autosomal dominant genes, (α-synuclein and LRRK2) and three autosomal recessive genes (parkin, DJ-1 and PINK1) have been repetitively found mutated in inherited PD (Kitada et al., 1998; Bonifati et al., 2002; Paisán-Ruíz et al., 2004; Valente et al., 2004; Zimprich et al., 2004). In brief, α-synuclein was the first gene in which a mutation was identified to cause an autosomal dominant form of Parkinsonism (Polymeropoulos et al., 1997). Furthermore, it was found to be the principal constituent of Lewy bodies (Spillantini et al., 1997). Its function is currently not known although it seems to be involved in fatty acid metabolism and synaptic transmission (Sharon et al., 2003).

LRRK2, whose function is also unknown, is a complex kinase for which it has been proposed that a simple gain of function could lead to toxicity (Greggio et al., 2006).

Parkin or PARK2 is an E3 ubiquitin ligase that has been shown to ubiquitinate substrates and to trigger proteasome-dependent degradation or autophagy. PTEN-induced putative kinase 1 (PINK1) or PARK6 is a mitochondrial protein kinase whose activity is required for Parkin-dependent mitophagy, a process that has been linked to neurodegeneration. In fact, PINK1 and Parkin act jointly in mitochondrial quality control by sensing mitochondrial dysfunction on the outer mitochondrial membrane and coupling it with a program of organelle degradation (Narendra et al., 2008).

DJ-1 or PARK7 is an atypical peroxidase with neuroprotective activity which affects sensitivity to oxidative stress.

Ubiquitin Carboxy Terminal Hydrolase L1 or PARK5

Ubiquitin Carboxy Terminal Hydrolase L1 (Uchl1) is an abundant neuronal enzyme representing 1-5% of total brain protein (Wilkinson et al., 1989). It possesses a well characterized de-ubiquitinating activity that catalyzes the hydrolysis of carboxyl-terminal esters and amides of ubiquitin to generate free monomeric ubiquitin (Larsen et al., 1996). Furthemore, Uchl1 associates with monoubiquitin and elevates the half-life of monoubiquitin in neurons, probably by preventing its degradation in lysosomes.

Interestingly, a natural Uchl1-null mutant is the Gad mouse (Gracile axonal dystrophy), a mouse model of a recessively transmitted neurodegenerative disease characterized by progressive axonal degeneration. Loss of functional Uchl1 leads to a decrease of free ubiquitin (Ub) and subsequent inadequate ubiquitinilation of proteins. A decreased Ub-dependent degradation is clearly upstream the accumulation of nondegradated Ub-proteins observed within the spheroid bodies in Gad mice (Castegna et al., 2004).

General involvement of UCHL1 in neurodegeneration has been assessed for Spinocerebellar ataxia (Fernandez-Funez et al., 2000) and Hungtinton's disease (Nazé et al., 2002), while its role in the pathogenesis of PD is still debated. A missense mutation in the UCHL1 gene leading to I93M substitution at the protein level has been reported in two affected siblings in a German family with an autosomal inherited form of PD. However, the existence of an unaffected carrier of the I93M mutation has questioned the link between I93M mutation and PD (Leroy et al., 1998). Intriguingly, I93M Uchl1 transgenic mice exhibit a clear nigrostiatal degeneration and progressive dopaminergic cell loss (Setsuie and Wada, 2007). Moreover, I93M UCHL1 shows decreased solubility and display aberrant interaction with several cellular proteins, including tubulin whose polimerization is severely unbalanced in presence of mutant I93M or carbonyl-modified UCHL1 (an oxidized form of UCHL1 often found in PD *post-mortem* brains) (Kabuta et al., 2008).

In search for additional I93M mutants, a previously unrecognized polymorphism in the Uchl1 gene (S18Y) was discovered and subsequently found to be linked to a decreased susceptibility to PD (Levecque et al., 2001). Protection of S18Y allele is dependent on the dosage, meaning that homozygotes have significantly lower risk than heterozygotes. The protection exerted by S18Y is not simply linked to UCHL1 hydrolytic activity because S18Y variant showed similar hydrolase properties as the

wild type. This fact suggested the existence of a distinct enzymatic activity that confers a gain-of-toxic-function for I93M mutant and protective properties to S18Y variant. This second activity was identified in the 2002 by the group of Peter Lansbury in a novel dimerization-dependent ubiquitin-ligase activity. UCHL1 was reported to form K63 polyubiquitin chain *in vitro*, using α-synuclein as a model substrate. While I93M and wt UCHL1 increased the α-synuclein levels in transfected cells inhibiting its degradation, S18Y did not (Liu et al., 2002).

Uchl1 ligase activity was found to be diminished for S18Y variant, which had indeed a dominant negative effect toward I93M mutant *in vitro*, thus explaining the incomplete penetrance of I93M mutation (Liu et al., 2002).

Kabuta et al. also showed an aberrant interaction between mutant I93M UCHL1 and protein involved in chaperon mediated autophagy (CMA) machinery: LAMP2A, Hsp70 and Hsp90. I93M UCHL1 was proposed to be a negative regulator of the CMA pathway and to have also a role in the inhibition of α-synuclein shunting to lysosomes (Kabuta et al., 2008).

Recent studies have shown classical Lewy pathology in a deceased sibling of a family affected by 193M UCHL1 mutation who developed, in addition to DOPA-responsive Parkinsonism, marked cognitive deficits (Leroy et al., 1998).

From a clinical point of view, UCHL1 has been extensively studied in *post mortem* brains of neurodegenerative diseases. In Alzheimer's Disease (AD) brains UCHL1 was also commonly found in neurofibrillary tangles with decreased levels of soluble protein (Choi et al., 2003). Downregulation and extensive oxidative modifications have been observed in *post mortem* brains of both AD and PD idiopathic forms (Butterfield et al., 2002; Castegna et al., 2002). Aberrant ubiquitin hydrolase and/or ligase activity occurring after oxidative modifications and/or downregulation of UCHL1 might lead to dysfunction of the neuronal ubiquitination/de-ubiquitination machinery, thus causing synaptic deterioration and neuronal degeneration. Furthermore, oxidative modification can make UCHL1 itself more resistant to proteolysis and promote aggregation into hallmark lesions of AD and PD brains (Lowe et al., 1990; Choi et al., 2003). In fact, UCHL1 has been found in neurofibrillary tangles and the level of soluble UCHL1 protein was inversely proportional to tangle number. These observations together with the lower hydrolytic activity shown by oxidized forms of UCHL1 raise the possibility that its role may be the de-ubiquitination of posphorylated tau protein and prevention of its aggregation *in*

vivo. Importantly, transduction of Uchl1 protein restored enzymatic and synaptic activity in hyppocampal slices treated with oligomeric Ab42 peptides and in APP/Ps1 mice model of AD (Gong et al., 2006).

A potential link of UCHL1 with α-synuclein pathology is supported by the observation that inhibition of UCHL1 activity in fetal rat ventral mesencephalic cultures is associated with α-synuclein aggregates (McNaught et al., 2002).

Increased intracellular aggregates containing ubiquitinated proteins have been found in human SK-N-SH cells after UCHL1 inhibition by prostaglandins (Li et al., 2004). These findings suggest that reduced UCHL1 activity impairs Ubiquitin Proteasome System (UPS) function and protein degradation, thus facilitating the accumulation of abnormal protein aggregates. In line with this, reduced Uchl1 mRNA and protein is found in PD and in Dementia with Lewy Bodies (DLB) (Barrachina et al., 2006).

Molecular Mechanism of Translational Control

The mammalian translational machinery is a tightly regulated system composed by eukaryotic initiation, elongation, and termination factors that are responsible for the recruitment of ribosomes to the 5'cap structure of cytoplasmic RNAs and for the following step of polypeptide chain synthesis.

Two predominant pathways translate mammalian mRNA through cap-dependent and independent mechanisms.

Cap-Dependent Translation

The rate-limiting step of protein synthesis is translation initiation. During this process the small ribosome subunit 40S is loaded on the 7metil-GTP-capped mRNA and scans in the 3' direction for the AUG start codon where the complete ribosome is subsequently assembled to begin polypeptide formation.

The recruitment of small ribosomal subunit requires the assembly of the eukaryotic Initiation Factor 4F (eIF4F) complex on the 5'cap structure of mRNA. eIF4E or cap-recognizing protein binds to the 5'7mG of mRNAs and promotes the assembly of eIF4A and eIF4G. The inhibited hyperphosphorylated eukaryotic Initiation Factor 4E-Binding Protein 1 (4E-BP1) releases eIF4E, allowing eIF4F complex to form. 4E-BP1 is a target of highly regulated signaling pathways that control its phosphorilation status and thus its ability to bind to eIF4E.

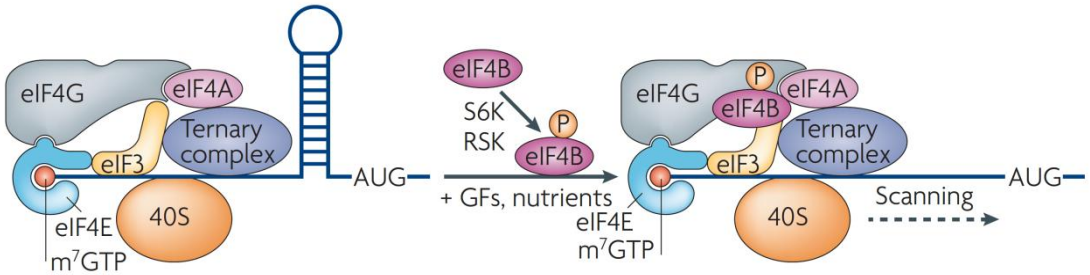

Figure 12. Regulating cap-dependent translation initiation. Following 40S ribosomal S6K-mediated phosphorylation, eIF4B is recruited to the pre-initiation complex and enhances the RNA helicase activity of eIF4A. GF, growth factor. Modified from Ma and Blenis, 2009.

Some mRNAs contain inhibitory secondary structures at their 5'UTRs. They may encode proteins that are involved in promoting cell growth and proliferation. Normal

processivity of translational machine requires that highly structured 5'UTR are first linearized. This is achieved through an initiation factor belonging to the family of RNA helicases, eIF4A which unwinds the RNA as long as the initiation complex is forming on the 5'cap of these mRNAs. Basic eIF4A activity is significantly enhanced when associated to its regulatory factor eIF4B, a target of 40S ribosomal protein S6 kinase (S6K). S6K phosphorilates eIF4B near its RNA-binding site, thus promoting its association to eIF4A (**Fig. 12**). Mutant eIF4B that cannot be modified by S6K is inactive *in vitro*, confirming that phosphorilation is both sufficient and necessary for its recruitment to the translation-initiation complex.

Cap-Independent Translation

RNA genomes of picornaviruses, such as encephalomyocarditis virus (EMCV) and poliovirus, have properties that are incompatible with initiation by 5′end–dependent scanning. In 1988, it was discovered that picorna viral mRNAs are translated by a mechanism, distinct from shunting, that enables ribosomes to initiate translation effectively on highly structured regions located within the 5'non-translated region (NTRs) (Pelletier et al., 1988). These regions were named Internal Ribosomal Entry Sites (IRESs). Picornaviral 5'NTRs can range in length from 610 to 1500 nucleotides, are highly structured, and contain multiple nonconserved AUG triplets upstream of the initiation codon that should act as strong barriers to scanning ribosomes.

Interestingly, several cellular oncogenes, growth factors and proteins involved in the regulation of programmed cell death, cell cycle progression and stress response contain IRES elements in their 5'UTRs. Internal initiation of translation escapes many control mechanisms that regulate cap-dependent translation. Thus, a distinguishing hallmark of IRES-mediated translation is that it allows for enhanced or continued protein expression under conditions where normal, cap-dependent translation is shut-off or compromised. For instance, IRES elements were found to be active during irradiation (Gu et al., 2009), hypoxia (Lang et al., 2002), angiogenesis (Nagamachi et al., 2010), apoptosis (Spriggs et al., 2005), and amino acid starvation (Gilbert et al., 2007).

The repression of global protein synthesis associated with such stresses is in part a consequence of phospholylation of Ser51 on the α subunit of the translation initiation

factor eIF2, which is a heterotrimer consisting of α, β, and γ subunits. During one of the first step of translation, eIF2 binds to GTP and the initiator Met-tRNA$_i^{Met}$ to form the Ternary Complex (TC), which subsequently binds to the 40S ribosomal subunit to compose the 43S PreInitiation Complex (PIC). In a second step GTP is hydrolyzed; for recurring initiation, the GDP must be released and eIF2 charged with fresh GTP. This reaction is catalyzed by eIF2β. After phosphorylation of eIF2α subunit of eIF2 the TC formation is inhibited, leading to a global repression of protein synthesis (**Fig. 13**).

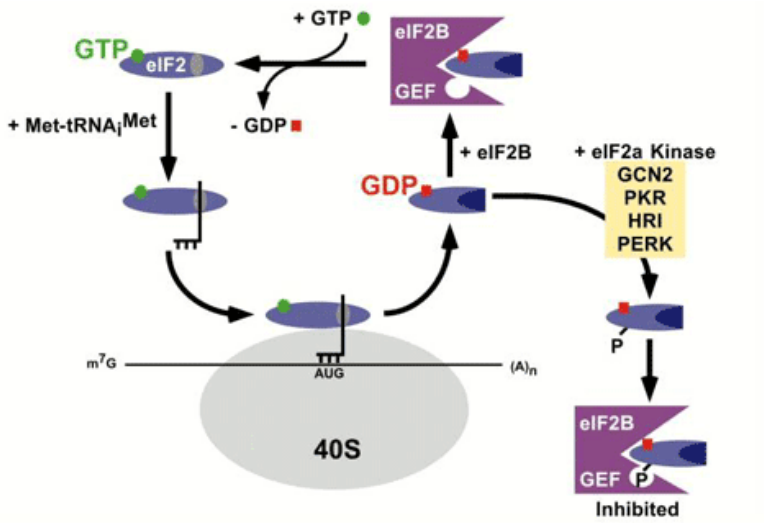

Figure 13. Recycling of EiF2 by EiF2B and regulation by Eif2A kinases. The γ subunit of eIF2 binding to GTP is essential for the TC of eIF2, GTP and Met-tRNA$_i^{Met}$. During the course of translation initiation the GTP bound by eIF2 is hydrolyzed to GDP and eIF2 is released from the ribosome in a binary complex with GDP. As eIF2 has a much higher affinity for binding GDP than GTP, a guanine-nucleotide exchange factor termed eIF2β is required.

Paradoxically, inhibition of eIF2 by phosphorylated eIF2α leads to upregulated translation of mRNAs with particular motifs in their 5'UTRs; these motifs are recognizable as upstream Open Reading Frames (uORFs) and IRES (Tzamarias et al., 1989; Vattem and Wek, 2004; Stoneley and Willis, 2004; Komar and Hatzoglou, 2011).

In the genome of *Saccharomyces cerevisiae* a single eIF2α kinase has been found and named General Control Non-derepressing 2 (GCN2). GCN2 is activated in response to nutrient deprivation and in particular to amino acids starvation (Kimball, 2001).

Mammals have 4 different eIF2α kinases: the mammalian ortholog to GCN2, the Protein Kinase R (PKR), the Heme-Regulated Inhibitor kinase (HRI), and the PKR-like endoplasmic reticulum (ER)-localized kinase (PERK). Each of these kinases is activated upon distinct stresses: GCN2 after deprivation of essential amino acids, PKR after viral infection with double-stranded RNA and interferon response, HRI during heme limitation and PERK during ER stress or Unfolded Protein Response (UPR).

Phosphorylation of eIF2α is essential for both the shut-off of global translation and recovery from stress. For instance, when unfolded protein accumulates in the lumen of ER, activated PERK mediates the phosphorylation of eIF2α. PERK-mediated phoshorylation of eIF2α represses the synthesis of proteins targeted to the ER thereby minimizing further accumulation of unfolded proteins. Lower cellular availability of eIF2α-GTP bound complexes increases the chance that mRNAs with internal AUG are translated (**Fig. 14**).

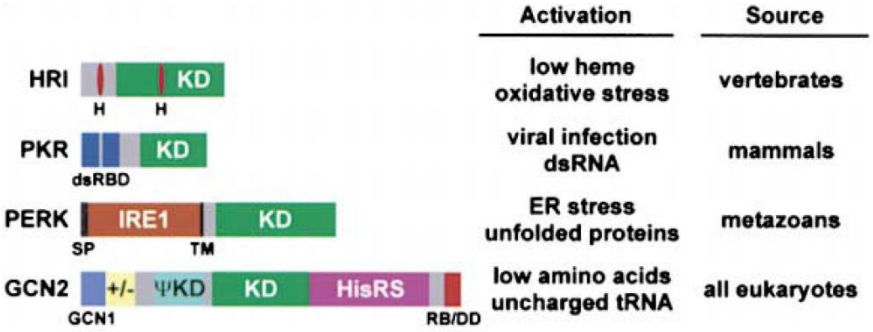

Figure 14. Kinases as sensors of cellular stress.

These shown protein kinases are activated following heme-deprivation (HRI), virus infection (PKR), ER stress (PERK), and amino acid starvation (GCN2). Subsequent phosphorylation of eIF2α on Ser-51 inhibits eIF2β and thus impairs general translation.

Together, these observations suggest that IRES and uORF mediate the translation initiation of certain mRNAs, representing a regulatory mechanism that helps the cell cope with transient stress. It is thus reasonable that each of the eIF2α kinases would be required for a recovery program specific to its activating stress, hence influencing the translation efficiency of different subsets of mRNAs. Moreover, IRES activity may also participate in the maintenance of normal physiological processes such as adequate synthesis of some proteins during cell cycle progression (Fingar et al., 2003).

Rapamycin

The ability of a cell to respond to an environmental stress is a fundamental property which allows cell survival. Cells respond to changes in environmental conditions by altering gene expression and proteins are produced as a consequence of new mRNA synthesis. However, translation is a tightly regulated molecular step and it has a fundamental role in forming the proteome of a cell.

To grow and proliferate cells must ensure that sufficient resources are available to drive protein production. When amino acids availability becomes limiting, protein production has to be down-regulated, keeping the spare energetic resources to survive.

Mammalian cells have evolved a fine mechanism of translational control in response to nutrient availability, cellular energy, stress, hormones and growth factors stimuli, which targets translational initiation. A key pathway that responds to environmental cues and integrates protein synthesis rate with external conditions involves the mammalian Target Of Rapamycin (mTOR). mTOR is the catalytic subunit of two molecular complexes: mTORC1 and mTORC2. mTORC1 is a serine/threonine protein kinase which includes mTOR, Raptor (regulatory-associated protein of mTOR) and Mammalian Lethal with SEC13 protein 8 (MLST8) (**Fig. 15**).

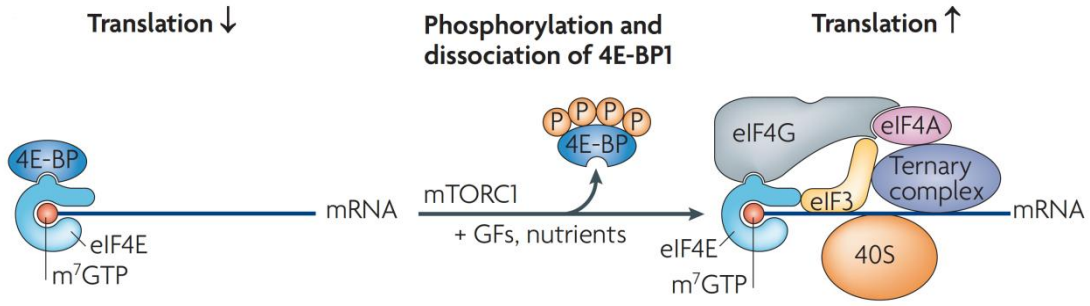

Figure 15. Regulating cap-dependent translation initiation. Hypophosphorylated 4E-BPs bind tightly to eIF4E, thereby preventing its interaction with eIF4G and thus inhibiting translation. mTORC1-mediated phosphorylation of 4EBPs releases the 4E-BP1 from eIF4E, resulting in the recruitment of eIF4G to the 5'cap, and thereby allowing translation initiation to proceed. Modified from Ma and Blenis, 2009.

mTOR signaling is activated downstream to numerous growth stimuli responding mainly to the Akt/PI3K pathway. Thus, TOR signaling coordinates cell growth and metabolism in response to physiological changes and elicits its control mainly via

phosphorilaton of its major downstream targets, 4E-BP1 and S6K. Phosphorilated 4EBP releases the 4E-BP from eIF4E, resulting in the recruitment of eIF4G to the 5′cap, and thereby allowing translation initiation to proceed.

Rapamycin is a macrolide antibiotic produced by *Streptomyces hygroscopicus*, which binds and inhibits mTOR. Inhibited mTOR prevents further phosphorylation of S6K, 4E-BP1 and, indirectly, other proteins involved in transcription, translation and cell cycle control.

Inhibition of cap-dependent translation is essential for survival under stress conditions. Many cellular stressors result in the rapid cessation of overall cap-dependent translation and promotion of cap-independent translation of several prosurvival factors. Overexpression of the translational inhibitor 4E-BP1 or treatment with mTOR inibitor rapamycin has been shown to possess viable therapeutic potential for PD (Tain et al., 2009; Liu et al., 2013).

It has been proved that 4E-BP1 mediates the survival response of cells exposed to various stresses (Clemens, 2001; Richter and Sonenberg, 2005). A regulated control of translation is believed to be the strategy used by cells to elicit a rapid response to toxic insults aiming to immediately change protein synthesis from pre-existing mRNAs pools.

In *D. melanogaster* PINK1 and parkin mutants exhibit dopaminergic neurodegeneration, locomotor deficits and mitochondrial dysfunction, representing a reliable animal model of PD. A genetic screening on *D. melanogaster* mutants has identified Thor as a modifier capable to influence the *Parkin-/-* genotype. *Thor* encodes for the sole orthologue of the mammalian 4E-BP1. Loss of *D. melanogaster* 4E-BP1 Thor markedly reduced the viability of double mutants for parkin and PINK1. On the contrary, overexpression of 4E-BP1 was sufficient to suppress all the pathologic phenotype in *Parkin/PINK1* double mutants, included neurodegeneration (Tain et al., 2009). The same protective effect *in vivo* is achieved by rapamycin-driven pharmacological inhibition of TOR.

Rapamycin has been recently found to provide neuroprotection in PD models (Malagelada et al., 2010). Primary neurons pre-exposed to rapamycin are protected by different neurotoxins that are known to recapitulate PD pathogenesis. More importantly, the infusion of rapamycin in the brain of mice treated with the PD mimicking drug MPTP (1-metil 4-phenil 1,2,3,6-tetrahydro-piridin) rescues neurons from undergoing degeneration.

The neuroprotection is exerted at different levels: 1) Rapamycin promotes autophagy in neurons; protein aggregates and organelles damaged by PD-mimicking neurotoxins would be cleared by autophagic process; 2) Rapamycin suppresses the expression of pro-cell death proteins known to induce neuronal apoptosis; one of these proteins is RTP801, a transcription factor that is induced during PD and neuronal oxidative stress (Ryu et al., 2002; Malagelada et al., 2006); 3) Rapamycin maintains the activation status of neuroprotective signaling pathways in neurons such as the pro-survival Akt pathway (Malagelada et al., 2008). Importantly, rapamycin treatment is also able to rescue mitochondrial defects in parkin-mutant PD patient cells (Siddiqui et al., 2012).

Other studies have shown that rapamycin significantly reduces the toxic buildup of protein aggregates such as amyloid beta and huntingtin proteins *in vivo* and *in vitro* models of AD and Huntington's Disease (HD) (Yu et al., 2005; Sarkar and Rubinsztein, 2008).

In Vitro Transcription and Translation Systems

Cell-free protein synthesis (CFPS) is not a new concept and it is based on the demonstration that cell integrity is not necessary for protein translation. Instead of relying on living cells, CFPS is carried out in an artificial buffer supplemented with a crude cell lysate, an energy supply, amino acids, and an exogenously mRNA or DNA template. The biggest advantage is that CFPS offers the quickest way to link a phenotype (protein) to a genotype (gene).

Indeed, most of the knowledge on the genetic code, mRNA, ribosome functions, protein factors involved in translation, translation stages including initiation, translational control, and co-translational protein folding, was obtained thanks to the use of cell-free systems. Like PCR, which uses cellular replication machinery to create a DNA amplifier, cell-free protein synthesis is emerging as a transformative technology with broad applications in protein engineering, biopharmaceutical development, and post-genomic research.

In order to produce high quantity of biologically active proteins *in vitro*, cell culturing and transfection of an expression vector carrying cDNA are time consuming, and undesirable proteolytic processing might happen in the mammalian cell culture system.

The protein expression field has traditionally been dominated by cell-based expression systems, initially including both conventional (*Escherichia coli*, *Saccharomyces cerevisiae*) and non-conventional (e.g., *Pichia pastoris*, *Thermus thermophilus*) host organisms that have been developed as 'cell factories'.

However, to fulfill their function proteins must adopt a precise three-dimensional conformation, the native state, acquired during cellular protein folding. This process is universally conserved in all organisms and enables bacteria to produce large amounts of human proteins. Although *Escherichia coli* is the simplest and by far the most widely used organism, the folding pathway of many recombinant proteins is often impaired in that host. Consequently, the misfolded polypeptides aggregate and form inclusion bodies instead of the native protein.

In this scenario, cell-free protein synthesis has rapidly emerged as an important complementary approach, rivaling cell-based protein production in terms of both convenience and scalability, and becoming widely recognized as a valuable tool for protein engineering (Kai et al., 2012).

Since viral RNA polymerases became commercially available, *in vitro* transcription/translation systems have allowed us to conveniently produce recombinant proteins of interest from cDNA. Such translation systems include the rabbit reticulocyte lysate system (Asselbergs et al., 1980), Hela cell lysate system (Mikami et al., 2008), wheat germ extract system (Lodish and Rose, 1977), and insect cell extract (Tarui et al., 2000). Some of the translation mixtures are further supplemented with T7 RNA polymerase and nucleotides, which enables the synthesis of recombinant protein from cDNA in a single tube within a few hours. Furthermore, programming a cell-free system with PCR products was made possible by adding a potent inhibitor of exonucleases, naturally present in bacterial lysate, thus increasing considerably the lifetime of linear DNA templates. With this development, all techniques of mutagenic PCR, used in protein engineering (site-directed or random mutagenesis, exchange exchange of codons, insertion or deletion, gene fusion, etc.), can be directly coupled with protein production (Burks et al., 1997).

The choice of a translation mixture over the others is imposed by the aim of the following analysis. For instance, Wang et al. have recently reported that among wheat germ extract, HeLa cell lysate, and rabbit reticulocyte lysate, only the latter was able to produce a biologically active neurotrophic factor. They presumed that the tertiary structure of the translation product(s) in the wheat germ extract and Hela cell lysate significantly differ from those in the reticulocyte lysate. Thus, the reticulocyte lysate translation system can be applied to high-throughput screening of active gene products (Wang et al., 2011b).

In addition to structural studies, the possibility of incorporating unnatural and chemically modified amino acids into proteins synthesized in cell-free systems raises new possibilities in functional studies, protein engineering and pharmaceutical research. The absence of cells permits the preparative scale synthesis of cytotoxic proteins and polypeptides, including various cell regulators and other factors crucial for cell life.

In addition to the principal contributions of the cell-free method to the basic science, possibilities for technological applications of cell-free translation systems have arisen. The development of continuous cell-free translation systems with perpetual supply of consumable substrates and removal of reaction products made the process of *in vitro* synthesis of individual proteins sustainable and productive (Spirin, 2004).

Advances in cell-free protein synthesis in recent years, particularly the ability to reconstitute protein synthesis from well-defined, purified components, has transformed the approach from a specialized analytical tool to a powerful preparative method with broad applicability. The Protein synthesis Using Recombinant Elements (PURE) approach to cell-free protein synthesis is based on modular reconstitution of the translational machinery of the cell from affinity purified protein components (Shimizu et al., 2005), including initiation factors, elongation factors, release factors, ribosome recycling factors, 20 aminoacyl tRNA synthetases, methionyl tRNA formyltransferase and pyrophosphatase, all bearing a 6 x His tag that can be utilized in 'reverse purification' of products, extracting the tagged proteins by metal affinity chromatography. These recombinant components are combined with ribosomes and tRNAs isolated from specially engineered *E. coli* strains, together with all of the necessary NTPs and amino acids, an ATP-generating catalytic module and Recombinant T7 RNA Polymerase (RNAP), creating a self-contained reaction system that can be programmed for protein synthesis using a variety of DNA templates. The advantages of the PURE systems include reduced levels of contaminating proteases, nucleases, and phosphatases, greater reproducibility resulting from more defined chemistry, and the flexibility of a modular system. Because it is modular, the PURE system supports a variety of modifications for specialized applications, including ribosome display and site-selective incorporation of non-natural amino acids (Whittaker, 2012).

MATERIALS AND METHODS

Plasmids

AS Uchl1 ΔA (ΔAlu, 1000-1045) mutant was obtained by subsequent cloning of PCR fragment I (NheI-EcoRI site) and PCR fragment II (EcoRI-HindII site) into pcDNA3.1(-). Primers used to obtain fragments I and II from AS Uchl1 were:

PCR fragment I: For mAS Uchl1 fl: 5'-ACAAAGCTCAGCCCACACGT-3'
Rev pre-SINE B2: 5'-CAATGGATTCCATGT-3'

PCR fragment II: For post-ALU: 5'-GATATAAGGAGAATCTG-3'
Rev mAS Uchl1 fl: 5'-CATAGGGTTCATT-3'

AS Uchl1 ΔS (ΔSINEB2, 764-934) mutant was obtained with a similar strategy than AS Uchl1 ΔA and the following primers:

PCR fragment I: For mAS Uchl1 fl: 5'-ACAAAGCTCAGCCCACACGT-3'
Rev pre-SINE B2: 5'-CAA TGGATTCCATGT-3'

PCR fragment II: For post-SINE B2: 5'-GAATTCCTCCAGTCTCTTA-3'
Rev mAS Uchl1 fl: 5'-CATAGGGTTCATT-3'

AS Uchl1 ΔAS (ΔAlu+SINEB2, 764-1045) mutant was obtained with a similar strategy than AS Uchl1 ΔA and the following primers:

PCR fragment I: For mAS Uchl1 fl 5'-ACAAAGCTCAGCCCACACGT-3'
Rev pre-SINE B2 5'-CAATGGATTCCATGT-3'

PCR fragment II: For post-ALU 5'-GATATAAGGAGAATCTG-3'
Rev mAS Uchl1 fl 5'-CATAGGGTTCATT-3'

AS Uchl1(ASf) (flipped Alu+SINEB2): PCR fragment obtained with the following primers was cloned in the unique EcoRI site of AS Uchl1 ΔAS:

For SINE B2 inside: 5'-TGCTAGAGGAGG-3'

Rev Alu inside: 5'-GTCAGGCAATCC-3'

AS Uchl1(Sf) (flipped SINEB2): PCR fragment obtained with the following primers was cloned in the unique EcoRI site of AS Uchl1 ΔS:

For SINE B2 inside: 5'-TGCTAGAGGAGG-3'

Rev SINE B2 flip: 5'-AAAGAGATGGC-3'

AS Uxt was amplified by PCR starting from FANTOM clone 4833404H03 (GenBank AK029359.1) and cloned into pcDNA3.1(-) using XbaI and HindIII restriction sites with the following primers: mAS Uxt F: 5'-CAACGTTGGGGATGACTTCT-3'
mAS Uxt R: 5'-TCGATTCCCATTACCCACAT-3'

AS Uchl1-73bp was obtained by annealing and extension of two 3'end overlapping oligonucleotides to generate the 73 bp antisense Uchl1 overlap region. Annealed fragment was obtained with:

AS Uchl1 73 bp forward:

5'-TCGGGGTTAATCTCCATCGGCTTCAGCTGCATCTTCGCGGATGGCACC-3'

AS Uchl1 73 bp reverse:

5'-CGGCTCCTCGGGTTTGTGTCTGCAGGTGCCATCCGCGAAGATGCAG-3'

Fragment was digested with XhoI and EcoRV and ligated into Δ5' AS Uchl1 deletion mutant (Carrieri et al., 2012).

AS SCR(73 bp) mutant was obtained with a similar strategy as AS Uchl1-73bp. The annealing extension was performed with oligonucleotides with scrambled (SCR) sequence.

AS SCR forward:

5'-CATCACCCCAAGAAAAGCGGGAACGGTAGCTGGGTCTTGTTAAGATT-3'

AS SCR reverse:

5'-CCTCGTTCCGATGGTTAAGACTCGGAATCTTAACAAGACCCAG-3'

AS GFP plasmid was generated with a similar strategy as AS Uchl1-73bp. Seventy-two base pairs corresponding to nucleotide -40/+32 with respect to the ATG of GFP coding sequence in pEGFP-C2 vector (Clontech) were chosen as target sequence for artificial antisense DNA generation.

GFP antisense forward:

5'-CCGGTGAACAGCTCCTCGCCCTTGCTCACCATGGTGGCGACCGGTAGC-3'

GFP antisense reverse:

5'-TAGTGAACCGTCAGATCCGCTAGCGCTACCGGTCGCCACCATGGTGA-3'

Cells

MN9D cells were obtained from Prof Michael J. Zigmond at University of Pittsburg. Cells were seeded in 100-mm dishes in Dulbecco's modified Eagle's (DMEM) medium containing 10% fetal bovine serum (Invitrogen) supplemented with penicillin (50 units/ml) and streptomycin (50 units/ml). For experiments, cells were plated and grown overnight; approximately 50% confluent cells were treated with 1 μM rapamycin (R0395, Sigma) or DMSO vehicle for 45'.

For the establishment of stable cell lines (shRNA -15/14, shRNA scrambled, pcDNA 3.1- and AS Uchl1DSINEB2), MN9D cells were seeded in 100-mm Petri dishes and

transfected with Lipofectamine 2000 (Invitrogen) according to the manufacturer's instruction. Stable clones were selected by 500 mM neomycin (N1142, Sigma). HEK cells (Sigma) were cultured under standard condition in DMEM containing 10% fetal bovine serum supplemented with antibiotics.

HEK cells (Sigma) were cultured under standard condition in DMEM containing 10% fetal bovine serum supplemented with antibiotics.

Transient transfections were done with Lipofectamine 2000 (Invitrogen). For all experiments, S and AS plasmids were transfected at 1:6 ratio.

qRT-PCR

Total RNA was extracted using Trizol reagent (Invitrogen) according to manufacturer's instructions. Purified RNA was subjected to DNase I treatment (Ambion) and 1µg was retro-transcribed using iScript cDNA Synthesis Kit (BioRad). qPCR was carried out using SYBR Green fluorescence dye (2X iQ5 SYBR Green supermix, BioRad). GAPDH and β-actin were used as normalizing controls in all experiments. The amplified transcripts were quantified using the comparative Ct method: relative expression in each sample was calculated by the formula 2^ΔΔCt and the differences in gene expression were presented as normalized fold expression.

Below are the used primers:

Gapdh F: 5'-GCAGTGGCAAAGTGGAGATT-3'

Gapdh R: 5'-GCAGAAGGGGCGGAGATGAT-3'

Beta-actin F: 5'- CACACCCGCCACCAGTTC-3'

Beta-actin R: 5'- CCCATTCCCACCATCACACC-3'

Uchl1 F: 5'-CCCGCCGATAGAGCCAAG-3'

Uchl1 R: 5'-ATGGTTCACTGGAAAGGG-3'

AS Uchl1 F: 5'CTGGTGTGTATCTCTTATGC-3'

AS Uchl1 R: 5'CTCCCGAGTCTCTGTAGC-3'

AS Uchl1 overlap F: 5'-GCACCTGCAGACACAAACC-3'

AS Uchl1 overlap R: 5'-TCTCTCAGCTGCTGGAATCA-3'

GFP F: 5'-GCCCGACAACCACTACCTGAG-3'

GFP R: 5'-CGGCGGTCACGAACTCCAG-3'

hUCHL1 S: 5'-GCCAATAATCAAGACAAAC-3'

hUCHL1 AS: 5'-CATTCGTCCATCAAGTTC-3'

hAS UCHL1 S: 5'-AAACCCATCCTTTCACCATCC-3'

hAS UCHL1 AS: 5'-TTCCTATCTTCAGCCACATCAC-3'
AS Uxt F: 5'-CAACGTTGGGGATGACTTCT-3'
AS Uxt R: 5'-TCGATTCCCATTACCCACAT-3'
Uxt F: 5'-TTGAGCGACTCCAGGAAACT-3'
Uxt R: 5'-GAGTCCTGGTGAGGCTGTC-3'

Western Blot

Cells were lysed in 2X SDS sample buffer. Proteins were separated in 15% SDS–polyacrylamide gel and transferred to nitrocellulose membranes. Immunoblotting was performed with the following primary antibodies: anti-UCHL1 (3524, Cell Signaling), anti-UXT (11047-1-AP, Proteintech Group), anti-GFP (A6455, Invitrogen), anti-FLAG (F7425, Sigma–Aldrich), and anti-β-Actin (A5441, Sigma). For the mTOR pathway: anti-phospho-p70 S6 kinase (Thr 389) (9234), anti-phospho-4E-BP1 (Ser 65) (9451), anti-p70 S6 kinase (9202), anti-4E-BP1 (9452), were all purchased from Cell Signaling. Signals were revealed after incubation with recommended secondary antibodies conjugated with horseradish peroxidase by using enhanced chemiluminescence for UCHL1 (WBKLS0500, Millipore Immobilion Western Chemioluminescent HRP substrate) and ECL detection reagent (RPN2105, GE Healthcare).

Cellular Fractionation

The protocol for nucleo-cytoplasmic fractionation was adapted from Wang et al 2006 and the subcellular enrichment was confirmed by detection of nuclear and cytoplasmic proteins. RNA was extracted using Trizol reagent (Invitrogen) according to manufacturer's instructions and subjected to DNAse I treatment (Ambion).

Polysomes Profiles

Polysomes profiles were obtained using sucrose density gradients. MN9D cells were treated with 1 μg/ml rapamycin for 35', then with 100 μg/ml cycloheximide for 10' prior lysis in 150 μl lysis buffer (50 mM Tris-HCl pH7.5, 100 mM NaCl, 30 mM MgCl2, 100 μg/ml cycloheximide, 0.1% NP-40, 40 U/ml RNasin®, protease inhibitors cocktail). Whole cell extracts were clarified at 15000g for 10' at 4°C. The equivalent of 5-10 absorbance units at 254 nm of the clarified cell extract was layered onto 15%-55% (w/v) sucrose gradient (50 mM Tris/acetate pH 7.5, 50 mM NH4Cl,

12 mM MgCl2 and 1 mM DTT) and centrifuged at 39000 rpm for 210' in a Beckman SW41Ti rotor at 4°C. The gradient was pump out by upward displacement and absorbance at 254 nm was monitored using BioLogic LP software (Bio-Rad). Fractions of 1 ml were collected, 1 ml Trizol reagent (Invitrogen) was added and, RNA was extracted following manufacturer's instructions. A fixed volume of each RNA sample was then retro-transcribed and percentage of mRNA in each fraction was calculated as relative Ct value to total RNA.

Pulse Labelling and Immunoprecipitation.

To monitor *de novo* protein synthesis, HEK cells were transiently transfected with pEGFP-C2 plasmid (Clontech) in combination with antisense GFP or empty control vector. After 24 hours, medium was replaced with methionine/cysteine-free DMEM for 1 hour. Then, cells were labeled with 100 μCi/ml of [^{35}S]methionine/cysteine (EasyTag, Perkin-Elmer) for 1 hour. Labeled cells were collected, lysed in RIPA buffer (150 mM NaCl, 50 mM Tris pH8, 1 mM EDTA, 1% NP40, 0.5% deoxycholic acid and 0.1% SDS) and used for immunoprecipitation with anti-GFP antibody (Invitrogen) overnight. Immune complexes were isolated with protein G-sepharose beads (Amersham) and separated on 10% SDS–PAGE. Newly translated GFP was visualized by autoradiography. Densitometric analysis was performed on high-resolution images with Photoshop-CS5. Normalization was obtained relative to input.

Northern Blot.

500 μl of polysome fractions were digested with 100 μg/ml proteinase K in 1% SDS and 10 μg glycogen (Invitrogen) at 37°C for 1 hour. RNA was obtained by phenol/chloroform extraction and resuspended in formaldehyde/formamide MOPS buffer. Samples were incubated for 5' at 65°C before being loaded into formaldehyde 1% agarose gel and run at 90V for 4 hours at 4°C. RNA was transferred onto Amersham Hybond-XL nylon membranes and UV-crosslinked. A Uchl1-specific RNA probe complementary to the distal 600 bps of mouse Uchl1 cDNA was *in vitro* transcribed in the presence of 50 μCi of α-^{32}P-UTP (Perkin-Elmer). After treatment with DNase I (Ambion), the radiolabelled riboprobe was purified on RNeasy columns (Qiagen). Membranes were pre-hybridized for 3 hours at 65°C with NorthernMax prehybridization/hybridization buffer (Ambion) supplemented with 50 μg/ml salmon sperm DNA (Invitrogen), and hybridized with Uchl1 riboprobe overnight at 65°C in

the same buffer. After extensive washes (most stringent conditions were 0.2X SSC/0.1% SDS at 65°C), membranes were exposed to autoradiography at -80°C with intensifying screens.

Uncoupled *In Vitro* Transcription and Translation Assay

Plasmids were linearized by HindIII digestion and column purified prior to *in vitro* transcription with mMESSAGE mMACHINE® T7 Kit (Ambion). After treatment with DNase I (Ambion) the RNA was purified on RNeasy columns (Qiagen).

The obtained RNA was added to commercially available lysates for *in vitro* translation following manufacturer's instruction: Rabbit Reticulocyte Lysate System, TnT® T7 Insect Cell Extract Protein Expression System, and Wheat Germ Extract were all purchased by Promega. Produced proteins were detected by Western Blot with anti-GFP (A6455, Invitrogen) antibody. Signals were revealed after incubation with recommended secondary antibodies conjugated with horseradish peroxidase by using ECL detection reagent (RPN2105, GE Healthcare).

PRELIMINARY DATA OF PROFESSOR S. GUSTINCICH LABORATORY

from Claudia Carrieri's Thesis "Uchl1 Protein Synthesis Upon Rapamycin Treatment Involves Its Antisense RNA Through Embedded SINEB2 Repeat".

Among the mouse synthenic genomic loci of genes associated to PD a spliced long noncoding (lncRNA) transcript (Rik6430596G22 – GenBank AK078321.1) was identified in Uchl1 gene mapping in antisense direction to its coding counterpart. This 5' head to head transcript that initiates within the second intron of Uchl1 mRNA and overlaps its first 73 bps including the ATG codon (-40/+33 from ATG) was named antisense Uchl1 (AS Uchl1) (**Fig. 16**).

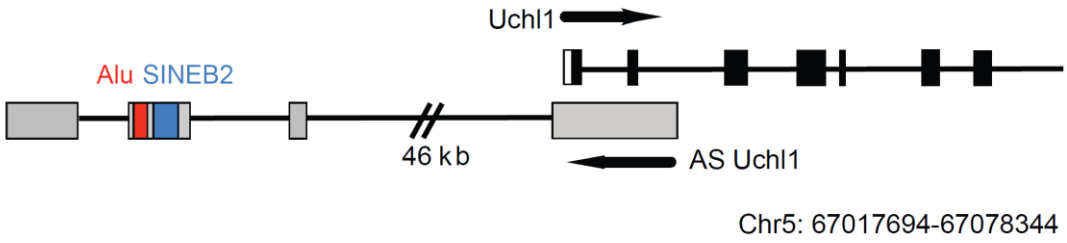

Figure 16. Uchl1/AS Uchl1 genomic organization. Uchl1 exons are in black; 3' and 5'UTRs are in white; AS Uchl1 exons are in grey; repetitive elements are in red (Alu) and blue (SINEB2); introns are indicated as lines.

To elucidate the expression pattern of Uchl1 sense/antisense (S/AS) pair several neuronal cell lines, a panel of mouse adult tissues and macroscopically dissected brain regions were analyzed. AS Uchl1 was expressed in MN9D dopaminergic cells while it was absent in non dopaminergic cell lines. In the mouse adult brain AS Uchl1 expression was restricted to the ventral midbrain and cortex. In particular AS Uchl1 was enriched in dopaminergic cells, where the two transcripts were localized in different subcellular compartments: mature Uchl1 mRNA was mainly present in the cytoplasm, while AS Uchl1 was enriched in the nucleus.

Moreover AS Uchl1 and Uchl1 were downregulated in neurochemical models of PD as expected from the literature on PD *post-mortem* brains which reported Uchl1 protein downregulation and inactivation.

Transient overexpression of antisense Uchl1 in MN9D cells caused no significant change in endogenous Uchl1 mRNA expression. Notably, a strong and reproducible upregulation of Uchl1 protein was detected suggesting that AS Uchl1 regulates UCHL1 expression at a post-transcriptional level (**Fig. 17**).

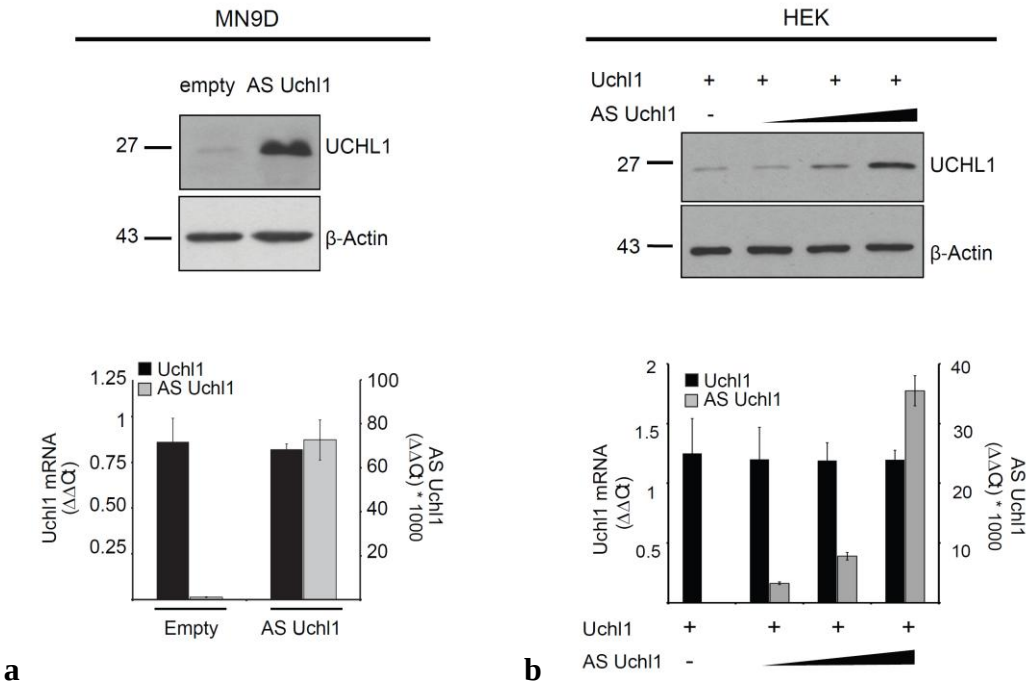

Figure 17. AS Uchl1 regulates Uchl1 translation. a, AS Uchl1-transfected dopaminergic MN9D cells show increased levels of endogenous Uchl1 protein relative to empty vector control, with unchanged mRNA quantity. **b**, Increasing doses of transfected AS Uchl1 titrate quantity of translated Uchl1 protein in HEK 293T cells. No changes in Uchl1 mRNA levels are detected. Data in **a** and **b** indicate mean ± s.d., $n \geq 3$.

To identify sequences and/or structural elements of AS Uchl1 mRNA that elicit its functional activity on Uchl1 protein, deletion mutants were produced and tested in MN9D cells as well as in co-transfection in HEK cells. Δ5' AS Uchl1 lacked the first exon cointaining the 5'sequence overlapping Uchl1, while Δ3' AS Uchl1 did not contain the last three exons of the antisense transcript (**Fig. 18a**). Neither the Δ3' nor the Δ5' transcripts were able to upregulate endogenous Uchl1 protein levels in dopaminergic MN9D (**Fig. 18b**) and in cotransfection in HEK cells (**Fig. 18c**). Titration of the endogenous level of Uchl1 in transfected MN9D cells was evaluated with qRT-PCR, and no significant change in its mRNA expression was noticed. These results suggest that both 5' and 3' components are required for AS Uchl1 function.

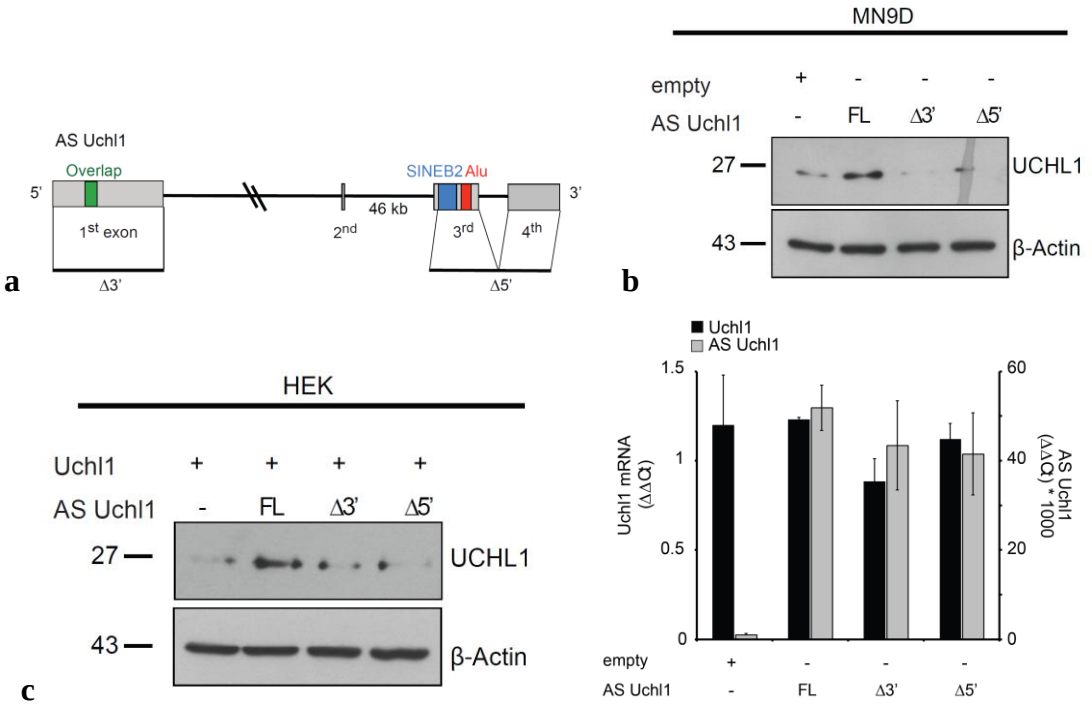

Figure 18. Full length AS Uchl1 is required for UCHL1 upregulation. a, Scheme of Δ5' or Δ3' deletion mutants is shown. **b**, Full-length (FL) AS Uchl1 is required for regulating endogenous UCHL1 level in MN9D cells; units for numbers along the left of gels indicate kDa. **c**, FL AS Uchl1 is required for regulating overexpressed UCHL1 level in HEK cells (left panel); units for numbers along the left of gels indicate kDa. qRT-PCR (right panel) from MN9D cells transfected with Δ5' and Δ3' AS Uchl1 mutants; relative abundance of endogenous Uchl1 mRNA and overexpressed deletion mutants are shown. Data indicate mean ± s.d., n ≥ 3.

Among several stressors that have been implicated in PD pathogenesis inhibition of mTOR by rapamycin treatment of MN9D cells induced an increase in UCHL1 levels similar to the overexpression of AS Uchl1. Rapamycin treatment did not affect Uchl1 mRNA level and the stability of its protein (**Fig. 19**). At a subcellular analysis rapamycin substantially induced AS Uchl1 shuffle to the cytoplasm. This redistribution was confirmed by a concomitant decrease in its nuclear steady-state levels, and by the absence of any *de novo* transcription (**Fig. 19**). Uchl1 mRNA showed no change in subcellular distribution, *de novo* transcription or total cellular content (**Fig. 19**), suggesting that AS Uchl1 localization can be regulated by the mTOR pathway, and its cytoplasmic level correlates with the expression of Uchl1 protein.

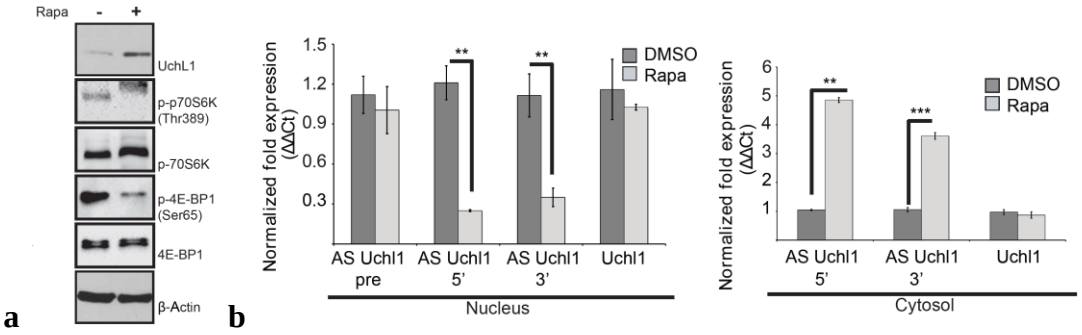

Figure 19. Rapamycin induction of Uchl1 protein and AS Uchl1 shuffling. a, Uchl1 protein level is increased in rapamycin-treated MN9D cells. Rapamycin inhibition of mTOR pathway is verified with anti-p-p70S6K and anti-p-4E-BP1 antibodies. **b**, AS Uchl1 translocates from the nucleus (left) to the cytoplasm (right) upon rapamycin treatment in MN9D cells. mRNA levels were measured by qRT-PCR with 5' or 3' primers. Data indicate mean ± s.d., n ≥ 3. **p < 0.01; ***p < 0.005.

Furthermore, a causal link between rapamycin induction of Uchl1 protein and AS Uchl1 expression was proved through silencing of AS Uchl1 expression in MN9D cells, indicating that AS Uchl1 mediates rapamycin-induced Uchl1 protein upregulation (**Fig. 20**).

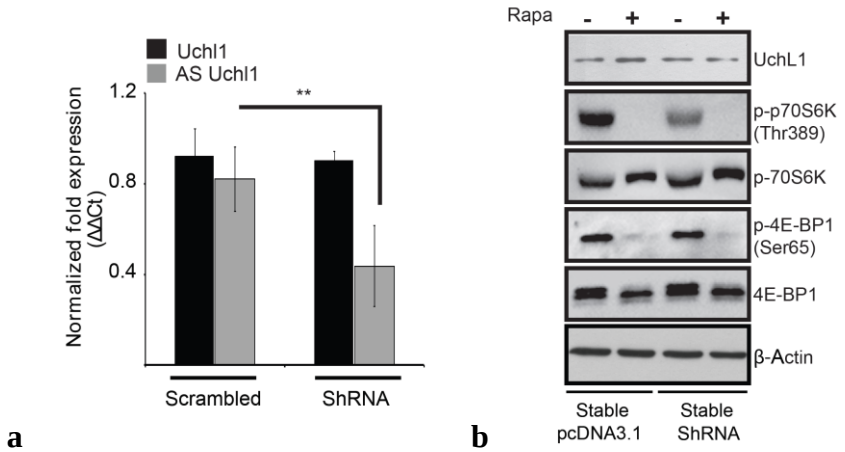

Figure 20. AS Uchl1 is required for rapamycin-induction of Uchl1 protein. a, Silencing AS Uchl1 transcription (shRNA) in MN9D cells does not affect Uchl1 mRNA levels. Data indicate mean ± s.d., n≥ 3. **p < 0.01; ***p < 0.005. **b**, Uchl1 protein level is increased in rapamycin-treated MN9D cells but not in AS Uchl1-silenced MN9D cells. Rapamycin inhibition of mTOR pathway is verified with anti-p-p70S6K and anti-p-4E-BP1 antibodies.

RESULTS

Analysis of Polysome Association upon Rapamycin Treatment.

Association of Uchl1 mRNA to polysomes was then monitored upon rapamycin treatment to assess the role of translation in Uchl1 protein induction. MN9D cells were treated with Rapamycin 1μg/ml for 45' and with vehicle DMSO as control. Cytoplasmic extracts were prepared and fractionated through sucrose gradients. Nine fractions were collected from each gradient while recording the absorbance profile. Distribution of specific transcripts was assayed with qRT-PCR. Uchl1 mRNA was found increased in fraction 8 upon rapamycin treatment, showing an enhanced polysome association (**Fig. 21**). mRNA of β-actin show a pattern similar for DMSO and rapamycin treated cells since no variation of polysomal association can be observed in the different growth conditions (**Fig. 21**).

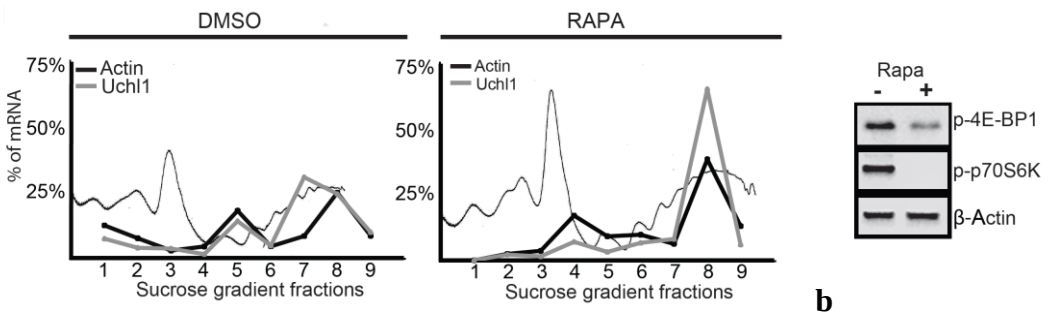

Figure 21. Uchl1 associated with polysomal fractions upon rapamycin treatment. a, qRT-PCR for Uchl1, and β-Actin was performed on RNA extracted from 9 sucrose gradient fractions of MN9D cells treated with rapamycin or vehicle alone (DMSO), as indicated. Association with each fraction is shown as percentage of total mRNA. Absorbance profile is outlined in the background of each plot. **b**, Inhibition of mTOR was verified with anti-p-p70S6K (Thr389) and anti-p-4E-BP1 (Ser65) antibodies.

The association of Uchl1 mRNA with polysomes was then monitored by northern blotting. MN9D cells were treated with rapamycin 1μg/ml for 45' and with vehicle DMSO as control. Cytoplasmic extracts were prepared and fractionated through sucrose gradients. Nine fractions were collected from each gradient while recording the absorbance profile. The purified RNA was blotted and Uchl1 mRNA was detected by radiolabelled RNA probe generated through *in vitro* transcription of the distal 600 bps of Uchl1 transcript. In basal conditions, Uchl1 mRNA was associated with translating ribosomes. Rapamycin treatment induced a significant shift of Uchl1

mRNA to heavier polysomes (**Fig. 22**), consistent with an enhanced rate of translation initiation; this increase of Uchl1 mRNA association to heavier polysomes did not occur in control cells. The analysis of the whole polysomal profile showed a clear shift of Uchl1 mRNA toward the heaviest fraction upon rapamycin treatment, confirming the redistribution previously detected by qRT-PCR (**Fig. 22**).

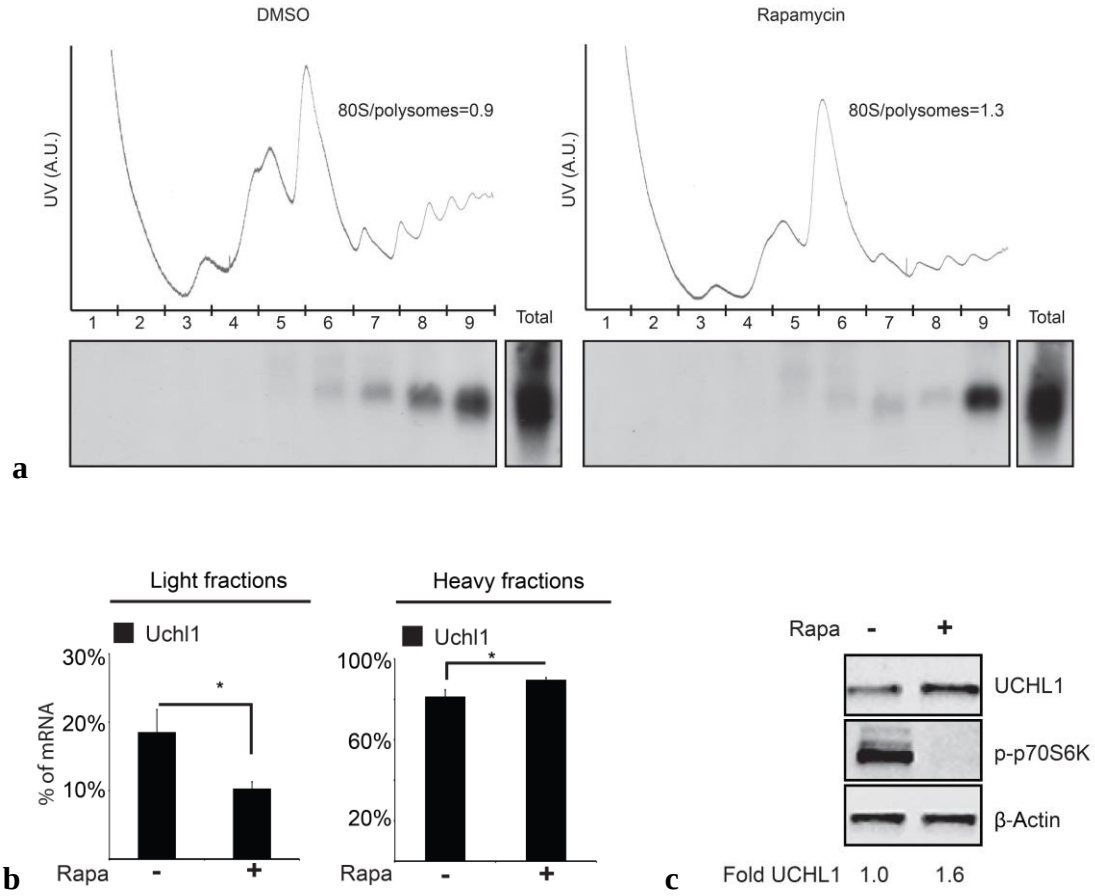

Figure 22. Uchl1 mRNA increases association to heavy polysomes upon rapamycin treatment of MN9D cells. a, RNA purified from 9 sucrose gradient fractions was used for Northern Blot analysis with radioactive riboprobes for Uchl1 mRNA. **b**, Quantification of Uchl1 mRNA signals is obtained by the addition of the fractions corresponding to the light subpolysomal mRNPs and the heavy polysomes from three replica. Data indicate mean ± s.d. *p < 0.05. **c**, Total protein lysates from the same cell preparation were analyzed for the level of expression of UCHL1 and β-Actin; inhibition of mTOR was verified with anti-p-p70S6K (Thr389) antibody.

AS Uchl1 Causes Uchl1 Protein Upregulation in an Embedded SINEB2-Dependent Fashion.

Repeatmasker analysis of AS Uchl1 revealed the presence of two embedded repetitive sequences, SINEB2 and Alu, within the 3' half of the transcript. Therefore, additional deletion mutants were synthesized to assess the role of these embedded repetitive elements in Uchl1 protein upregulation: the ΔSINEB2+Alu (ΔAS) (764-1045), the ΔSINEB2 (ΔS) (764-934) and the ΔAlu (ΔA) (1000-1045). While the ΔAlu mutant showed a comparable effect on Uchl1 protein upregulation as full length AS Uchl1, the ΔSINEB2+Alu and the ΔSINEB2 mutants were unable to do so proving a functional role of the embedded SINEB2 (**Fig. 23**).

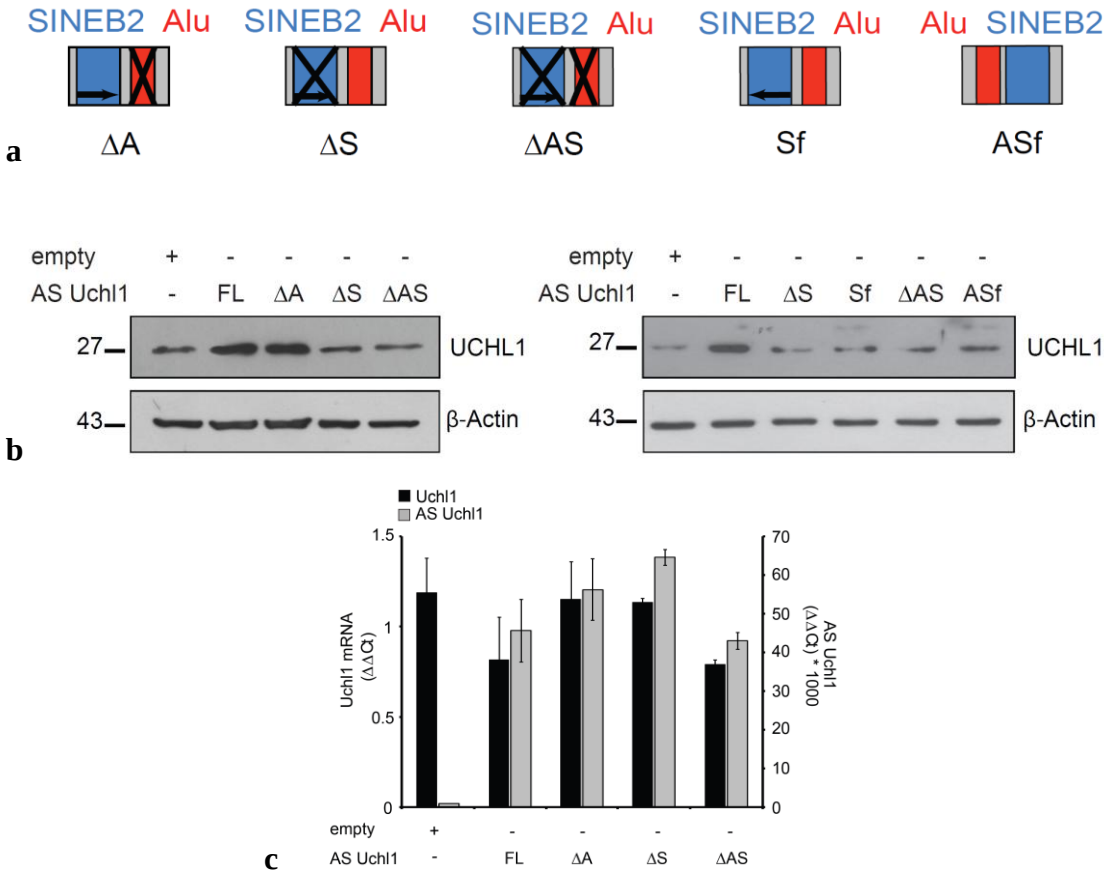

Figure 23. AS Uchl1 regulates Uchl1 translation via embedded SINEB2. a, Scheme of mutants is shown in 5' to 3' orientation. ΔA, ΔAlu; ΔS, ΔSINEB2; ΔAS, ΔAlu1+SINEB2; Sf, SINEB2 flipped; ASf, Alu1+SINEB2 flipped. **b**, Inverted SINEB2 is sufficient to control endogenous UCHL1 levels in MN9D cells. Units for numbers along the left of gels indicate kDa. **c**, Endogenous Uchl1 mRNA levels are not altered by overexpression of AS Uchl1 mutants. In qRT-PCR from MN9D cells transfected with ΔA, ΔS and ΔAS AS Uchl1 mutants relative abundance of endogenous Uchl1 mRNA and over-expressed deletion mutants are shown. Data indicate mean ± s.d., $n \geq 3$.

No change in Uchl1 mRNA level was observed. Since the deletion mutant ΔSINEB2 lacks 170 nucleotides potentially impairing AS Uchl1 RNA secondary structure, a mutant was produced with the SINEB2 sequence flipped in between nucleotide 764-934. Interestingly, SINEB2 flip was unable to increase Uchl1 protein levels in transient transfection thus proving the orientation-dependent activity of the SINEB2 domain (**Fig. 23**). Together, these data indicated that AS Uchl1 function of translation enhancer resided in the SINEB2 sequence embedded in its 3' tail and in its inverted orientation. Furthermore, ΔSINEB2 AS Uchl1 demonstrated to have a negative dominant effect on full length AS Uchl1 endogenously expressed in MN9D cells.

Rapamycin Causes Uchl1 Protein Upregulation in an Embedded SINEB2-Dependent Fashion.

As previously demonstrated in Professor S. Gustincich laboratory, the effects of rapamycin on Uchl1 protein levels were concomitant to AS Uchl1 RNA redistribution from the nucleus to the cytoplasm and UCHL1 induction required the expression of AS Uchl1. As an indipendent model, stable cell lines constitutively expressing ΔSINEB2 AS Uchl1 and empty vector as control were established taking advantage of the dominant negative properties of this deletion construct on the activity of the endogenous full length AS Uchl1 in MN9D cells.

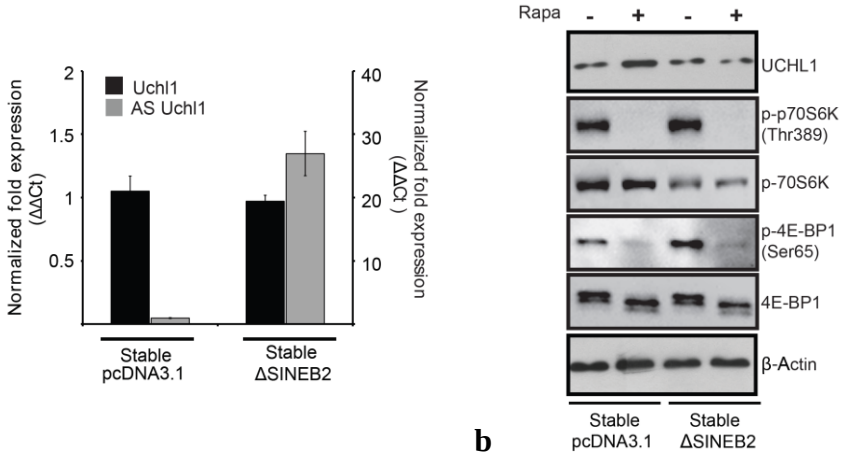

Figure 24. Deletion of embedded SINEB2 in AS Uchl1 inhibits rapamycin-induced Uchl1 protein upregulation. a, Expression of ΔSINEB2 AS Uchl1 does not affect Uchl1 mRNA levels in comparison to pcDNA3.1 control cells. Data indicate mean ± s.d., n ≥ 3. **b,** Deletion of embedded SINEB2 from AS Uchl1 inhibits rapamycin-induced Uchl1 protein upregulation. Inhibition of mTOR was verified with anti-p-p70S6K (Thr389) and anti-p-4E-BP1 (Ser65) antibodies.

MN9D cells were stably transfected with ΔSINEB2 AS Uchl1 and pcDNA3.1 as control and ΔSINEB2 AS Uchl1 was checked by qRT-PCR. Expression of ΔSINEB2 AS Uchl1 does not affect Uchl1 mRNA levels in stably transfected MN9D cells (**Fig. 24**). As expected, when polyclonal stable MN9D cells for empty vector pcDNA3.1 were treated with rapamycin, Uchl1 protein was found increased. In presence of the dominant negative form of ΔSINEB2 AS Uchl1, this upregulation was no longer visible (**Fig. 24**). These results suggested that deletion of embedded SINEB2 from AS Uchl1 is sufficient to inhibit rapamycin-induced Uchl1 protein upregulation.

Taking advantage of MN9D cells stably transfected for ΔSINEB2 AS Uchl1 we analyzed the polysomal association of Uchl1 mRNA upon rapamycin treatment to further assess if translation of Uchl1 mRNA was affected by the deletion of embedded SINEB2 of AS Uchl1.

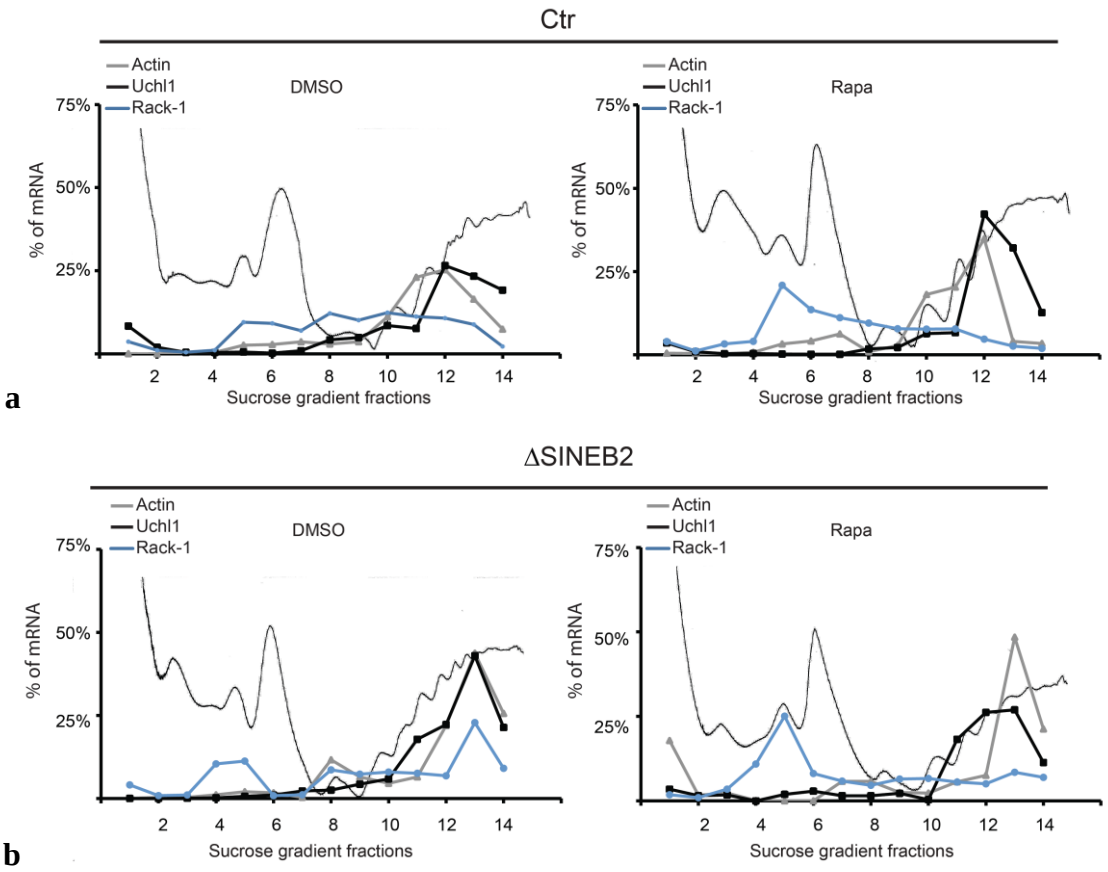

Figure 25. Uchl1 mRNA association to heavy polysomes depends on a functional AS Uchl1. qRT-PCR for **a**, control pcDNA3.1 stable MN9D cells (Ctr) and **b**, mutant ΔSINEB2 AS Uchl1 stable MN9D cells treated with rapamycin or vehicle alone (DMSO) was performed on RNAs purified from 14 sucrose gradient fractions. Association with each fraction is shown as linear plot of the percentage of total RNA; the plot is superimposed on the absorbance profile of the gradient.

MN9D cells were treated with rapamycin 1μg/ml for 45' and with vehicle DMSO as control. Cytoplasmic extracts were prepared and fractionated through sucrose gradients. Fourteen fractions were collected from each gradient while recording the absorbance profile. Distribution of specific transcripts was assayed with qRT-PCR. Uchl1 mRNA was found increased in fraction 12 of 1.54 fold upon rapamycin treatment, showing an enhanced polysome association in control pcDNA3.1 stable MN9D cells (**Fig. 25**). mRNAs of β-Actin show a pattern similar for DMSO and rapamycin treated cells since no variation of polysomal association can be observed in the different growth conditions (**Fig. 25**). This increase of Uchl1 mRNA association to heavier polysomes upon rapamycin treatment did not occur in cells overexpressing the dominant-negative form of antisense Uchl1 (**Fig. 25**). Rack1 transcript distribution was also studied as representative of TOP mRNAs which translation is specifically suppressed by rapamycin (Jefferies et al., 1997). As expected, Rack-1 mRNA was mostly associated with polysomes in growing cells (DMSO), but shifted to subpolysomal particles after rapamycin treatment (**Fig. 25**).

AS Uchl1 Identifies a New Functional Class of Long Noncoding Antisense RNAs. The collection of FANTOM3 non-coding cDNAs was bioinformatically screened for clones representing natural antisense transcript 5' head to head overlapping to protein coding genes. This list was subsequently analyzed for the presence of embedded SINEB2 of the B3 types in reverse complement orientation in the 3' half of AS RNA. 31 transcripts and S/AS pairs were thus identified (**Table 2**).

Riken Acc.	*AS to gene*	*NCBI Acc.*	*Orientation*	*Type*
AK019925	Ccdc44	NM_027346	RC	SINE/B2 #B3
AK029359	Uxt	NM_013840	RC	SINE/B2 #B3
AK032194	Nars2	NM_153591	RC	SINE/B2 #B3
AK032215	Nudt9	NM_028794	RC	SINE/B2 #B3
AK034331	n/a	NM_001012311	RC	SINE/B2 #B3
AK035015	Nrm	NM_134122	RC	SINE/B2 #B3
AK035406	Sv2b	NM_153579	RC	SINE/B2 #B3
AK041236	Ccdc88a	NM_176841	RC	SINE/B2 #B3
AK041654	Rcc	NM_133878	RC	SINE/B2 #B3
AK041742	Abhd11	NM_145215	RC	SINE/B2 #B3
AK042861	Wfdc5	NM_145369	RC	SINE/B2 #B3
AK044205	Rhod	NM_007485	RC	SINE/B2 #B3
AK045677	Eln	NM_007925	RC	SINE/B2 #B3
AK046828	n/a	NM_177006	RC	SINE/B2 #B3
AK047213	Uhmk1	NM_010633	RC	SINE/B2 #B3
AK048309	Epb4.9	NM_013514	RC	SINE/B2 #B3
AK053130	Rabgap1l	NM_001038621	RC	SINE/B2 #B3
AK054076	Gadd45a	NM_007836	RC	SINE/B2 #B3
AK078161	Nck1	NM_010878	RC	SINE/B2 #B3
AK078321	Uchl1	NM_011670	RC	SINE/B2 #B3
AK080749	Pgls	NM_025396	RC	SINE/B2 #B3
AK090347	3110005G23Rik	NM_028427	RC	SINE/B2 #B3
AK132441	A130022J15Rik	NM_175313	RC	SINE/B2 #B3
AK135599	Ednra	NM_010332	RC	SINE/B2 #B3
AK143014	Cdkn2aip	NM_172407	RC	SINE/B2 #B3
AK143784	Txnip	NM_001009935	RC	SINE/B2 #B3
AK145079	Gsk3b	NM_019827	RC	SINE/B2 #B3
AK149843	Cmtm6	NM_026036	RC	SINE/B2 #B3
AK163105	E4f1	NM_007893	RC	SINE/B2 #B3
AK165234	Dtx3	NM_030714	RC	SINE/B2 #B3
AK169421	n/a	NM_001110101	RC	SINE/B2 #B3

Table 2. Family of FANTOM3 non-coding RNA clones that are antisense to protein coding genes and contain embedded SINEB2 in inverted orientation. In red, S/AS pairs tested.

On the bases of the expression of their protein coding mRNA counterpart in MN9D dopaminergic cells (Biagioli et al., 2009), an antisense RNA (Rik4833404H03 – GeneBank AK029359.1) to the Ubiquitously eXpressed Transcript (Uxt, NM_013840) was then chosen (**Fig. 26**) and tested for its ability to induce upregulation of the sense protein coding overlapping gene. Transfection of antisense Uxt (AS Uxt) in MN9D dopaminergic cell shows transient upregulation of Uxt protein product with no change in the total mRNA levels (**Fig. 26**) indicating that AS Uxt was able to increase protein levels post-transcriptionally likewise AS Uchl1.

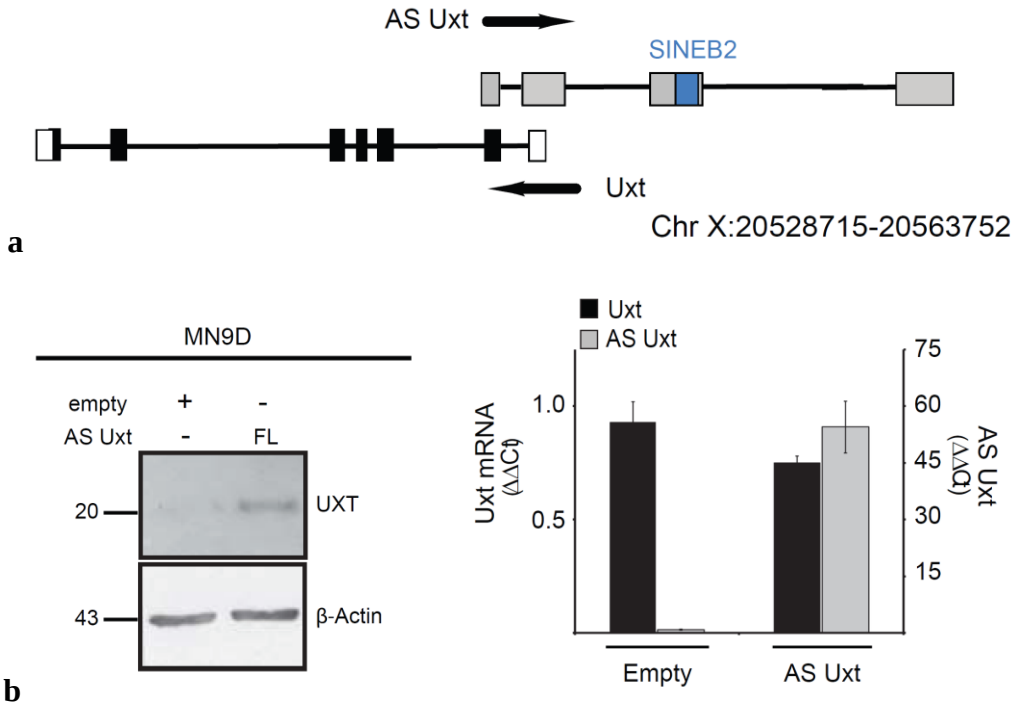

Figure 26. Natural antisense lncRNAs increases target protein level. a, Scheme of Uxt/antisense Uxt genomic organization. **b**, Antisense Uxt increases endogenous UXT protein levels (left; units for numbers along the left of gels indicate kDa) without affecting RNA levels (right) in transfected MN9D cells. Data indicate mean ± s.d., n ≥ 3.

Synthetic Antisense lncRNAs Increase Target Protein Levels.

With the series of deletion mutants so far tested two likely functional domains were identified in AS Uchl1 transcript: the 5'end region overlapping Uchl1 mRNA and the inverted SINEB2 sequence along the 3' tail. In order to take advantage of the enhancement of translation due to the SINEB2 repeat but driven by the 5' overlapping region we obtained an artificial construct subcloning the 73 bp overlapping (OL) sequence to Uchl1 mRNA immediately close to the repetitive elements in Δ5' AS Uchl1 which lacks the first exon of full length AS Uchl1 and therefore the overlap to its sense RNA. This shorter version of AS Uchl1 was named AS Uchl1-73bp (**Fig. 27**). Nevertheless the lacking of more than 300 bp from the first exon of AS Uchl1, AS Uchl1-73bp increased UCHL1 levels as much as the full-length clone (**Fig. 27**).

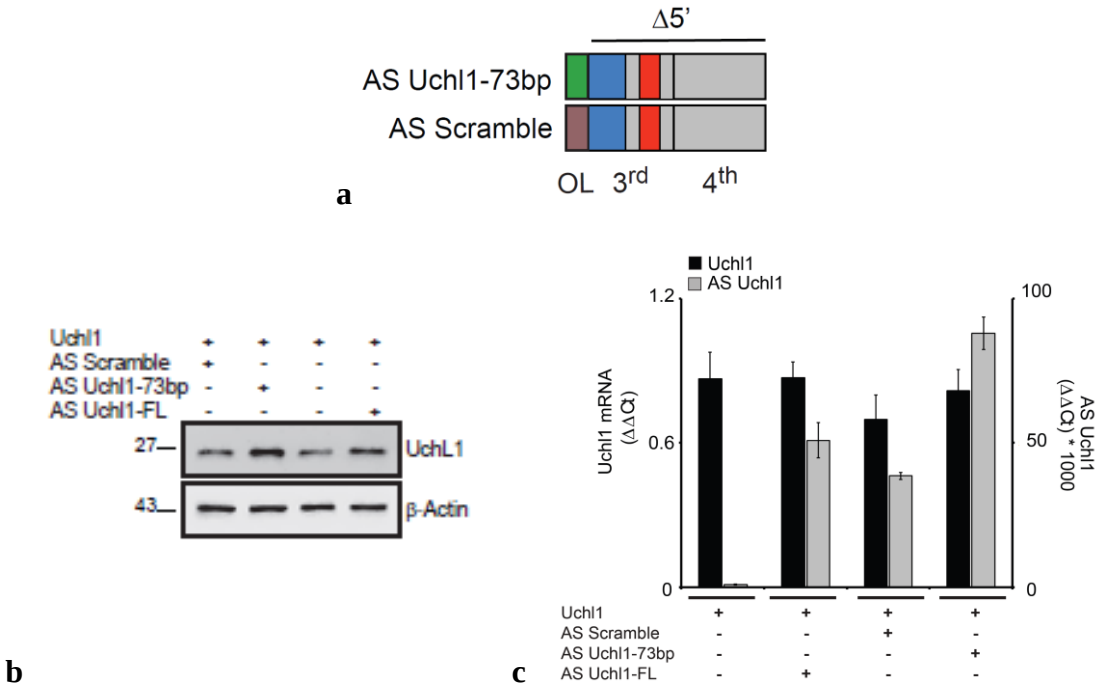

Figure 27. Synthetic short AS Uchl1 is able to increase UCHL1. a, Scheme of mutant and scramble control in 5' to 3' orientation. **b**, A 73 bp overlap (OL) of AS Uchl1 is sufficient to increase UCHL1 in transfected HEK cells. Units for numbers along the left of gels indicate kDa. **c**, qRT-PCR from transfected HEK cells with AS Uchl1-73bp. Relative abundance of endogenous Uchl1 mRNA and over-expressed deletion mutants are shown. Antisense scramble (AS SCR) and full length AS Uchl1 (FL) were used as negative and positive controls, respectively. Data indicate mean ± s.d., n ≥ 3.

Of the two functional domains identified in AS Uchl1 the SINEB2 repetitive element conferred the protein synthesis activation domain whereas the 5' region likely provided the specificity for the sense target gene. To further investigate the combined activity of an OL region and the SINEB2 sequence from AS Uchl1 a chimerical AS RNA was obtained by swapping the 5'end OL with a sequence antisense to an mRNA of choice. We thus synthesized a 72 nucleotide-long artificial sequence antisense to the AUG-containing region as transcribed from pEGFP, and inserted it into Δ5' AS Uchl1 to generate antisense GFP (AS GFP) (**Fig. 28a**).

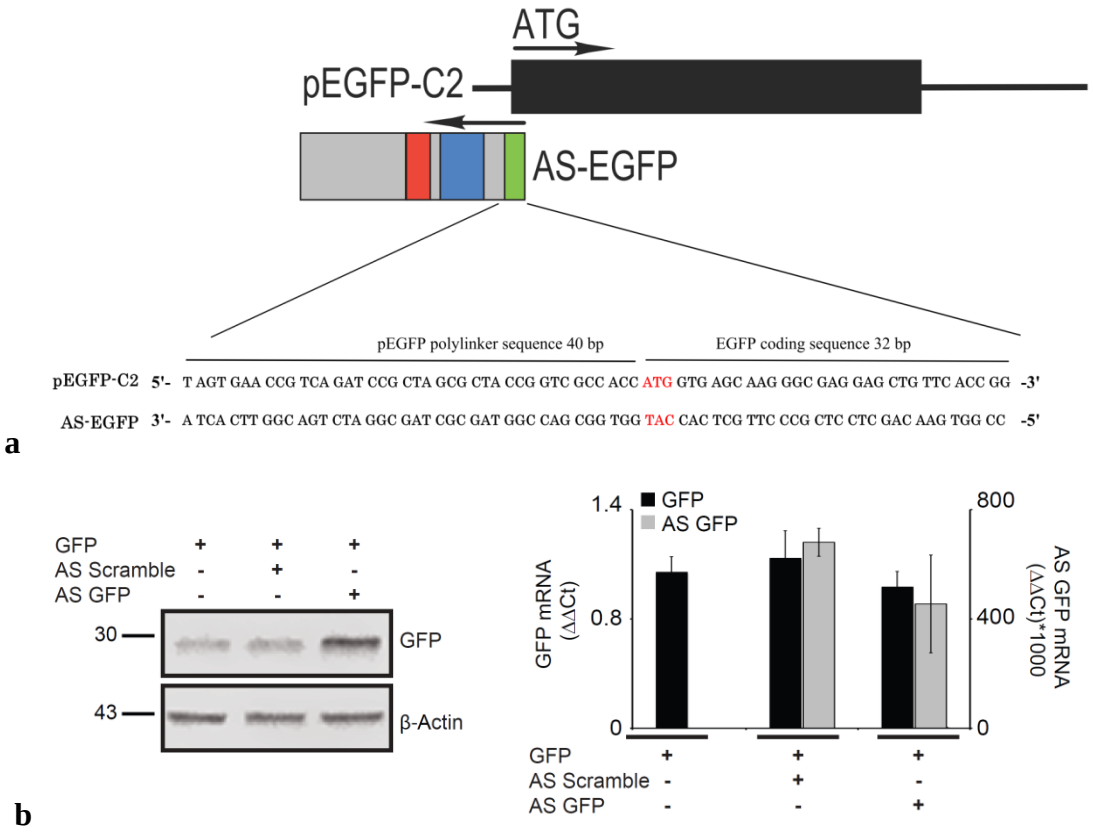

Figure 28. Synthetic antisense lncRNA increases target protein levels. a, Scheme of antisense GFP construct. Δ5'AS Uchl1 with repetitive elements (SINEB2, blue; Alu, red) and overlap (green) regions are indicated. **b**, Inverted SINEB2 plus the overlap sequence increase GFP levels in transfected HEK cells (left, units for numbers along the left of gels indicate kDa) without affecting its transcription (right). Data indicate mean ± s.d., n ≥ 3.

Co-transfection of AS GFP with pEGFP strongly increased GFP protein but not GFP mRNA levels in HEK cells (**Fig. 28b**). Moreover when we pulsed cells with radioactive methionine and immunoprecipitated GFP, AS GFP expression induced an increase in radioactively labelled, neo-synthesized GFP, without affecting mRNA levels (**Fig. 29**). Taken together, these results demonstrated that the antisense RNA enhancement of translation was redirected through the replacement of its 5' overlapping region.

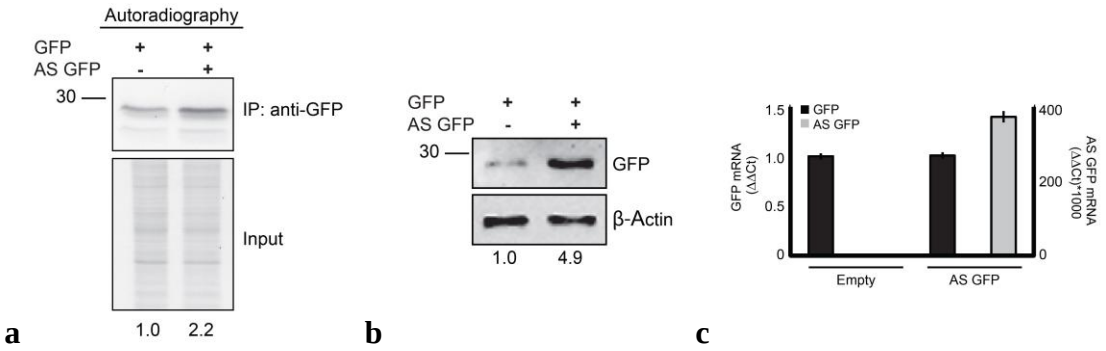

Figure 29. AS GFP enhances GFP *de novo* synthesis. HEK cells were transfected with pEGFP plasmid and control vector (-) or AS GFP; 24 hours after transfection cells were pulse-labeled with [^{35}S]-Methionine/Cysteine for 1 hour. Labeled cells were lysed and immunoprecipitated with anti-GFP antibody. An aliquote of protein extract was used to monitor inputs. **a**, Autoradiography of IP and input. Bands of translated GFP were quantified relative to inputs. **b**, Expression of transfected constructs was analyzed in the same cells by western blotting to detect GFP protein (β-Actin served as a loading control, units for numbers along the left of gels indicate kDa). **c**, qRT-PCR to detect GFP and AS GFP transcripts. Expression was normalized to β-Actin and mRNA levels in cells transfected with GFP plus empty vector was set to 1.

Uncoupled *In Vitro* Transcription and Translation for GFP S/AS Pair.

In order to develop a high-throughput assay to test more chimerical AS RNAs we set up an uncoupled *in vitro* transcription and translation procedure taking advantage of commercially available lysates and extracts. Clones for GFP, AS GFP, and AS SCR as negative control were linearized at the 3'end of vector multiple cloning site and *in vitro* transcribed by T7 RNA polymerase. After DNase treatment RNAs were purified, quantified, and loaded onto denaturing formaldehyde agarose gel (**Fig. 30**). Different quantities and combinations of sense (S) and antisense (AS) RNAs were then added directly to translation-competent lysates. After the *in vitro* translation reaction samples were analyzed by western blotting with antibody against GFP. All lysates were tested for competence of GFP translation alone (**Fig. 30**). The wheat germ system proved to be the most efficient lysate since as few as 5 µl of extract were sufficient for producing GFP protein at detectable levels.

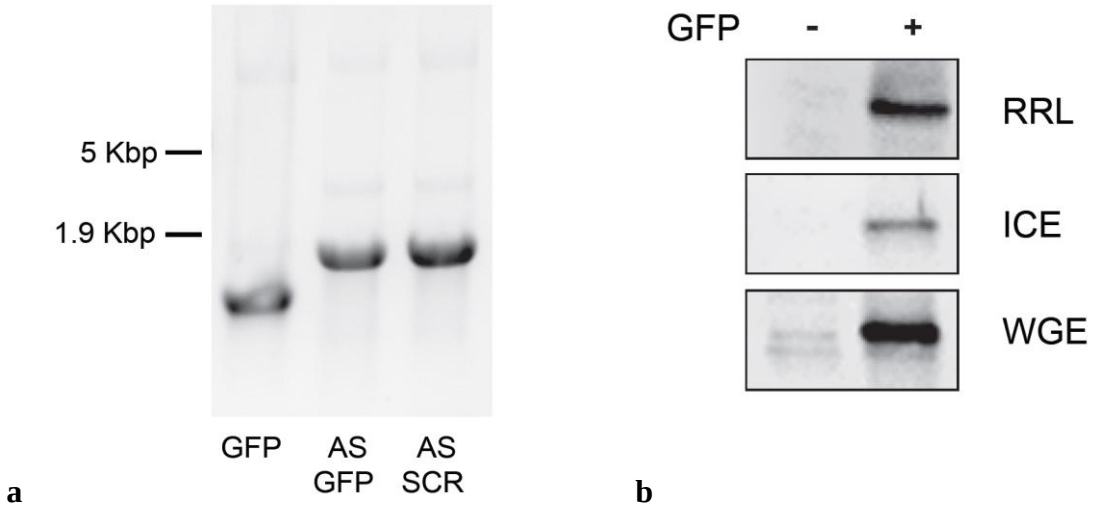

Figure 30. Control of uncoupled *in vitro* transcription and translation assay. a, *In vitro* transcribed RNAs loaded onto denaturing formaldehyde 1% agarose gel; expected size for GFP transcript is 0.75 Kbp and 1.2 Kbp for AS GFP and AS SCR. **b**, Lysates for *in vitro* translation are tested for GFP translation, Rabbit Reticulocyte Lysate (RRL), Insect Cell Extract (ICE), Wheat Germ Extract (WGE).

15 µl of rabbit reticulocyte lysate were used in every *in vitro* translation reaction. To test the assay several quantities of sense GFP RNA were tested together with increasing quantities of antisense GFP RNA. The highest GFP protein induction was achieved with S/AS RNA ratio of 1:3. In rabbit reticulocyte system we detected an average enhancement of GFP translation of 1.7 fold ($n \geq 10$) when AS GFP RNA was added to GFP mRNA (**Fig. 31**). For insect cell extract the reactions were also performed with 15 µl of lysate. Keeping the S/AS RNA ratio to 1:3 we obtained an average induction of GFP protein translation of 1.7 fold ($n \geq 3$) when AS GFP RNA was added together with GFP mRNA (**Fig. 31**). Performing the same experiment in wheat germ extract we reported an induction of GFP protein production of 2.1 fold ($n \geq 8$) in presence of AS GFP RNA (**Fig. 31**). These data indicated that the mechanism underneath AS GFP translation enhancement is evolutionary conserved in three very different organisms, such as rabbit, insect and wheat.

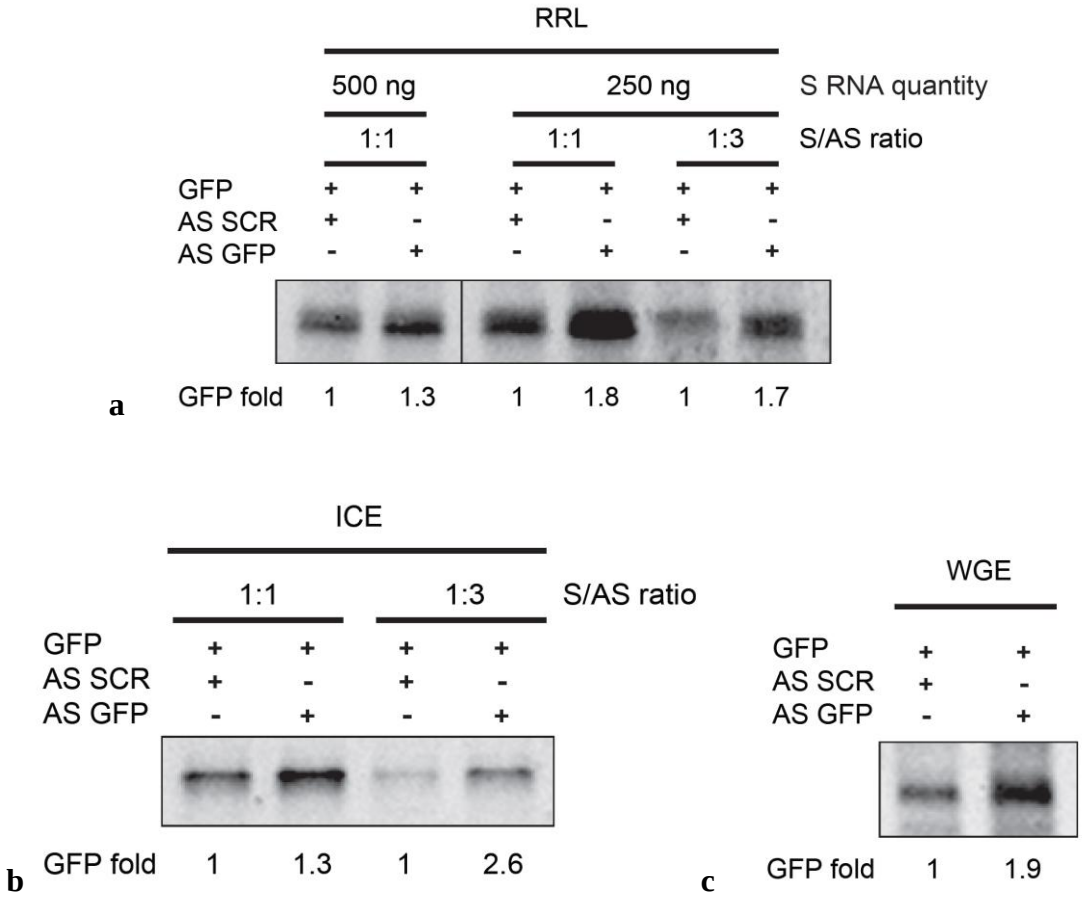

Figure 31. *In vitro* translation of GFP S/AS pair in different lysates. a, *In vitro* translation in rabbit reticulocyte lysate with two quantities of S RNA and two S/AS RNA ratios for one of them. **b**, *In vitro* translation in insect cell extract with two S/AS RNA ratios. **c**, Example of *in vitro* translation in wheat germ extract with S/AS RNA ratio of 1:3. For **a**, **b**, and **c** GFP was quantified by ImageJ and AS SCR control samples were set to 1.

DISCUSSION

Initially classified as "transcriptional noise" long noncoding RNAs (lncRNAs) are today defined as RNA genes able to orchestrate genetic regulatory outputs (Rinn and Chang, 2012). The renewed interest in RNA biology is particularly focused on the central nervous system where neural cells are highly transcriptionally active and exhibit robust expression of lncRNAs (Gustincich et al., 2006). In fact, in the central nervous system lncRNAs show precise patterns of expression in terms of time and regional, cellular, or subcellular localization and these dynamics mediate several nervous system processes and neurological disease states.

In the broad class of lncRNAs, antisense RNAs (AS RNA) represent a powerful subclass for one main reason: AS RNAs contain both the information necessary for target recognition, which is the overlapping sequence with protein coding transcript, and additional analogical or digital features for interaction with RNA binding proteins and/or co-factors. AS RNAs can thus be the perfect candidate for post-transcriptional regulation of gene expression.

Here we report a novel function for a SINEB2 repeat embedded in an antisense lncRNAs AS Uchl1, specifically expressed and enriched in the nucleus of mouse dopaminergic cells. AS Uchl1 is involved in the post-transcriptional control of gene expression of its sense mRNA Uchl1 through the SINEB2 repetitive element embedded in its sequence. Furthermore, we showed how this natural antisense noncoding transcript was successfully modified to obtain a chimerical lncRNA antisense to GFP. In conclusion we proposed an *in vitro* translation assay as possible high throughput screening for future artificial AS lncRNAs as inducer of translation.

AS Uchl1 as Stress-Responding LncRNA.

Previous experiments indicated that AS Uchl1 overexpression was able to drive Uchl1 protein upregulation with a post-transcriptional mechanism. Moreover, rapamycin treatment of mouse dopaminergic cells induced a similar upregulation of Uchl1 protein only in the presence of AS Uchl1 shuffling from nucleus to cytoplasm. These findings are consistent with the idea that acute stress response does not increase production of new transcripts, but affects the post-transcriptional regulation of previously synthesized mRNAs that already compose the cytoplasmic cohort. To further investigate the effect of cytoplasmic AS Uchl1 on Uchl1 translation we analyzed the polysomal profile of rapamycin-treated cells by two different technical

approaches, qRT-PCR and northern blotting. Both experiments showed an increased association of Uchl1 mRNA to heavy polysomes upon rapamycin treatment and confirmed the involvement of protein translation in AS Uchl1 function.

Rapamycin impairs Cap-dependent initiation of translation by blocking mTORC1 kinase. The same arrest occurs upon stress, when Cap-dependent translation of most proteins is greatly reduced and the expression of a small group of proteins, such as heat shock and pro-survival proteins, is enhanced. How the translation of certain mRNAs is temporarily halted and simultaneously increased for another subset of proteins is still not clear. Proposed mechanisms take into account two well known viral strategies, Internal Ribosome Entry Site or IRES (Jang et al., 1988; Pelletier et al., 1988) and ribosome shunting (Fütterer et al., 1993). Both strategies overcome host translation through the direct translocation of the ribosome from the upstream initiation complex to the start codon without the need for eIF4A helices activity to unwind RNA secondary structures. Indeed, IRES-mediated translation is prominent in conditions of stress, for instance Endoplasmic Reticulum (ER) stress, hypoxia, nutrient limitation, mitosis and cell differentiation (Komar and Hatzoglou, 2011).

In *D. melanogaster* models of PD rapamycin suppressed the pathological phenotype by promoting the activation of 4E-BP (Tain et al., 2009). In mice rapamycin shows both *in vitro* and *in vivo* protection for dopaminergic neurons upon neurochemical intoxication (Malagelada et al., 2010) and alleviates L-DOPA induced diskynesia in humans (Santini et al., 2009). The protective effect exerted by rapamycin on neurons has been explained by both induction of autophagy (Sarkar et al., 2009; Dehay et al., 2010) and suppression of RTP801 translation (Malagelada et al., 2006).

According to our data after rapamycin treatment of mouse dopaminergic cells AS Uchl1 re-localize into the cytoplasm and rescues Uchl1 from occurring block of translation. Moreover, the expression of full length AS Uchl1 is required for rapamycin-induction of UCHL1. In particular, the inverted SINEB2 element embedded in AS Uchl1 transcript has a crucial role in this stress-induced response.

Interestingly, Uchl1 is a pro-survival protein for neurons and for this reason the manipulation of its expression has been proposed for intervention in neurodegenerative diseases, including PD and AD. We propose that the antisense-driven elevation of Uchl1 protein in dopaminergic cells occurring upon rapamycin might be an additional molecular event to explain the neuroprotective property of this drug.

A New Class of LncRNAs.

The mechanism proposed for AS Uchl1 suggests the intriguing hypothesis that it might exist a pool of cellular nuclear-retained RNAs, normally kept latent in the nucleus, that are ready to respond to acute stimuli by changing their subcellular location. We already know that stress-dependent nuclear-cytoplasm shuttling of lncRNAs seems to be a common strategy to regulate translation since CTN-RNA, another nuclear-retained lncRNA, unveiled a cryptic protein coding sequence at its 3'end when in the cytoplasm (Prasanth et al., 2005). By changing location, RNA molecules can be able to exert their specific function, i.e. for AS Uchl1 using the SINEB2 module to increase protein translation and the 5' overlap to target the sense mRNA. We thus clustered several antisense transcripts that are overlapping 5' head-to-head to RefSeq genes in mouse and have a SINEB2 element in reverse complement within their sequence. From this list we experimentally found that a second antisense RNA (AS Uxt) is able to drive protein upregulation of its protein-coding overlapping partner. These results suggest that AS Uchl1 and AS Uxt may be a representative member of a new functional class of lncRNAs which are part of S/AS pairs in the mammalian genome. They require a 5' end overlap to their sense counterpart and a SINEB2 repeat along their 3' tail. The region at the 5' provides specificity to a protein-coding mRNA partner transcribed from the complementary strand, while the inverted SINEB2 element is required for translational activation.

It will be interesting in the future to capture all the transcripts that contain a reverse complement SINEB2 element via Deep Sequencing of 5'RACE products obtained from SINEB2 internal primer, thus profiling all the cellular pool of non-coding RNAs that can use this SINEB2 module to enhance translation. It is also reasonable that all the ncRNA molecules capable to reprogram translation of cognate protein-coding mRNAs via a SINEB2 module may represent potential pharmacological targets, together with involved protein interactors still to identify.

AS LncRNAs as Therapeutic Tool

Besides the role that ncRNAs have in several biological systems, they have emerged as particularly relevant players in a sophisticated place like the CNS, where the major diversity of ncRNAs is found (Mercer et al., 2008). LncRNAs generally play a role by modulating transcription, post-transcriptional processing, and translation of mRNAs.

In the central nervous system they play additional roles in mediating nervous system development, homeostasis, stress responses and plasticity (Qureshi et al., 2010). Moreover, lncRNAs are involved in the pathophysiology of a spectrum of CNS pathologies including neurodevelopmental, neurodegenerative, neuro-oncological and psychiatric diseases.

LncRNAs are implicated in the pathophysiology of neurodevelopmental disorders associated with genomic imprinting, such as Prader–Willi syndrome (PWS) and Angelman syndrome (AS) (Koerner et al., 2009).

As an example of neurodegenerative disorder, deregulation of lncRNAs has been assessed for AD, where the levels of lncRNA AS BACE1 are correlated with higher BACE1 protein which, in turn, leads to increased production of Aβ peptide (Faghihi et al., 2008). Another study utilized human AD brain tissue to link alterations in levels of lncRNA BC200 with AD pathogenesis. Increased levels of BC200 were found in brain regions that are preferentially affected in AD (Mus et al., 2007).

Moreover lncRNAs are known targets of the master epigenetic regulator REST/NRSF (repressor element-1 silencing transcription factor/neuron-restrictive silencing factor) in both mouse and human (Johnson et al., 2009). Deregulation of REST and CoREST functions is linked to a range of central nervous system pathologies that include cancer (glioblastoma, medulloblastoma, and neuroblastoma), neurodegenerative disease (Huntington's disease), neurodevelopmental disorder (Down syndromeand X-linked mental retardation), epilepsy, and ischemia (Qureshi and Mehler, 2009).

Neurological disorders like epileptogenesis involve BC1/BC200 brain-specific lncRNAs and Evf2, since they modulate neural network plasticity and excitability (Mercer et al., 2008; Qureshi et al., 2010).

In addition to neurological diseases, a number of psychiatric disorders have also been associated with lncRNAs. For example, the disruption of the DISC sense/antisense genomic locus, which encodes both the DISC1 protein-coding gene and the DISC2 lncRNA, has been linked to the risk of developing schizophrenia, schizoaffective

disorder, bipolar disorder, major depression, and autistic spectrum disorders (Chubb et al., 2008; Williams et al., 2009).

The discovery of new noncoding molecules and their function in the brain can constitute a starting point for the development of novel diagnostic and/or therapeutic approaches directed for example, to those lncRNAs whose downregulation or overexpression is aberrant in central nervous system disorders.

Historically, it has been easier to identify drug compounds and research tools that inhibit or downregulate a drug target than to identify agents that are capable of inducing its activation or upregulation. In fact, the majority of currently available drugs exhibit an inhibitory mechanism of action and there is a relative lack of pharmaceutical agents that are capable of increasing the activity of single effectors or pathways. Indeed, the upregulation of many genes, including tumour suppressors, growth factors, transcription factors and genes that are deficient in various genetic diseases would be desired in specific situations. For instance, in the case of neurodegenerative disorders their progression, at least when they are treated relatively early, could conceivably be alleviated by boosting the activities of neuroprotective growth factors.

Current strategies to upregulate specific therapeutic targets include nuclear receptor ligands, chromatin modulators, enzyme replacement, artificial transcription factors, and miRNA modulators. Although these strategies are promising, none of them can afford the upregulation of endogenous genes in a locus-specific manner.

However, by targeting a regulatory ncRNA it may be possible to upregulate an endogenous gene in a natural fashion. This may, for example, be relevant to diseases arising as a result of haploinsufficiency, in which patients have only one functional copy of a given gene owing to mutations, or in cases where both copies are less active than normal. As such, identifying and inhibiting ncRNAs that can regulate the expression of such genes may lead to enhanced activation of at least one functional copy and restoration of the normal cell phenotype.

Finally, a possible advantage of targeting lncRNAs is their relatively low abundance compared to mRNAs. Indeed, if these lncRNAs are transcriptional regulators, a small number of copies may suffice to show efficacy. Therefore, lncRNA inhibitors could potentially be administered at a lower dose than a conventional oligonucleotide used for mRNA knockdown.

Of particular importance is the observation that the inhibition of many antisense transcripts can derepress and therefore elevate levels of the sense transcript partner (known as discordant regulation) or, less often, decrease the expression of the sense transcript (known as concordant regulation) (Wahlestedt, 2006; Faghihi et al., 2010).
In the case of the lncRNA we report here, the antisense noncoding transcript is not a real target for PD therapy but it could be a drug tool itself. In fact, through an increase of AS Uchl1 expression the level of Uchl1 protein could be restored in dopaminergic cells of PD patients. One of the main advantages in upregulating an endogenous gene in a locus-specific manner, as in AS Uchl1 example, is the reduction of off-target effects.
Concerns remain for the delivery of a therapeutic RNA transcript, especially as the central nervous system is involved. Achieving safe and efficient *in vivo* delivery remains a crucial hurdle and several strategies to overcome such hurdles are currently being investigated, including various delivery approaches: for example, the use of viral vectors such as adenoviruses and retroviruses, as well as non-viral vectors such as polyplexes, lipoplexes and peptide- or protein-based systems (Bennett and Swayze, 2010).

Repetitive Elements

Despite the higher number of insertions, repetitive elements are not evenly distributed throughout the genome. For instance, inverted Alu elements in close proximity to each other are less frequently identified in the human genome than Alu insertions in the same orientation (Stenger et al., 2001) and this can only partially be attributed to insertional bias of insertions in the same orientation (Chen et al., 2008). Indeed, inverted repeats likely represent hotspots of genomic instability, as seen in studies with yeast (Lobachev et al., 2000). Inverted Alu elements that are closely spaced appear to build hairpin structures, which can cause Double Strand Breaks (DSBs) of the DNA and excision of inverted Alu elements from the human genome. Moreover, hairpin structures involving Alu elements appear to cause replication stalling and collapse of the replication fork, which can lead to DSBs and/or intra- or intermolecular template switch (Voineagu et al., 2008).

In this study we report a new function for an inverted SINEB2 element embedded in AS lncRNA transcripts, which also contain a 5' region of overlap to the relative sense mRNA transcript. While the physical interaction between the transcripts of Uchl1 S/AS pair is a speculation for now, the mechanism underlying AS Uchl1 enhancement of Uchl1 translation is still unknown. Deletion mutants affecting internal domains of the SINEB2 element, such as the A and B boxes of the internal promoter for RNA pol III, could further restrict the length of the functional domain of AS Uchl1.

The upregulation of Uchl1 protein involves an initial shuffling of AS Uchl1 from nucleus to cytoplasm and a following shift of Uchl1 mRNA to highly translating polysomes. This latter passage depends on the inverted SINEB2 repeat present along AS Uchl1 sequence. Next step in order to get a hint of the implicated cellular pathways would be the identification of proteins interacting with AS Uchl1 and in particular with the SINEB2 sequence.

Even though lncRNAs exhibited poor sequence conservation across species (Taft et al., 2007), RNA structure is arguably more highly conserved than its sequence (Mathews et al., 2010), which indicates that conventional sequence alignment across species may not reveal functionally conserved RNA motifs. SINE elements have a highly conserved secondary structure that derives from the RNA molecule from which they emerged (tRNA for mouse SINEB2 repeats) and is likely conserved when embedded in larger transcripts. The study of the three-dimensional structure of AS Uchl1 SINEB2 element and structure-function analysis could further help to elucidate the physical interactions of this functional domain with cellular proteins.

In Vitro Translation Assay of Artificial AS LncRNAs.

We demonstrated how AS Uchl1 function could be redirect and exploited for inducing the translation of a target protein, such as GFP, in cells through the replacement of its 5' overlapping region. Here, we propose an uncoupled *in vitro* transcription and translation assay as initial screening for functional chimerical AS lncRNAs designed according to AS Uchl1 functional domains and sequence. All three tested commercially available lysates for *in vitro* translation (rabbit reticulocyte

lysate, insect cell extract, and wheat germ) were able to recapitulate the enhancement of protein synthesis driven by AS GFP in cells.

In particular, the wheat germ extract showed the highest efficiency of translation considering the low amount of extract sufficient to produce GFP at detectable levels. Since we are interested in observing a translational upregulation alone, the choice of one lysate over the others is not dictated by the need to eventually produce a functional protein. As far as the enhancement of translation is conserved among lysates which are obtained from different organisms, intrinsic differences in post-translation modifications are not relevant.

Indeed, a lot of questions remain open concerning the mechanism of translation induction of this newly identified class of AS lncRNAs. The identification of the protein interactors to AS Uchl1 transcript and its inverted SINEB2 element could be a valuable starting point for further experimental hypothesis. Then, the generalization of a mechanism of translation enhancement has to take into account the complexity of a cell and adapt to the variety of its proteome.

In conclusion, the *in vitro* translation protocol could be a useful and rapid assay to screen for functional AS GFP deletion mutants, but its technical potential as high throughput screening of AS lncRNAs as enhancer of translation needs further experimental trials.

BIBLIOGRAPHY

Abelson, J.F. (2005). Sequence Variants in SLITRK1 Are Associated with Tourette's Syndrome. Science *310*, 317–320.

Akasaki, T., Nikaido, M., Nishihara, H., Tsuchiya, K., Segawa, S., and Okada, N. (2010). Characterization of a novel SINE superfamily from invertebrates: "Ceph-SINEs" from the genomes of squids and cuttlefish. Gene *454*, 8–19.

Allen, E., Xie, Z., Gustafson, A.M., and Carrington, J.C. (2005). microRNA-Directed Phasing during Trans-Acting siRNA Biogenesis in Plants. Cell *121*, 207–221.

Allen, T.A., Von Kaenel, S., Goodrich, J.A., and Kugel, J.F. (2004). The SINE-encoded mouse B2 RNA represses mRNA transcription in response to heat shock. Nat. Struct. 38 Mol. Biol. *11*, 816–821.

Amaral, P.P., and Mattick, J.S. (2008). Noncoding RNA in development. Mamm. Genome *19*, 454–492.

Aravin, A.A., and Bourc'his, D. (2008). Small RNA guides for de novo DNA methylation in mammalian germ cells. Genes Dev. *22*, 970–975.

Aravin, A., Gaidatzis, D., Pfeffer, S., Lagos-Quintana, M., Landgraf, P., Iovino, N., Morris, P., Brownstein, M.J., Kuramochi-Miyagawa, S., Nakano, T., et al. (2006). A novel class of small RNAs bind to MILI protein in mouse testes. Nature.

Asselbergs, F.A., Meulenberg, E., Venrooij, W.J., and Bloemendal, H. (1980). Preferential Translation of mRNAs in an mRNA-Dependent Reticulocyte Lysate. Eur. J. Biochem. *109*, 159–165.

Barrachina, M., Castaño, E., Dalfó, E., Maes, T., Buesa, C., and Ferrer, I. (2006). Reduced ubiquitin C-terminal hydrolase-1 expression levels in dementia with Lewy bodies. Neurobiol. Dis. *22*, 265–273.

Bartel, D.P. (2004). MicroRNAs: genomics, biogenesis, mechanism, and function. Cell *116*, 281–297.

Bennett, C.F., and Swayze, E.E. (2010). RNA targeting therapeutics: molecular mechanisms of antisense oligonucleotides as a therapeutic platform. Annu. Rev. Pharmacol. Toxicol. *50*, 259–293.

Bentwich, I., Avniel, A., Karov, Y., Aharonov, R., Gilad, S., Barad, O., Barzilai, A., Einat, P., Einav, U., Meiri, E., et al. (2005). Identification of hundreds of conserved and nonconserved human microRNAs. Nat. Genet. *37*, 766–770.

Bernheimer, H., Birkmayer, W., Hornykiewicz, O., Jellinger, K., and Seitelberger, F. (1973). Brain dopamine and the syndromes of Parkinson and Huntington. Clinical, morphological and neurochemical correlations. J. Neurol. Sci. *20*, 415–455.

Bertone, P., Stolc, V., Royce, T.E., Rozowsky, J.S., Urban, A.E., Zhu, X., Rinn, J.L., Tongprasit, W., Samanta, M., Weissman, S., et al. (2004). Global Identification of Human Transcribed Sequences with Genome Tiling Arrays. Science *306*, 2242–2246.

Bhat, R.A., and Thimmappaya, B. (1983). Two small RNAs encoded by Epstein-Barr virus can functionally substitute for the virus-associated RNAs in the lytic growth of adenovirus 5. Proc. Natl. Acad. Sci. *80*, 4789–4793.

Biagioli, M., Pinto, M., Cesselli, D., Zaninello, M., Lazarevic, D., Roncaglia, P., Simone, R., Vlachouli, C., Plessy, C., and Bertin, N. (2009). Unexpected expression of α-and β-globin in mesencephalic dopaminergic neurons and glial cells. Proc. Natl. Acad. Sci. *106*, 15454–15459.

Bonifati, V., Rizzu, P., van Baren, M.J., Schaap, O., Breedveld, G.J., Krieger, E., Dekker, M.C.J., Squitieri, F., Ibanez, P., Joosse, M., et al. (2002). Mutations in the DJ-1 Gene Associated with Autosomal Recessive Early-Onset Parkinsonism. Science *299*, 256–259.

Borodulina, O.R., and Kramerov, D.A. (2008). Transcripts synthesized by RNA polymerase III can be polyadenylated in an AAUAAA-dependent manner. RNA *14*, 1865–1873.

Brennecke, J., Hipfner, D.R., Stark, A., Russell, R.B., and Cohen, S.M. (2003). bantam Encodes a Developmentally Regulated microRNA that Controls Cell Proliferation and Regulates the Proapoptotic Gene hid in Drosophila. Cell *113*, 25–36.

Brennecke, J., Malone, C.D., Aravin, A.A., Sachidanandam, R., Stark, A., and Hannon, G.J. (2008). An epigenetic role for maternally inherited piRNAs in transposon silencing. Science *322*, 1387–1392.

Burks, E.A., Chen, G., Georgiou, G., and Iverson, B.L. (1997). In vitro scanning saturation mutagenesis of an antibody binding pocket. Proc. Natl. Acad. Sci. *94*, 412–417.

Butterfield, D.A., Castegna, A., Lauderback, C.M., and Drake, J. (2002). Evidence that amyloid beta-peptide-induced lipid peroxidation and its sequelae in Alzheimer's disease brain contribute to neuronal death. Neurobiol. Aging *23*, 655–664.

Carrieri, C., Cimatti, L., Biagioli, M., Beugnet, A., Zucchelli, S., Fedele, S., Pesce, E., Ferrer, I., Collavin, L., Santoro, C., et al. (2012). Long non-coding antisense RNA controls Uchl1 translation through an embedded SINEB2 repeat. Nature *491*, 454–457.

Castegna, A., Aksenov, M., Thongboonkerd, V., Klein, J.B., Pierce, W.M., Booze, R., Markesbery, W.R., and Butterfield, D.A. (2002). Proteomic identification of oxidatively modified proteins in Alzheimer's disease brain. Part II: dihydropyrimidinase-related protein 2, α-enolase and heat shock cognate 71. J. Neurochem. *82*, 1524–1532.

Castegna, A., Thongboonkerd, V., Klein, J., Lynn, B.C., Wang, Y.-L., Osaka, H., Wada, K., and Butterfield, D.A. (2004). Proteomic analysis of brain proteins in the gracile axonal dystrophy (gad) mouse, a syndrome that emanates from dysfunctional ubiquitin carboxyl-terminal hydrolase L-1, reveals oxidation of key proteins. J. Neurochem. *88*, 1540–1546.

Chekanova, J.A., Gregory, B.D., Reverdatto, S.V., Chen, H., Kumar, R., Hooker, T., Yazaki, J., Li, P., Skiba, N., Peng, Q., et al. (2007). Genome-Wide High-Resolution Mapping of Exosome Substrates Reveals Hidden Features in the Arabidopsis Transcriptome. Cell *131*, 1340–1353.

Chen, J.-L., and Greider, C.W. (2004). Telomerase RNA structure and function: implications for dyskeratosis congenita. Trends Biochem. Sci. *29*, 183–192.

Chen, J., Sun, M., Kent, W.J., Huang, X., Xie, H., Wang, W., Zhou, G., Shi, R.Z., and Rowley, J.D. (2004). Over 20% of human transcripts might form sense-antisense pairs. Nucleic Acids Res. *32*, 4812–4820.

Chen, L.-L., DeCerbo, J.N., and Carmichael, G.G. (2008). Alu element-mediated gene silencing. EMBO J. *27*, 1694–1705.

Cheng, J., Kapranov, P., Drenkow, J., Dike, S., Brubaker, S., Patel, S., Long, J., Stern, D., Tammana, H., Helt, G., et al. (2005). Transcriptional Maps of 10 Human Chromosomes at 5-Nucleotide Resolution. Science *308*, 1149–1154.

Chiu, Y.-L., Witkowska, H.E., Hall, S.C., Santiago, M., Soros, V.B., Esnault, C., Heidmann, T., and Greene, W.C. (2006). High-molecular-mass APOBEC3G complexes restrict Alu retrotransposition. Proc. Natl. Acad. Sci. *103*, 15588–15593.

Choi, J., Levey, A.I., Weintraub, S.T., Rees, H.D., Gearing, M., Chin, L.-S., and Li, L. (2003). Oxidative Modifications and Down-regulation of Ubiquitin Carboxyl-terminal Hydrolase L1 Associated with Idiopathic Parkinson's and Alzheimer's Diseases. J. Biol. Chem. *279*, 13256–13264.

Chu, W.M., Liu, W.M., and Schmid, C.W. (1995). RNA polymerase III promoter and terminator elements affect Alu RNA expression. Nucleic Acids Res. *23*, 1750–1757.

Chubb, J.E., Bradshaw, N.J., Soares, D.C., Porteous, D.J., and Millar, J.K. (2008). The DISC locus in psychiatric illness. Mol. Psychiatry *13*, 36–64.

Churakov, G., Smit, A.F.A., Brosius, J., and Schmitz, J. (2005). A Novel Abundant Family of Retroposed Elements (DAS-SINEs) in the Nine-Banded Armadillo (Dasypus novemcinctus). Mol. Biol. Evol. *22*, 886–893.

Churakov, G., Sadasivuni, M.K., Rosenbloom, K.R., Huchon, D., Brosius, J., and Schmitz, J. (2010). Rodent Evolution: Back to the Root. Mol. Biol. Evol. *27*, 1315–1326.

Clemens, M. (1987). Translational control. Developments in development. Nature *330*, 699–700.

Clemens, M.J. (2001). Translational regulation in cell stress and apoptosis. Roles of the eIF4E binding proteins. J. Cell. Mol. Med. *5*, 221–239.

Core, L.J., Waterfall, J.J., and Lis, J.T. (2008). Nascent RNA sequencing reveals widespread pausing and divergent initiation at human promoters. Science *322*, 1845–1848.

Croce, C.M., and Calin, G.A. (2005). miRNAs, cancer, and stem cell division. Cell *122*, 6–7.

Dagan, T., Sorek, R., Sharon, E., Ast, G., and Graur, D. (2004). AluGene: a database of Alu elements incorporated within protein-coding genes. Nucleic Acids Res. *32*, 489D–492.

Dahary, D., Elroy-Stein, O., and Sorek, R. (2005). Naturally occurring antisense: Transcriptional leakage or real overlap? Genome Res. *15*, 364–368.

Daniels, G.R., and Deininger, P.L. (1983). A second major class of Alu family repeated DNA sequences in a primate genome. Nucleic Acids Res. *11*, 7595–7610.

Dehay, B., Bove, J., Rodriguez-Muela, N., Perier, C., Recasens, A., Boya, P., and Vila, M. (2010). Pathogenic Lysosomal Depletion in Parkinson's Disease. J. Neurosci. *30*, 12535–12544.

Deininger, P.L., Jolly, D.J., Rubin, C.M., Friedmann, T., and Schmid, C.W. (1981). Base sequence studies of 300 nucleotide renatured repeated human DNA clones. J. Mol. Biol. *151*, 17–33.

Deragon, J.-M., and Zhang, X. (2006). Short Interspersed Elements (SINEs) in Plants: Origin, Classification, and Use as Phylogenetic Markers. Syst. Biol. *55*, 949–956.

Dermitzakis, E.T. (2003). Evolutionary Discrimination of Mammalian Conserved Non-Genic Sequences (CNGs). Science *302*, 1033–1035.

Derrien, T., Johnson, R., Bussotti, G., Tanzer, A., Djebali, S., Tilgner, H., Guernec, G., Martin, D., Merkel, A., Knowles, D.G., et al. (2012). The GENCODE v7 catalog of human long noncoding RNAs: Analysis of their gene structure, evolution, and expression. Genome Res. *22*, 1775–1789.

Dewannieux, M., Esnault, C., and Heidmann, T. (2003). LINE-mediated retrotransposition of marked Alu sequences. Nat. Genet. *35*, 41–48.

Djebali, S., Davis, C.A., Merkel, A., Dobin, A., Lassmann, T., Mortazavi, A., Tanzer, A., Lagarde, J., Lin, W., Schlesinger, F., et al. (2012). Landscape of transcription in human cells. Nature *489*, 101–108.

Ebralidze, A.K., Guibal, F.C., Steidl, U., Zhang, P., Lee, S., Bartholdy, B., Jorda, M.A., Petkova, V., Rosenbauer, F., Huang, G., et al. (2008). PU.1 expression is modulated by the balance of functional sense and antisense RNAs regulated by a shared cis-regulatory element. Genes Dev. *22*, 2085–2092.

Ehringer, H., and Hornykiewicz, O. (1960). [Distribution of noradrenaline and dopamine (3-hydroxytyramine) in the human brain and their behavior in diseases of the extrapyramidal system]. Klin. Wochenschr. *38*, 1236–1239.

Esnault, C., Maestre, J., and Heidmann, T. (2000). Human LINE retrotransposons generate processed pseudogenes. Nat. Genet. *24*, 363–367.

Espinoza, C.A., Goodrich, J.A., and Kugel, J.F. (2007). Characterization of the structure, function, and mechanism of B2 RNA, an ncRNA repressor of RNA polymerase II transcription. RNA *13*, 583–596.

Faghihi, M.A., and Wahlestedt, C. (2009). Regulatory roles of natural antisense transcripts. Nat. Rev. Mol. Cell Biol. *10*, 637–643.

Faghihi, M.A., Modarresi, F., Khalil, A.M., Wood, D.E., Sahagan, B.G., Morgan, T.E., Finch, C.E., Laurent III, G.S., Kenny, P.J., and Wahlestedt, C. (2008). Expression of a noncoding RNA is elevated in Alzheimer's disease and drives rapid feed-forward regulation of β-secretase. Nat. Med. *14*, 723–730.

Faghihi, M.A., Zhang, M., Huang, J., Modarresi, F., Van der Brug, M.P., Nalls, M.A., Cookson, M.R., St-Laurent, G., 3rd, and Wahlestedt, C. (2010). Evidence for natural antisense transcript-mediated inhibition of microRNA function. Genome Biol. *11*, R56.

Fejes-Toth, K., Sotirova, V., Sachidanandam, R., Assaf, G., Hannon, G.J., Kapranov, P., Foissac, S., Willingham, A.T., Duttagupta, R., Dumais, E., et al. (2009). Post-transcriptional processing generates a diversity of 5′-modified long and short RNAs. Nature *457*, 1028–1032.

Fernandez-Funez, P., Nino-Rosales, M.L., de Gouyon, B., She, W.C., Luchak, J.M., Martinez, P., Turiegano, E., Benito, J., Capovilla, M., Skinner, P.J., et al. (2000). Identification of genes that modify ataxin-1-induced neurodegeneration. Nature *408*, 101–106.

Fingar, D.C., Richardson, C.J., Tee, A.R., Cheatham, L., Tsou, C., and Blenis, J. (2003). mTOR Controls Cell Cycle Progression through Its Cell Growth Effectors S6K1 and 4E-BP1/Eukaryotic Translation Initiation Factor 4E. Mol. Cell. Biol. *24*, 200–216.

Fornace, A.J., Jr, and Mitchell, J.B. (1986). Induction of B2 RNA polymerase III transcription by heat shock: enrichment for heat shock induced sequences in rodent cells by hybridization subtraction. Nucleic Acids Res. *14*, 5793–5811.

Fütterer, J., Kiss-László, Z., and Hohn, T. (1993). Nonlinear ribosome migration on cauliflower mosaic virus 35S RNA. Cell *73*, 789–802.

Gebauer, F., and Hentze, M.W. (2004). Molecular mechanisms of translational control. Nat. Rev. Mol. Cell Biol. *5*, 827–835.

Gilbert, N., and Labuda, D. (1999). CORE-SINEs: eukaryotic short interspersed retroposing elements with common sequence motifs. Proc. Natl. Acad. Sci. *96*, 2869–2874.

Gilbert, W.V., Zhou, K., Butler, T.K., and Doudna, J.A. (2007). Cap-Independent Translation Is Required for Starvation-Induced Differentiation in Yeast. Science *317*, 1224–1227.

Ginger, M.R., Shore, A.N., Contreras, A., Rijnkels, M., Miller, J., Gonzalez-Rimbau, M.F., and Rosen, J.M. (2006). A noncoding RNA is a potential marker of cell fate during mammary gland development. Proc. Natl. Acad. Sci. *103*, 5781–5786.

Giraldez, A.J., Cinalli, R.M., Glasner, M.E., Enright, A.J., Thomson, M.J., Baskerville, S., Hammond, S.M., Bartel, D.P., and Schier, A.F. (2005). MicroRNAs Regulate Brain Morphogenesis in Zebrafish. Science *308*, 833–838.

Girard, A., Sachidanandam, R., Hannon, G.J., and Carmell, M.A. (2006). A germline-specific class of small RNAs binds mammalian Piwi proteins. Nature.

Gogolevsky, K.P., Vassetzky, N.S., and Kramerov, D.A. (2008). Bov-B-mobilized SINEs in vertebrate genomes. Gene *407*, 75–85.

Gogolevsky, K.P., Vassetzky, N.S., and Kramerov, D.A. (2009). 5S rRNA-derived and tRNA-derived SINEs in fruit bats. Genomics *93*, 494–500.

Goldman, J.E., Yen, S.H., Chiu, F.C., and Peress, N.S. (1983). Lewy bodies of Parkinson's disease contain neurofilament antigens. Science *221*, 1082–1084.

Gong, C., and Maquat, L.E. (2011). "Alu"strious long ncRNAs and their roles in shortening mRNA half-lives. Cell Cycle *10*, 1882–1883.

Gong, B., Cao, Z., Zheng, P., Vitolo, O.V., Liu, S., Staniszewski, A., Moolman, D., Zhang, H., Shelanski, M., and Arancio, O. (2006). Ubiquitin Hydrolase Uch-L1 Rescues β-Amyloid-Induced Decreases in Synaptic Function and Contextual Memory. Cell *126*, 775–788.

Goodyer, C.G., Zheng, H., and Hendy, G.N. (2001). Alu elements in human growth hormone receptor gene 5'untranslated region exons. J. Mol. Endocrinol. *27*, 357–366.

Greggio, E., Jain, S., Kingsbury, A., Bandopadhyay, R., Lewis, P., Kaganovich, A., van der Brug, M.P., Beilina, A., Blackinton, J., Thomas, K.J., et al. (2006). Kinase activity is required for the toxic effects of mutant LRRK2/dardarin. Neurobiol. Dis. *23*, 329–341.

Grivna, S.T., Pyhtila, B., and Lin, H. (2006). MIWI associates with translational machinery and PIWI-interacting RNAs (piRNAs) in regulating spermatogenesis. Proc. Natl. Acad. Sci. *103*, 13415–13420.

Gu, L., Zhu, N., Zhang, H., Durden, D.L., Feng, Y., and Zhou, M. (2009). Regulation of XIAP Translation and Induction by MDM2 following Irradiation. Cancer Cell *15*, 363–375.

Guenther, M.G., Levine, S.S., Boyer, L.A., Jaenisch, R., and Young, R.A. (2007). A Chromatin Landmark and Transcription Initiation at Most Promoters in Human Cells. Cell *130*, 77–88.

Gustincich, S., Sandelin, A., Plessy, C., Katayama, S., Simone, R., Lazarevic, D., Hayashizaki, Y., and Carninci, P. (2006). The complexity of the mammalian transcriptome. J. Physiol. *575*, 321–332.

Hasegawa, Y., Brockdorff, N., Kawano, S., Tsutui, K., Tsutui, K., and Nakagawa, S. (2010). The Matrix Protein hnRNP U Is Required for Chromosomal Localization of Xist RNA. Dev. Cell *19*, 469–476.

Häsler, J., Samuelsson, T., and Strub, K. (2007). Useful "junk": Alu RNAs in the human transcriptome. Cell. Mol. Life Sci. *64*, 1793–1800.

Hastings, M.L., Milcarek, C., Martincic, K., Peterson, M.L., and Munroe, S.H. (1997). Expression of the thyroid hormone receptor gene, erbAα, in B lymphocytes: alternative mRNA processing is independent of differentiation but correlates with antisense RNA levels. Nucleic Acids Res. *25*, 4296–4300.

He, X.-P., Bataille, N., and Fried, H.M. (1994). Nuclear export of signal recognition particle RNA is a facilitated process that involves the Alu sequence domain. J. Cell Sci. *107*, 903–912.

Huarte, M., Guttman, M., Feldser, D., Garber, M., Koziol, M.J., Kenzelmann-Broz, D., Khalil, A.M., Zuk, O., Amit, I., Rabani, M., et al. (2010). A Large Intergenic Noncoding RNA Induced by p53 Mediates Global Gene Repression in the p53 Response. Cell *142*, 409–419.

Hulme, A.E., Bogerd, H.P., Cullen, B.R., and Moran, J.V. (2007). Selective inhibition of Alu retrotransposition by APOBEC3G. Gene *390*, 199–205.

Imamura, T., Yamamoto, S., Ohgane, J., Hattori, N., Tanaka, S., and Shiota, K. (2004). Non-coding RNA directed DNA demethylation of Sphk1 CpG island. Biochem. Biophys. Res. Commun. *322*, 593–600.

Iorio, M.V., Ferracin, M., Liu, C.-G., Veronese, A., Spizzo, R., Sabbioni, S., Magri, E., Pedriali, M., Fabbri, M., and Campiglio, M. (2005). MicroRNA gene expression deregulation in human breast cancer. Cancer Res. *65*, 7065–7070.

Jang, K.L., and Latchman, D.S. (1992). The herpes simplex virus immediate-early protein ICP27 stimulates the transcription of cellular Alu repeated sequences by increasing the activity of transcription factor TFIIIC. Biochem. J. *284 (Pt 3)*, 667–673.

Jang, K.L., Collins, M.K., and Latchman, D.S. (1992). The human immunodeficiency virus tat protein increases the transcription of human Alu repeated sequences by increasing the activity of the cellular transcription factor TFIIIC. J. Acquir. Immune Defic. Syndr. *5*, 1142–1147.

Jang, S.K., Kräusslich, H.G., Nicklin, M.J., Duke, G.M., Palmenberg, A.C., and Wimmer, E. (1988). A segment of the 5' nontranslated region of encephalomyocarditis virus RNA directs internal entry of ribosomes during in vitro translation. J. Virol. *62*, 2636–2643.

Janowski, B.A., Younger, S.T., Hardy, D.B., Ram, R., Huffman, K.E., and Corey, D.R. (2007). Activating gene expression in mammalian cells with promoter-targeted duplex RNAs. Nat. Chem. Biol. *3*, 166–173.

Jefferies, H.B., Fumagalli, S., Dennis, P.B., Reinhard, C., Pearson, R.B., and Thomas, G. (1997). Rapamycin suppresses 5'TOP mRNA translation through inhibition of p70s6k. EMBO J. *16*, 3693–3704.

Johnson, R., Teh, C.H.-L., Jia, H., Vanisri, R.R., Pandey, T., Lu, Z.-H., Buckley, N.J., Stanton, L.W., and Lipovich, L. (2009). Regulation of neural macroRNAs by the transcriptional repressor REST. RNA New York N *15*, 85–96.

Jurka, J. (1997). Sequence patterns indicate an enzymatic involvement in integration of mammalian retroposons. Proc. Natl. Acad. Sci. *94*, 1872–1877.

Kabuta, T., Setsuie, R., Mitsui, T., Kinugawa, A., Sakurai, M., Aoki, S., Uchida, K., and Wada, K. (2008). Aberrant molecular properties shared by familial Parkinson's disease-associated mutant UCH-L1 and carbonyl-modified UCH-L1. Hum. Mol. Genet. *17*, 1482–1496.

Kai, L., Roos, C., Haberstock, S., Proverbio, D., Ma, Y., Junge, F., Karbyshev, M., Dötsch, V., and Bernhard, F. (2012). Systems for the cell-free synthesis of proteins. Methods Mol. Biol. Clifton NJ *800*, 201–225.

Kajikawa, M., and Okada, N. (2002). LINEs mobilize SINEs in the eel through a shared 3′ sequence. Cell *111*, 433–444.

Kapitonov, V.V., and Jurka, J. (2003). A Novel Class of SINE Elements Derived from 5S rRNA. Mol. Biol. Evol. *20*, 694–702.

Kapranov, P., Drenkow, J., Cheng, J., Long, J., Helt, G., Dike, S., and Gingeras, T.R. (2005). Examples of the complex architecture of the human transcriptome revealed by RACE and high-density tiling arrays. Genome Res. *15*, 987–997.

Kapranov, P., Cheng, J., Dike, S., Nix, D.A., Duttagupta, R., Willingham, A.T., Stadler, P.F., Hertel, J., Hackermuller, J., Hofacker, I.L., et al. (2007a). RNA Maps Reveal New RNA Classes and a Possible Function for Pervasive Transcription. Science *316*, 1484–1488.

Kapranov, P., Willingham, A.T., and Gingeras, T.R. (2007b). Genome-wide transcription and the implications for genomic organization. Nat. Rev. Genet. *8*, 413–423.

Kapusta, A., Kronenberg, Z., Lynch, V.J., Zhuo, X., Ramsay, L., Bourque, G., Yandell, M., and Feschotte, C. (2013). Transposable Elements Are Major Contributors to the Origin, Diversification, and Regulation of Vertebrate Long Noncoding RNAs. PLoS Genet. *9*, e1003470.

Kawahara, Y., and Nishikura, K. (2006). Extensive adenosine-to-inosine editing detected in Alu repeats of antisense RNAs reveals scarcity of sense–antisense duplex formation. FEBS Lett. *580*, 2301–2305.

Kawaji, H., Nakamura, M., Takahashi, Y., Sandelin, A., Katayama, S., Fukuda, S., Daub, C.O., Kai, C., Kawai, J., Yasuda, J., et al. (2008). Hidden layers of human small RNAs. BMC Genomics *9*, 157.

Kim, T.-K., Hemberg, M., Gray, J.M., Costa, A.M., Bear, D.M., Wu, J., Harmin, D.A., Laptewicz, M., Barbara-Haley, K., Kuersten, S., et al. (2010). Widespread transcription at neuronal activity-regulated enhancers. Nature *465*, 182–187.

Kimball, S.R. (2001). Regulation of translation initiation by amino acids in eukaryotic cells. Prog. Mol. Subcell. Biol. *26*, 155–184.

Kino, T., Hurt, D.E., Ichijo, T., Nader, N., and Chrousos, G.P. (2010). Noncoding RNA gas5 is a growth arrest- and starvation-associated repressor of the glucocorticoid receptor. Sci. Signal. *3*, ra8.

Kishore, S., and Stamm, S. (2006). The snoRNA HBII-52 Regulates Alternative Splicing of the Serotonin Receptor 2C. Science *311*, 230–232.

Kiss, T. (2002). Small nucleolar RNAs: an abundant group of noncoding RNAs with diverse cellular functions. Cell *109*, 145–148.

Kitada, T., Asakawa, S., Hattori, N., Matsumine, H., Yamamura, Y., Minoshima, S., Yokochi, M., Mizuno, Y., and Shimizu, N. (1998). Mutations in the parkin gene cause autosomal recessive juvenile parkinsonism. Nature *392*, 605–608.

Klattenhoff, C., and Theurkauf, W. (2007). Biogenesis and germline functions of piRNAs. Development *135*, 3–9.

Klein, M.E., Impey, S., and Goodman, R.H. (2005). Role reversal: the regulation of neuronal gene expression by microRNAs. Curr. Opin. Neurobiol. *15*, 507–513.

Koerner, M.V., Pauler, F.M., Huang, R., and Barlow, D.P. (2009). The function of non-coding RNAs in genomic imprinting. Dev. Camb. Engl. *136*, 1771–1783.

De Kok, J.B., Verhaegh, G.W., Roelofs, R.W., Hessels, D., Kiemeney, L.A., Aalders, T.W., Swinkels, D.W., and Schalken, J.A. (2002). DD3PCA3, a very sensitive and specific marker to detect prostate tumors. Cancer Res. *62*, 2695–2698.

Komar, A.A., and Hatzoglou, M. (2011). Cellular IRES-mediated translation: The war of ITAFs in pathophysiological states. Cell Cycle *10*, 229–240.

Korneev, S.A., Park, J.-H., and O'Shea, M. (1999). Neuronal expression of neural nitric oxide synthase (nNOS) protein is suppressed by an antisense RNA transcribed from an NOS pseudogene. J. Neurosci. *19*, 7711–7720.

Korneev, S.A., Korneeva, E.I., Lagarkova, M.A., Kiselev, S.L., Critchley, G., and O'Shea, M. (2008). Novel noncoding antisense RNA transcribed from human anti-NOS2A locus is differentially regulated during neuronal differentiation of embryonic stem cells. RNA *14*, 2030–2037.

Kramerov, D.A., and Vassetzky, N.S. (2005). Short retroposons in eukaryotic genomes. Int. Rev. Cytol. *247*, 165–221.

Kramerov, D.A., and Vassetzky, N.S. (2011). Origin and evolution of SINEs in eukaryotic genomes. Heredity *107*, 487–495.

Krayev, A.S., Kramerov, D.A., Skryabin, K.G., Ryskov, A.P., Bayev, A.A., and Georgiev, G.P. (1980). The nucleotide sequence of the ubiquitous repetitive DNA sequence B1 complementary to the most abundant class of mouse fold-back RNA. Nucleic Acids Res. *8*, 1201–1215.

Kubodera, T., Watanabe, M., Yoshiuchi, K., Yamashita, N., Nishimura, A., Nakai, S., Gomi, K., and Hanamoto, H. (2003). Thiamine-regulated gene expression of Aspergillus oryzae thiA requires splicing of the intron containing a riboswitch-like domain in the 5′-UTR. FEBS Lett. *555*, 516–520.

Kuersten, S., and Goodwin, E.B. (2003). The power of the 3′ UTR: translational control and development. Nat. Rev. Genet. *4*, 626–637.

Kumar, M., and Carmichael, G.G. (1998). Antisense RNA: function and fate of duplex RNA in cells of higher eukaryotes. Microbiol. Mol. Biol. Rev. *62*, 1415–1434.

Kwek, K.Y., Murphy, S., Furger, A., Thomas, B., O'Gorman, W., Kimura, H., Proudfoot, N.J., and Akoulitchev, A. (2002). U1 snRNA associates with TFIIH and regulates transcriptional initiation. Nat. Struct. Biol. *9*, 800–805.

Labuda, D., and Zietkiewicz, E. (1994). Evolution of secondary structure in the family of 7SL-like RNAs. J. Mol. Evol. *39*, 506–518.

Labuda, D., Sinnett, D., Richer, C., Deragon, J.M., and Striker, G. (1991). Evolution of mouse B1 repeats: 7SL RNA folding pattern conserved. J. Mol. Evol. *32*, 405–414.

Lai, C.K., Miller, M.C., and Collins, K. (2003). Roles for RNA in telomerase nucleotide and repeat addition processivity. Mol. Cell *11*, 1673–1683.

Lander, E.S., Linton, L.M., Birren, B., Nusbaum, C., Zody, M.C., Baldwin, J., Devon, K., Dewar, K., Doyle, M., and FitzHugh, W. (2001). Initial sequencing and analysis of the human genome. Nature *409*, 860–921.

Landry, J.-R., Medstrand, P., and Mager, D.L. (2001). Repetitive Elements in the 5′ Untranslated Region of a Human Zinc-Finger Gene Modulate Transcription and Translation Efficiency. Genomics *76*, 110–116.

Lang, K.J., Kappel, A., and Goodall, G.J. (2002). Hypoxia-inducible factor-1α mRNA contains an internal ribosome entry site that allows efficient translation during normoxia and hypoxia. Mol. Biol. Cell *13*, 1792–1801.

Larsen, C.N., Price, J.S., and Wilkinson, K.D. (1996). Substrate binding and catalysis by ubiquitin C-terminal hydrolases: identification of two active site residues. Biochemistry (Mosc.) *35*, 6735–6744.

Lavorgna, G., Dahary, D., Lehner, B., Sorek, R., Sanderson, C.M., and Casari, G. (2004). In search of antisense. Trends Biochem. Sci. *29*, 88–94.

Lee, Y., Kim, M., Han, J., Yeom, K.-H., Lee, S., Baek, S.H., and Kim, V.N. (2004). MicroRNA genes are transcribed by RNA polymerase II. EMBO J. *23*, 4051–4060.

Leroy, E., Boyer, R., Auburger, G., Leube, B., Ulm, G., Mezey, E., Harta, G., Brownstein, M.J., Jonnalagada, S., Chernova, T., et al. (1998). The ubiquitin pathway in Parkinson's disease. Nature *395*, 451–452.

Levecque, C., Destée, A., Mouroux, V., Becquet, E., Defebvre, L., Amouyel, P., and Chartier-Harlin, M.C. (2001). No genetic association of the ubiquitin carboxy-terminal hydrolase-L1 gene S18Y polymorphism with familial Parkinson's disease. J. Neural Transm. Vienna Austria 1996 *108*, 979–984.

Li, J.-T., Zhang, Y., Kong, L., Liu, Q.-R., and Wei, L. (2008). Trans-natural antisense transcripts including noncoding RNAs in 10 species: implications for expression regulation. Nucleic Acids Res. *36*, 4833–4844.

Li, T.H., Kim, C., Rubin, C.M., and Schmid, C.W. (2000). K562 cells implicate increased chromatin accessibility in Alu transcriptional activation. Nucleic Acids Res. *28*, 3031–3039.

Li, Z., Melandri, F., Berdo, I., Jansen, M., Hunter, L., Wright, S., Valbrun, D., and Figueiredo-Pereira, M.E. (2004). Δ12-Prostaglandin J2 inhibits the ubiquitin hydrolase UCH-L1 and elicits ubiquitin–protein aggregation without proteasome inhibition. Biochem. Biophys. Res. Commun. *319*, 1171–1180.

Liu, K., Shi, N., Sun, Y., Zhang, T., and Sun, X. (2013). Therapeutic effects of rapamycin on MPTP-induced Parkinsonism in mice. Neurochem. Res. *38*, 201–207.

Liu, W.-M., Chu, W.-M., Choudary, P.V., and Schmid, C.W. (1995). Cell stress and translational inhibitors transiently increase the abundance of mammalian SINE transcripts. Nucleic Acids Res. *23*, 1758–1765.

Liu, Y., Fallon, L., Lashuel, H.A., Liu, Z., and Lansbury Jr, P.T. (2002). The UCH-L1 gene encodes two opposing enzymatic activities that affect α-synuclein degradation and Parkinson's disease susceptibility. Cell *111*, 209–218.

Lobachev, K.S., Stenger, J.E., Kozyreva, O.G., Jurka, J., Gordenin, D.A., and Resnick, M.A. (2000). Inverted Alu repeats unstable in yeast are excluded from the human genome. EMBO J. *19*, 3822–3830.

Lodish, H.F., and Rose, J.K. (1977). Relative importance of 7-methylguanosine in ribosome binding and translation of vesicular stomatitis virus mRNA in wheat germ and reticulocyte cell-free systems. J. Biol. Chem. *252*, 1181–1188.

Louro, R., Smirnova, A.S., and Verjovski-Almeida, S. (2009). Long intronic noncoding RNA transcription: Expression noise or expression choice? Genomics *93*, 291–298.

Lowe, J., McDermott, H., Landon, M., Mayer, R.J., and Wilkinson, K.D. (1990). Ubiquitin carboxyl-terminal hydrolase (PGP 9.5) is selectively present in ubiquitinated inclusion bodies characteristic of human neurodegenerative diseases. J. Pathol. *161*, 153–160.

Lunyak, V.V. (2008). Boundaries. Boundaries…Boundaries??? Curr. Opin. Cell Biol. *20*, 281–287.

Lunyak, V.V., Prefontaine, G.G., Nunez, E., Cramer, T., Ju, B.-G., Ohgi, K.A., Hutt, K., Roy, R., Garcia-Diaz, A., Zhu, X., et al. (2007). Developmentally Regulated Activation of a SINE B2 Repeat as a Domain Boundary in Organogenesis. Science *317*, 248–251.

Ly, H., Blackburn, E.H., and Parslow, T.G. (2003). Comprehensive Structure-Function Analysis of the Core Domain of Human Telomerase RNA. Mol. Cell. Biol. *23*, 6849–6856.

Ma, X.M., and Blenis, J. (2009). Molecular mechanisms of mTOR-mediated translational control. Nat. Rev. Mol. Cell Biol. *10*, 307–318.

Makalowska, I., Lin, C.-F., and Makalowski, W. (2005). Overlapping genes in vertebrate genomes. Comput. Biol. Chem. *29*, 1–12.

Makalowski, W. (2000). Genomic scrap yard: how genomes utilize all that junk. Gene *259*, 61–67.

Malagelada, C., Ryu, E.J., Biswas, S.C., Jackson-Lewis, V., and Greene, L.A. (2006). RTP801 Is Elevated in Parkinson Brain Substantia Nigral Neurons and Mediates Death in Cellular Models of Parkinson's Disease by a Mechanism Involving Mammalian Target of Rapamycin Inactivation. J. Neurosci. *26*, 9996–10005.

Malagelada, C., Jin, Z.H., and Greene, L.A. (2008). RTP801 Is Induced in Parkinson's Disease and Mediates Neuron Death by Inhibiting Akt Phosphorylation/Activation. J. Neurosci. *28*, 14363–14371.

Malagelada, C., Jin, Z.H., Jackson-Lewis, V., Przedborski, S., and Greene, L.A. (2010). Rapamycin Protects against Neuron Death in In Vitro andIn Vivo Models of Parkinson's Disease. J. Neurosci. *30*, 1166–1175.

Malone, C.D., and Hannon, G.J. (2009). Small RNAs as Guardians of the Genome. Cell *136*, 656–668.

Mariner, P.D., Walters, R.D., Espinoza, C.A., Drullinger, L.F., Wagner, S.D., Kugel, J.F., and Goodrich, J.A. (2008). Human Alu RNA Is a Modular Transacting Repressor of mRNA Transcription during Heat Shock. Mol. Cell *29*, 499–509.

Mathews, D.H., Moss, W.N., and Turner, D.H. (2010). Folding and finding RNA secondary structure. Cold Spring Harb. Perspect. Biol. *2*, a003665.

Mattick, J.S. (2004). RNA regulation: a new genetics? Nat. Rev. Genet. *5*, 316–323.

McNaught, K.S.P., Mytilineou, C., JnoBaptiste, R., Yabut, J., Shashidharan, P., Jenner, P., and Olanow, C.W. (2002). Impairment of the ubiquitin-proteasome system causes dopaminergic cell death and inclusion body formation in ventral mesencephalic cultures. J. Neurochem. *81*, 301–306.

Meier, U.T. (2005). The many facets of H/ACA ribonucleoproteins. Chromosoma *114*, 1–14.

Mello, C.C., and Conte, D. (2004). Revealing the world of RNA interference. Nature *431*, 338–342.

Mercer, T.R., Dinger, M.E., Sunkin, S.M., Mehler, M.F., and Mattick, J.S. (2008). Specific expression of long noncoding RNAs in the mouse brain. Proc. Natl. Acad. Sci. U. S. A. *105*, 716–721.

Mikami, S., Kobayashi, T., Masutani, M., Yokoyama, S., and Imataka, H. (2008). A human cell-derived in vitro coupled transcription/translation system optimized for production of recombinant proteins. Protein Expr. Purif. *62*, 190–198.

Mohammad, F., Mondal, T., and Kanduri, C. (2009). Epigenetics of imprinted long non-coding RNAs. Epigenetics *4*, 277–286.

Moore, M.J. (2005). From Birth to Death: The Complex Lives of Eukaryotic mRNAs. Science *309*, 1514–1518.

Morris, K.V., Chan, S.W.-L., Jacobsen, S.E., and Looney, D.J. (2004). Small Interfering RNA-Induced Transcriptional Gene Silencing in Human Cells. Science *305*, 1289–1292.

Morris, K.V., Santoso, S., Turner, A.-M., Pastori, C., and Hawkins, P.G. (2008). Bidirectional Transcription Directs Both Transcriptional Gene Activation and Suppression in Human Cells. PLoS Genet. *4*, e1000258.

Mus, E., Hof, P.R., and Tiedge, H. (2007). Dendritic BC200 RNA in aging and in Alzheimer's disease. Proc. Natl. Acad. Sci. U. S. A. *104*, 10679–10684.

Nagai, K., Oubridge, C., Kuglstatter, A., Menichelli, E., Isel, C., and Jovine, L. (2003). Structure, function and evolution of the signal recognition particle. EMBO J. *22*, 3479–3485.

Nagamachi, A., Htun, P.W., Ma, F., Miyazaki, K., Yamasaki, N., Kanno, M., Inaba, T., Honda, Z., Okuda, T., Oda, H., et al. (2010). A 5′ untranslated region containing the IRES element in the Runx1 gene is required for angiogenesis, hematopoiesis and leukemogenesis in a knock-in mouse model. Dev. Biol. *345*, 226–236.

Naguibneva, I., Ameyar-Zazoua, M., Polesskaya, A., Ait-Si-Ali, S., Groisman, R., Souidi, M., Cuvellier, S., and Harel-Bellan, A. (2006). The microRNA miR-181 targets the homeobox protein Hox-A11 during mammalian myoblast differentiation. Nat. Cell Biol. *8*, 278–284.

Narendra, D., Tanaka, A., Suen, D.-F., and Youle, R.J. (2008). Parkin is recruited selectively to impaired mitochondria and promotes their autophagy. J. Cell Biol. *183*, 795–803.

Nazé, P., Vuillaume, I., Destée, A., Pasquier, F., and Sablonnière, B. (2002). Mutation analysis and association studies of the ubiquitin carboxy-terminal hydrolase L1 gene in Huntington's disease. Neurosci. Lett. *328*, 1–4.

Nigumann, P., Redik, K., Mätlik, K., and Speek, M. (2002). Many Human Genes Are Transcribed from the Antisense Promoter of L1 Retrotransposon. Genomics *79*, 628–634.

Nishihara, H., Terai, Y., and Okada, N. (2002). Characterization of novel Alu-and tRNA-related SINEs from the tree shrew and evolutionary implications of their origins. Mol. Biol. Evol. *19*, 1964–1972.

Nishihara, H., Smit, A.F.A., and Okada, N. (2006). Functional noncoding sequences derived from SINEs in the mammalian genome. Genome Res. *16*, 864–874.

Nishikura, K. (2006). Editor meets silencer: crosstalk between RNA editing and RNA interference. Nat. Rev. Mol. Cell Biol. *7*, 919–931.

O'Donnell, K.A., and Boeke, J.D. (2007). Mighty Piwis Defend the Germline against Genome Intruders. Cell *129*, 37–44.

O'Donnell, K.A., Wentzel, E.A., Zeller, K.I., Dang, C.V., and Mendell, J.T. (2005). c-Myc-regulated microRNAs modulate E2F1 expression. Nature *435*, 839–843.

Ogiwara, I., Miya, M., and Ohshima, K. (2002). V-SINEs: A New Superfamily of Vertebrate SINEs That Are Widespread in Vertebrate Genomes and Retain a Strongly Conserved Segment within Each Repetitive Unit. Genome Res. *12*, 316–324.

Ohman, M. (2007). A-to-I editing challenger or ally to the microRNA process. Biochimie *89*, 1171–1176.

Ohshima, K., and Okada, N. (2005). SINEs and LINEs: symbionts of eukaryotic genomes with a common tail. Cytogenet. Genome Res. *110*, 475–490.

Paisán-Ruíz, C., Jain, S., Evans, E.W., Gilks, W.P., Simón, J., van der Brug, M., de Munain, A.L., Aparicio, S., Gil, A.M., and Khan, N. (2004). Cloning of the Gene Containing Mutations that Cause PARK8-Linked Parkinson's Disease. Neuron *44*, 595–600.

Panning, B., and Smiley, J.R. (1993). Activation of RNA polymerase III transcription of human Alu repetitive elements by adenovirus type 5: requirement for the E1b 58-kilodalton protein and the products of E4 open reading frames 3 and 6. Mol. Cell. Biol. *13*, 3231–3244.

Panning, B., and Smiley, J.R. (1995). Activation of Expression of Multiple Subfamilies of Human< i> Alu</i> Elements by Adenovirus Type 5 and Herpes Simplex Virus Type 1. J. Mol. Biol. *248*, 513–524.

Peaston, A.E., Evsikov, A.V., Graber, J.H., de Vries, W.N., Holbrook, A.E., Solter, D., and Knowles, B.B. (2004). Retrotransposons regulate host genes in mouse oocytes and preimplantation embryos. Dev. Cell *7*, 597–606.

Pelletier, J., Kaplan, G., Racaniello, V.R., and Sonenberg, N. (1988). Cap-independent translation of poliovirus mRNA is conferred by sequence elements within the 5'noncoding region. Mol. Cell. Biol. *8*, 1103–1112.

Peters, N.T., Rohrbach, J.A., Zalewski, B.A., Byrkett, C.M., and Vaughn, J.C. (2003). RNA editing and regulation of Drosophila 4f-rnp expression by sas-10 antisense readthrough mRNA transcripts. RNA *9*, 698–710.

Plath, K., Mlynarczyk-Evans, S., Nusinow, D.A., and Panning, B. (2002). Xist RNA and the mechanism of X chromosome inactivation. Annu. Rev. Genet. *36*, 233–278.

Poliseno, L., Salmena, L., Zhang, J., Carver, B., Haveman, W.J., and Pandolfi, P.P. (2010). A coding-independent function of gene and pseudogene mRNAs regulates tumour biology. Nature *465*, 1033–1038.

Polymeropoulos, M.H., Lavedan, C., Leroy, E., Ide, S.E., Dehejia, A., Dutra, A., Pike, B., Root, H., Rubenstein, J., Boyer, R., et al. (1997). Mutation in the Alpha-Synuclein Gene Identified in Families with Parkinson's Disease. Science *276*, 2045–2047.

Ponicsan, S.L., Kugel, J.F., and Goodrich, J.A. (2010). Genomic gems: SINE RNAs regulate mRNA production. Curr. Opin. Genet. Dev. *20*, 149–155.

Ponting, C.P., Oliver, P.L., and Reik, W. (2009). Evolution and Functions of Long Noncoding RNAs. Cell *136*, 629–641.

Prasanth, K.V., and Spector, D.L. (2007). Eukaryotic regulatory RNAs: an answer to the "genome complexity" conundrum. Genes Dev. *21*, 11–42.

Prasanth, K.V., Prasanth, S.G., Xuan, Z., Hearn, S., Freier, S.M., Bennett, C.F., Zhang, M.Q., and Spector, D.L. (2005). Regulating Gene Expression through RNA Nuclear Retention. Cell *123*, 249–263.

Preker, P., Nielsen, J., Kammler, S., Lykke-Andersen, S., Christensen, M.S., Mapendano, C.K., Schierup, M.H., and Jensen, T.H. (2008). RNA exosome depletion reveals transcription upstream of active human promoters. Science *322*, 1851–1854.

Qureshi, I.A., and Mehler, M.F. (2009). Regulation of non-coding RNA networks in the nervous system--what's the REST of the story? Neurosci. Lett. *466*, 73–80.

Qureshi, I.A., Mattick, J.S., and Mehler, M.F. (2010). Long non-coding RNAs in nervous system function and disease. Brain Res. *1338*, 20–35.

Richter, J.D., and Sonenberg, N. (2005). Regulation of cap-dependent translation by eIF4E inhibitory proteins. Nature *433*, 477–480.

Rinn, J.L., and Chang, H.Y. (2012). Genome Regulation by Long Noncoding RNAs. Annu. Rev. Biochem. *81*, 145–166.

Rodriguez, A., Griffiths-Jones, S., Ashurst, J.L., and Bradley, A. (2004). Identification of Mammalian microRNA Host Genes and Transcription Units. Genome Res. *14*, 1902–1910.

Rome, C., Loiseau, H., Arsaut, J., Roullot, V., and Couillaud, F. (2006). Diversity of contactin mRNA in human brain tumors. Mol. Carcinog. *45*, 774–785.

Roy-Engel, A.M., Salem, A.-H., Oyeniran, O.O., Deininger, L., Hedges, D.J., Kilroy, G.E., Batzer, M.A., and Deininger, P.L. (2002). Active Alu element "A-tails": size does matter. Genome Res. *12*, 1333–1344.

Rozhdestvensky, T.S., Crain, P.F., and Brosius, J. (2007). Isolation and posttranscriptional modification analysis of native BC1 RNA from mouse brain. RNA Biol. *4*, 11–15.

Rubin, C.M., VandeVoort, C.A., Teplitz, R.L., and Schmid, C.W. (1994). Alu repeated DNAs are differentially methylated in primate germ cells. Nucleic Acids Res. *22*, 5121–5127.

Rubin, C.M., Kimura, R.H., and Schmid, C.W. (2002). Selective stimulation of translational expression by Alu RNA. Nucleic Acids Res. *30*, 3253–3261.

Ryu, E.J., Harding, H.P., Angelastro, J.M., Vitolo, O.V., Ron, D., and Greene, L.A. (2002). Endoplasmic reticulum stress and the unfolded protein response in cellular models of Parkinson's disease. J. Neurosci. *22*, 10690–10698.

Santini, E., Heiman, M., Greengard, P., Valjent, E., and Fisone, G. (2009). Inhibition of mTOR signaling in Parkinson's disease prevents L-DOPA-induced dyskinesia. Sci. Signal. *2*, ra36.

Sarkar, S., and Rubinsztein, D.C. (2008). Huntington's disease: degradation of mutant huntingtin by autophagy: Degradation of mutant huntingtin by autophagy. FEBS J. *275*, 4263–4270.

Sarkar, S., Ravikumar, B., Floto, R.A., and Rubinsztein, D.C. (2009). Rapamycin and mTOR-independent autophagy inducers ameliorate toxicity of polyglutamine-expanded huntingtin and related proteinopathies. Cell Death Differ. *16*, 46–56.

Sastry, S.S., and Hoffman, P.L. (1995). The influence of RNA and DNA template structures during transcript elongation by RNA polymerases. Biochem. Biophys. Res. Commun. *211*, 106–114.

Schmid, C.W. (1996). Alu: structure, origin, evolution, significance and function of one-tenth of human DNA. Prog. Nucleic Acid Res. Mol. Biol. *53*, 283–319.

Schmitz, J., and Zischler, H. (2003). A novel family of tRNA-derived SINEs in the colugo and two new retrotransposable markers separating dermopterans from primates. Mol. Phylogenet. Evol. *28*, 341–349.

Schramm, L., and Hernandez, N. (2002). Recruitment of RNA polymerase III to its target promoters. Genes Dev. *16*, 2593–2620.

Schwartz, J.C., Younger, S.T., Nguyen, N.-B., Hardy, D.B., Monia, B.P., Corey, D.R., and Janowski, B.A. (2008). Antisense transcripts are targets for activating small RNAs. Nat. Struct. 38 Mol. Biol. *15*, 842–848.

Seila, A.C., Calabrese, J.M., Levine, S.S., Yeo, G.W., Rahl, P.B., Flynn, R.A., Young, R.A., and Sharp, P.A. (2008). Divergent transcription from active promoters. Science *322*, 1849–1851.

Serdobova, I.M., and Kramerov, D.A. (1998). Short retroposons of the B2 superfamily: evolution and application for the study of rodent phylogeny. J. Mol. Evol. *46*, 202–214.

Setsuie, R., and Wada, K. (2007). The functions of UCH-L1 and its relation to neurodegenerative diseases. Neurochem. Int. *51*, 105–111.

Sharon, R., Bar-Joseph, I., Frosch, M.P., Walsh, D.M., Hamilton, J.A., and Selkoe, D.J. (2003). The formation of highly soluble oligomers of α-synuclein is regulated by fatty acids and enhanced in Parkinson's disease. Neuron *37*, 583–595.

Shearwin, K., Callen, B., and Egan, J. (2005). Transcriptional interference – a crash course. Trends Genet. *21*, 339–345.

Shimizu, Y., Kanamori, T., and Ueda, T. (2005). Protein synthesis by pure translation systems. Methods *36*, 299–304.

Siddiqui, A., Hanson, I., and Andersen, J.K. (2012). Mao-B elevation decreases parkin's ability to efficiently clear damaged mitochondria: protective effects of rapamycin. Free Radic. Res. *46*, 1011–1018.

Singh, K., Carey, M., Saragosti, S., and Botchan, M. (1985). Expression of enhanced levels of small RNA polymerase III transcripts encoded by the B2 repeats in simian virus 40-transformed mouse cells. Nature *314*, 553–556.

Sinnett, D., Richer, C., Deragon, J.-M., and Labuda, D. (1991). Alu RNA secondary structure consists of two independent 7 SL RNA-like folding units. J. Biol. Chem. *266*, 8675–8678.

Sioud, M., and Røsok, O. (2004). Profiling microRNA expression using sensitive cDNA probes and filter arrays. BioTechniques *37*, 574–576, 578–580.

Smalheiser, N.R., and Torvik, V.I. (2005). Mammalian microRNAs derived from genomic repeats. Trends Genet. TIG *21*, 322–326.

Sobczak, K., and Krzyzosiak, W.J. (2002). Structural Determinants of BRCA1 Translational Regulation. J. Biol. Chem. *277*, 17349–17358.

Spillantini, M.G., Schmidt, M.L., Lee, V.M., Trojanowski, J.Q., Jakes, R., and Goedert, M. (1997). Alpha-synuclein in Lewy bodies. Nature *388*, 839–840.

Spirin, A.S. (2004). High-throughput cell-free systems for synthesis of functionally active proteins. Trends Biotechnol. *22*, 538–545.

Spriggs, K.A., Bushell, M., Mitchell, S.A., and Willis, A.E. (2005). Internal ribosome entry segment-mediated translation during apoptosis: the role of IRES-trans-acting factors. Cell Death Differ. *12*, 585–591.

Stenger, J.E., Lobachev, K.S., Gordenin, D., Darden, T.A., Jurka, J., and Resnick, M.A. (2001). Biased distribution of inverted and direct Alus in the human genome: implications for insertion, exclusion, and genome stability. Genome Res. *11*, 12–27.

Stoneley, M., and Willis, A.E. (2004). Cellular internal ribosome entry segments: structures, trans-acting factors and regulation of gene expression. Oncogene *23*, 3200–3207.

Sudarsan, N., Barrick, J.E., and Breaker, R.R. (2003). Metabolite-binding RNA domains are present in the genes of eukaryotes. RNA *9*, 644–647.

Sun, B.K., Deaton, A.M., and Lee, J.T. (2006). A Transient Heterochromatic State in Xist Preempts X Inactivation Choice without RNA Stabilization. Mol. Cell *21*, 617–628.

Sun, F.-J., Fleurdépine, S., Bousquet-Antonelli, C., Caetano-Anollés, G., and Deragon, J.-M. (2007). Common evolutionary trends for SINE RNA structures. Trends Genet. *23*, 26–33.

Taft, R.J., Pheasant, M., and Mattick, J.S. (2007). The relationship between non-protein-coding DNA and eukaryotic complexity. BioEssays *29*, 288–299.

Taft, R.J., Glazov, E.A., Cloonan, N., Simons, C., Stephen, S., Faulkner, G.J., Lassmann, T., Forrest, A.R.R., Grimmond, S.M., Schroder, K., et al. (2009). Tiny RNAs associated with transcription start sites in animals. Nat. Genet. *41*, 572–578.

Tain, L.S., Mortiboys, H., Tao, R.N., Ziviani, E., Bandmann, O., and Whitworth, A.J. (2009). Rapamycin activation of 4E-BP prevents parkinsonian dopaminergic neuron loss. Nat. Neurosci. *12*, 1129–1135.

Tam, O.H., Aravin, A.A., Stein, P., Girard, A., Murchison, E.P., Cheloufi, S., Hodges, E., Anger, M., Sachidanandam, R., Schultz, R.M., et al. (2008). Pseudogene-derived small interfering RNAs regulate gene expression in mouse oocytes. Nature *453*, 534–538.

Tarui, H., Imanishi, S., and Hara, T. (2000). A novel cell-free translation/glycosylation system prepared from insect cells. J. Biosci. Bioeng. *90*, 508–514.

The FANTOM Consortium (2005). The Transcriptional Landscape of the Mammalian Genome. Science *309*, 1559–1563.

Tufarelli, C., Stanley, J.A.S., Garrick, D., Sharpe, J.A., Ayyub, H., Wood, W.G., and Higgs, D.R. (2003). Transcription of antisense RNA leading to gene silencing and methylation as a novel cause of human genetic disease. Nat. Genet. *34*, 157–165.

Tzamarias, D., Roussou, I., and Thireos, G. (1989). Coupling of GCN4 mRNA translational activation with decreased rates of polypeptide chain initiation. Cell *57*, 947–954.

Uchida, T., Rossignol, F., Matthay, M.A., Mounier, R., Couette, S., Clottes, E., and Clerici, C. (2004). Prolonged Hypoxia Differentially Regulates Hypoxia-inducible Factor (HIF)-1 and HIF-2 Expression in Lung Epithelial Cells: IMPLICATION OF NATURAL ANTISENSE HIF-1. J. Biol. Chem. *279*, 14871–14878.

Ullu, E., and Tschudi, C. (1984). Alu sequences are processed 7SL RNA genes. Nature *312*, 171–172.

Ullu, E., and Weiner, A.M. (1985). Upstream sequences modulate the internal promoter of the human 7SL RNA gene. Nature *318*, 371–374.

Valente, E.M., Abou-Sleima, P.M., Caputo, V., Muqit, M.M.K., Harvey, K., Gispert, S., Ali, Z., Del Turco, D., Bentivoglio, A.R., Healy, D.G., et al. (2004). Hereditary Early-Onset Parkinson's Disease Caused by Mutations in PINK1. Science *304*, 1158–1160.

Vanhée-Brossollet, C., and Vaquero, C. (1998). Do natural antisense transcripts make sense in eukaryotes? Gene *211*, 1–9.

Vassetzky, N.S., Ten, O.A., and Kramerov, D.A. (2003). B1 and related SINEs in mammalian genomes. Gene *319*, 149–160.

Vattem, K.M., and Wek, R.C. (2004). Reinitiation involving upstream ORFs regulates ATF4 mRNA translation in mammalian cells. Proc. Natl. Acad. Sci. U. S. A. *101*, 11269–11274.

Veniaminova, N.A., Vassetzky, N.S., and Kramerov, D.A. (2007). B1 SINEs in different rodent families. Genomics *89*, 678–686.

Voineagu, I., Narayanan, V., Lobachev, K.S., and Mirkin, S.M. (2008). Replication stalling at unstable inverted repeats: interplay between DNA hairpins and fork stabilizing proteins. Proc. Natl. Acad. Sci. U. S. A. *105*, 9936–9941.

Vulliamy, T., Marrone, A., Goldman, F., Dearlove, A., Bessler, M., Mason, P.J., and Dokal, I. (2001). The RNA component of telomerase is mutated in autosomal dominant dyskeratosis congenita. Nature *413*, 432–435.

Wagner, S.D., Kugel, J.F., and Goodrich, J.A. (2009). TFIIF Facilitates Dissociation of RNA Polymerase II from Noncoding RNAs That Lack a Repression Domain. Mol. Cell. Biol. *30*, 91–97.

Wahlestedt, C. (2006). Natural antisense and noncoding RNA transcripts as potential drug targets. Drug Discov. Today *11*, 503–508.

Wahlestedt, C. (2013). Targeting long non-coding RNA to therapeutically upregulate gene expression. Nat. Rev. Drug Discov. *12*, 433–446.

Wang, G., and Reinke, V. (2008). A C. elegans Piwi, PRG-1, Regulates 21U-RNAs during Spermatogenesis. Curr. Biol. *18*, 861–867.

Wang, K.C., and Chang, H.Y. (2011). Molecular Mechanisms of Long Noncoding RNAs. Mol. Cell *43*, 904–914.

Wang, D., Garcia-Bassets, I., Benner, C., Li, W., Su, X., Zhou, Y., Qiu, J., Liu, W., Kaikkonen, M.U., Ohgi, K.A., et al. (2011a). Reprogramming transcription by distinct classes of enhancers functionally defined by eRNA. Nature *474*, 390–394.

Wang, R., Iwakura, Y., Araki, K., Sotoyama, H., Takei, N., and Nawa, H. (2011b). In vitro production of an active neurotrophic factor, neuregulin-1: Qualitative comparison of different cell-free translation systems. Neurosci. Lett. *497*, 90–93.

Wapinski, O., and Chang, H.Y. (2011). Long noncoding RNAs and human disease. Trends Cell Biol. *21*, 354–361.

Watanabe, T., Totoki, Y., Toyoda, A., Kaneda, M., Kuramochi-Miyagawa, S., Obata, Y., Chiba, H., Kohara, Y., Kono, T., Nakano, T., et al. (2008). Endogenous siRNAs from naturally formed dsRNAs regulate transcripts in mouse oocytes. Nature *453*, 539–543.

Wei, W., Gilbert, N., Ooi, S.L., Lawler, J.F., Ostertag, E.M., Kazazian, H.H., Boeke, J.D., and Moran, J.V. (2001). Human L1 Retrotransposition: cis Preference versus trans Complementation. Mol. Cell. Biol. *21*, 1429–1439.

Weichenrieder, O., Wild, K., Strub, K., and Cusack, S. (2000). Structure and assembly of the Alu domain of the mammalian signal recognition particle. Nature *408*, 167–173.

Weil, D., Power, M.-A., Webb, G.C., and Li, C.L. (1997). Antisense transcription of a murine FGFR-3 pseudogene duringfetaldevelopment. Gene *187*, 115–122.

Whittaker, J.W. (2012). Cell-free protein synthesis: the state of the art. Biotechnol. Lett. *35*, 143–152.

Wilkinson, K.D., Lee, K.M., Deshpande, S., Duerksen-Hughes, P., Boss, J.M., and Pohl, J. (1989). The neuron-specific protein PGP 9.5 is a ubiquitin carboxyl-terminal hydrolase. Science *246*, 670–673.

Williams, J.M., Beck, T.F., Pearson, D.M., Proud, M.B., Cheung, S.W., and Scott, D.A. (2009). A 1q42 deletion involving DISC1, DISC2, and TSNAX in an autism spectrum disorder. Am. J. Med. Genet. A. *149A*, 1758–1762.

Wilson, G.M., Vasa, M.Z., and Deeley, R.G. (1998). Stabilization and cytoskeletal-association of LDL receptor mRNA are mediated by distinct domains in its 3′ untranslated region. J. Lipid Res. *39*, 1025–1032.

Wu, Q., Kim, Y.C., Lu, J., Xuan, Z., Chen, J., Zheng, Y., Zhou, T., Zhang, M.Q., Wu, C.-I., and Wang, S.M. (2008). Poly A- Transcripts Expressed in HeLa Cells. PLoS ONE *3*, e2803.

Wutz, A., Rasmussen, T.P., and Jaenisch, R. (2002). Chromosomal silencing and localization are mediated by different domains of Xist RNA. Nat. Genet. *30*, 167–174.

Young, T.L., Matsuda, T., and Cepko, C.L. (2005). The Noncoding RNA Taurine Upregulated Gene 1 Is Required for Differentiation of the Murine Retina. Curr. Biol. *15*, 501–512.

Yu, W., Gius, D., Onyango, P., Muldoon-Jacobs, K., Karp, J., Feinberg, A.P., and Cui, H. (2008). Epigenetic silencing of tumour suppressor gene p15 by its antisense RNA. Nature *451*, 202–206.

Yu, W.H., Cuervo, A.M., Kumar, A., Peterhoff, C.M., Schmidt, S.D., Lee, J.-H., Mohan, P.S., Mercken, M., Farmery, M.R., Tjernberg, L.O., et al. (2005). Macroautophagy--a novel -amyloid peptide-generating pathway activated in Alzheimer's disease. J. Cell Biol. *171*, 87–98.

Zhou, B.-S., Beidler, D.R., and Cheng, Y.-C. (1992). Identification of antisense RNA transcripts from a human DNA topoisomerase I pseudogene. Cancer Res. *52*, 4280–4285.

Zietkiewicz, E., Richer, C., Sinnett, D., and Labuda, D. (1998). Monophyletic origin of Alu elements in primates. J. Mol. Evol. *47*, 172–182.

Zimprich, A., Biskup, S., Leitner, P., Lichtner, P., Farrer, M., Lincoln, S., Kachergus, J., Hulihan, M., Uitti, R.J., Calne, D.B., et al. (2004). Mutations in LRRK2 cause autosomal-dominant parkinsonism with pleomorphic pathology. Neuron *44*, 601–607.

LETTER

doi:10.1038/nature11508

Long non-coding antisense RNA controls *Uchl1* translation through an embedded SINEB2 repeat

Claudia Carrieri[1]*, Laura Cimatti[1]*, Marta Biagioli[1,2], Anne Beugnet[3], Silvia Zucchelli[1,2], Stefania Fedele[1], Elisa Pesce[3], Isidre Ferrer[4], Licio Collavin[5,6], Claudio Santoro[7], Alistair R. R. Forrest[8], Piero Carninci[8], Stefano Biffo[3,9], Elia Stupka[10] & Stefano Gustincich[1,2]

Most of the mammalian genome is transcribed[1–3]. This generates a vast repertoire of transcripts that includes protein-coding messenger RNAs, long non-coding RNAs (lncRNAs) and repetitive sequences, such as SINEs (short interspersed nuclear elements). A large percentage of ncRNAs are nuclear-enriched with unknown function[4]. Antisense lncRNAs may form sense–antisense pairs by pairing with a protein-coding gene on the opposite strand to regulate epigenetic silencing, transcription and mRNA stability[5–10]. Here we identify a nuclear-enriched lncRNA antisense to mouse ubiquitin carboxy-terminal hydrolase L1 (*Uchl1*), a gene involved in brain function and neurodegenerative diseases[11]. Antisense *Uchl1* increases UCHL1 protein synthesis at a post-transcriptional level, hereby identifying a new functional class of lncRNAs. Antisense *Uchl1* activity depends on the presence of a 5′ overlapping sequence and an embedded inverted SINEB2 element. These features are shared by other natural antisense transcripts and can confer regulatory activity to an artificial antisense to green fluorescent protein. Antisense *Uchl1* function is under the control of stress signalling pathways, as mTORC1 inhibition by rapamycin causes an increase in UCHL1 protein that is associated to the shuttling of antisense *Uchl1* RNA from the nucleus to the cytoplasm. Antisense *Uchl1* RNA is then required for the association of the overlapping sense protein-coding mRNA to active polysomes for translation. These data reveal another layer of gene expression control at the post-transcriptional level.

To discover non-coding antisense transcripts of sense–antisense (S–AS) pairs expressed in the brain, the mouse syntenic loci of genes involved in neurodegenerative diseases were identified computationally and examined in the Ensembl browser (http://www.ensembl.org). The FANTOM2 clone 6430596G22 was classified as a spliced antisense lncRNA of the *Uchl1* gene[11]; we refer to this as antisense *Uchl1*. UCHL1 is a neuron-restricted protein that acts as a deubiquitinating enzyme, ubiquitin ligase or monoubiquitin stabilizer[12]. An in-frame deletion in the *Uchl1* gene, as in gracile axonal dystrophy mice, leads to ataxia and axonal degeneration. Although an association of *UCHL1* gene mutations to familial Parkinson's disease has not been confirmed in independent families, oxidative inactivation of UCHL1 protein has been reported in Parkinson's disease and Alzheimer's disease brains[13–15].

Antisense *Uchl1* is a 5′ head-to-head transcript that initiates within the second intron of *Uchl1* and overlaps the first 73 nucleotides of the sense mRNA including the AUG codon. By 5′ rapid amplification of cDNA ends (RACE), the transcriptional start site (TSS) of antisense *Uchl1* was mapped to the second intron of *Uchl1* (Fig. 1a). The non-overlapping part of the transcript contains two embedded repetitive sequences, SINEB1 of the F1 subclass (Alu) and SINEB2 of the B3 subclass, identified by Repeatmasker[16–18]. The FANTOM2 clone spans a genomic region of 70 kilobases (kb) (Fig. 1a) and its genomic organization is conserved in mammals (Supplementary Fig. 1a).

Sense and antisense *Uchl1* expression in mouse and human tissues was similar (Fig. 1b and Supplementary Fig. 1b). In the mouse, antisense *Uchl1* RNA was highly expressed in the ventral midbrain (Fig. 1b) and in the MN9D dopaminergic cell line (data not shown). Mature *Uchl1* mRNA was observed mainly in the cytoplasm of dopaminergic neurons, whereas antisense *Uchl1* was enriched in the nucleus (Fig. 1c and Supplementary Fig. 2). Antisense *Uchl1* expression was confirmed by qRT–PCR from dopaminergic neurons purified with laser capture microdissection (LCM, Supplementary Fig. 3).

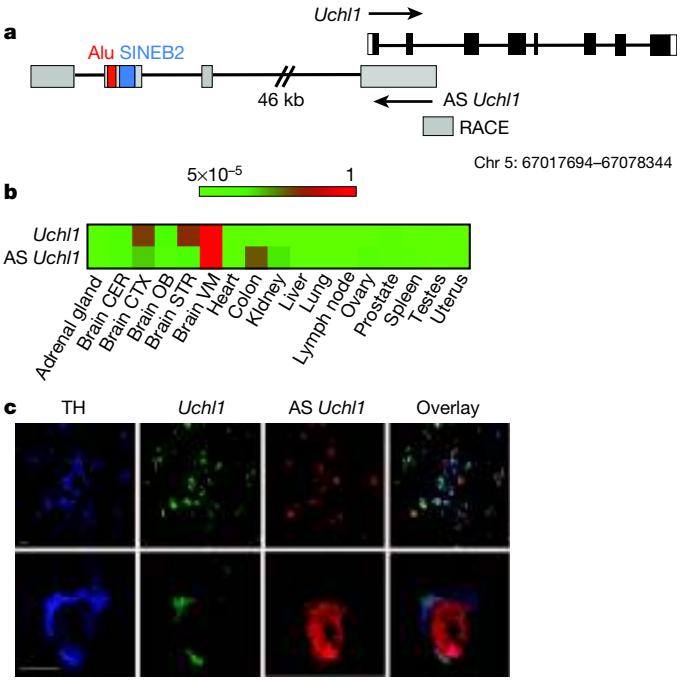

Figure 1 | Expression of antisense *Uchl1* in dopaminergic neurons. a, *Uchl1*/antisense (AS) *Uchl1* genomic organization. *Uchl1* exons are in black; 3′ and 5′ UTRs are in white; antisense *Uchl1* exons are grey; repetitive elements are in red (Alu) and blue (SINEB2). Introns are indicated as lines. **b**, Quantitative expression of *Uchl1* and antisense *Uchl1* in mouse tissues ($\Delta\Delta Ct/\Delta\Delta Ct_{max}$). CER, cerebellum; CTX, cortex; OB, olfactory bulb; STR, striatum; VM, ventral midbrain. **c**, Antisense *Uchl1* (red) and *Uchl1* (green) transcripts are expressed in the nucleus and cytoplasm of TH-positive dopaminergic neurons of the substantia nigra (blue).

[1]Area of Neuroscience, International School for Advanced Studies (SISSA), via Bonomea 265, 34136 Trieste, Italy. [2]The Giovanni Armenise-Harvard Foundation Laboratory, via Bonomea 265, 34136 Trieste, Italy. [3]Laboratory of Molecular Histology and Cell Growth, DIBIT, San Raffaele Scientific Institute, Via Olgettina 58, 20132 Milan, Italy. [4]Institute of Neuropathology, IDIBELL-University Hospital of Bellvitge, Carrer Feixa Llarga sn, 08907 Hospitalet de Llobregat, Spain. [5]Laboratorio Nazionale Consorzio Interuniversitario Biotecnologie (LNCIB), Area Science Park, Padriciano 99, 34149 Trieste, Italy. [6]Department of Life Sciences (DSV), University of Trieste, via Giorgeri 1, 34129 Trieste, Italy. [7]Department of Health Sciences, University of Eastern Piedmont, Viale Solaroli 17, 28100 Novara, Italy. [8]Omics Science Center, RIKEN Yokohama Institute, 1-7-22 Suehiro-chô, Tsurumi-ku, Yokohama, Kanagawa 230-0045, Japan. [9]Department of Environmental and Life Sciences, University of Eastern Piedmont, Viale T. Michel 11, 15121 Alessandria, Italy. [10]Center for Translational Genomics and Bioinformatics, San Raffaele Scientific Institute, Via Olgettina 58, 20132 Milan, Italy.
*These authors contributed equally to this work.

Transient expression of antisense *Uchl1* in MN9D cells caused no significant change in endogenous *Uchl1* mRNA expression. Notably, a strong and reproducible upregulation of UCHL1 protein was detected within 24 h (Fig. 2a). When increasing amounts of antisense *Uchl1* were co-transfected with murine *Uchl1* into HEK cells, which do not express either transcript, dose-dependent UCHL1 protein upregulation was recorded in the absence of any significant change in the quantity of exogenous *Uchl1* mRNA (Fig. 2b). These data indicate that antisense *Uchl1* regulates UCHL1 expression at a post-transcriptional level.

Antisense *Uchl1* deletion constructs lacking the 5′ first exon (antisense *Uchl1*(Δ5′)) or the last three exons (antisense *Uchl1*(Δ3′)) failed to induce UCHL1 protein in MN9D and HEK cells, suggesting that both 5′ and 3′ components are important to antisense *Uchl1* function (Fig. 2c and Supplementary Fig. 4a). Targeted deletion of the region containing the embedded SINEB2 and Alu repetitive sequences (ΔAS) was also able to prevent UCHL1 protein induction. Deletion of each repetitive element separately revealed that SINEB2 is the functional unit required by antisense *Uchl1* for increasing UCHL1 protein synthesis (Fig. 2d). In all cases no change in *Uchl1* mRNA level was detected (Supplementary Fig. 4b). A mutant with a flipped SINEB2 sequence was unable to increase UCHL1 protein levels, thus proving the orientation-dependent activity of the SINEB2 domain embedded within antisense *Uchl1* (Fig. 2d). Importantly, an artificial construct containing the 73-nucleotide overlapping sequence immediately close to the repetitive elements in antisense *Uchl1*(Δ5′) increased UCHL1 levels as much as the full-length clone (Fig. 2e and Supplementary Fig. 4c).

We then considered whether other SINEB2-containing lncRNAs may post-transcriptionally regulate the expression of their protein-coding partner, on the basis of similar structural elements. The FANTOM3 collection of non-coding cDNAs was bioinformatically screened for natural antisense transcripts that contain SINEB2 elements of the B3 subclass in the correct orientation and 5′ head-to-head overlapping to a protein-coding gene. This identified 31 S–AS pairs similar to the *Uchl1*/antisense *Uchl1* structure (Supplementary Fig. 5). By sequence alignment, we chose antisense *Uxt* (4833404H03), antisense of ubiquitously expressed transcript (*Uxt*), as the one with the most similar SINEB2 elements (Fig. 3a). Transfection of antisense *Uxt* in MN9D cells elicited an increase of UXT protein level with no change in *Uxt* mRNA (Fig. 3b), indicating that antisense *Uxt* was similarly able to increase protein levels post-transcriptionally.

These data indicate a model whereby lncRNAs regulate protein synthesis through the combined activities of two domains. The 5′ antisense

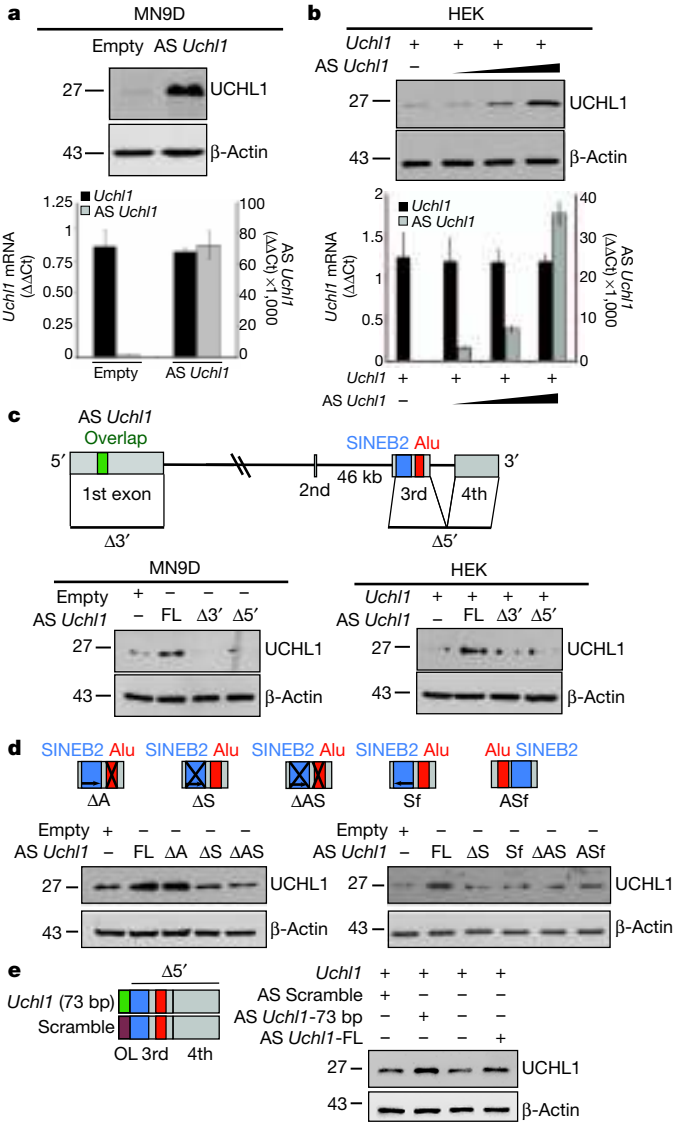

Figure 2 | Antisense *Uchl1* regulates UCHL1 protein levels via an embedded inverted SINEB2 element. **a**, Antisense *Uchl1*-transfected dopaminergic MN9D cells show increased levels of endogenous UCHL1 protein, with unchanged mRNA quantity. **b**, Increasing doses of transfected antisense *Uchl1* titrate UCHL1 protein but not mRNA levels in HEK cells. Data in **a** and **b** indicate mean ± s.d., $n \geq 3$. **c**, Full-length (FL) antisense *Uchl1* is required for regulating endogenous (MN9D cells, left panel) and overexpressed (HEK cells, right panel) UCHL1 protein levels. Scheme of Δ5′ or Δ3′ deletion mutants is shown. **d**, Inverted SINEB2 is sufficient to control endogenous UCHL1 protein levels in MN9D cells. Scheme of mutants is shown in 5′ to 3′ orientation. ΔA, ΔAlu; ΔS, ΔSINEB2; ΔAS, ΔAlu+SINEB2; Sf, SINEB2 flipped; ASf, Alu+SINEB2 flipped. **e**, A 73-bp overlap (OL) of antisense *Uchl1* is sufficient to increase UCHL1 in transfected HEK cells. Scheme of mutant and scramble control in 5′ to 3′ orientation. Units for numbers along the left of gels in **a**–**e** indicate kDa.

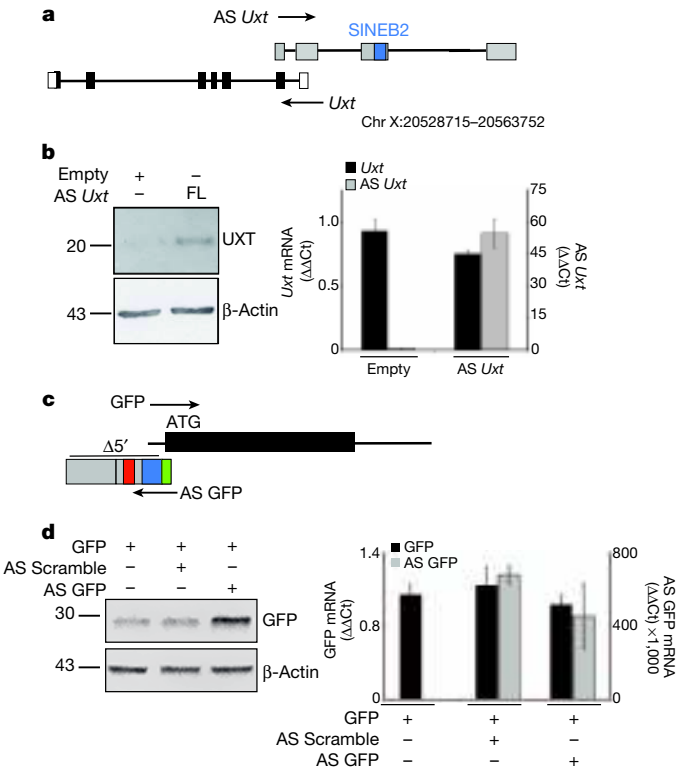

Figure 3 | Natural and synthetic antisense lncRNAs increase target protein levels. **a**, Scheme of *Uxt*/antisense *Uxt* genomic organization. **b**, Antisense *Uxt* increases endogenous UXT protein levels (left) without affecting RNA levels (right) in transfected MN9D cells. **c**, Scheme of antisense GFP construct. Δ5′ with repetitive elements (SINEB2, blue; Alu, red) and overlap (green) regions is indicated. **d**, Inverted SINEB2 plus the overlap sequence increase GFP levels in transfected cells. Data in **b** and **d** indicate mean ± s.d., $n \geq 3$.

region provides specificity for the sense target gene whereas the repetitive element confers the protein synthesis activation domain. The model predicts that by swapping the overlapping sequence one may increase the amount of proteins encoded by the mRNAs of choice acting at the post-transcriptional level. We thus synthesized a 72-nucleotide-long artificial sequence antisense to the AUG-containing region as transcribed from pEGFP, and inserted it into antisense *Uchl1*(Δ5′) to generate antisense GFP (Fig. 3c). Co-transfection of antisense GFP with pEGFP strongly increased GFP protein but not mRNA levels in HEK cells (Fig. 3d). When we pulsed cells with methionine for an hour and immunoprecipitated GFP, antisense GFP induced an increase in radioactively labelled, neo-synthesized GFP, without affecting mRNA levels (Supplementary Fig. 6).

To understand how the antisense *Uchl1* transcript operates and the physiological conditions in which it might act, we assayed several stimuli and/or drugs for their ability to modulate UCHL1 protein expression. Inhibition of mTORC1 signalling favoured an increase in UCHL1 levels in a range from 1.5- to 2.5-fold (Fig. 4a). This effect was evident with as low as 20 nM rapamycin (Supplementary Fig. 7) and was concomitant with dephosphorylation of mTOR targets p70S6K and 4E-BP1. Furthermore, the effect was not due to a stabilization of the protein, as co-application of cycloheximide decreased UCHL1 protein levels (Supplementary Fig. 8a). These data are surprising because rapamycin impairs formation of the CAP-dependent complex and hence translation of highly structured mRNAs[19]. However, in agreement with previous reports, in our experimental settings mTORC1 inhibition only slightly impairs the global rate of translation (Supplementary Fig. 8b). Under these conditions, it has been proposed that rapamycin may affect competition among different mRNAs[20]. If so, we proposed that inhibition of the CAP complex formation favours the translation of *Uchl1* mRNA with a mechanism that requires antisense *Uchl1*.

To test this model, we used two complementary approaches to establish a loss-of-function phenotype. First, we downregulated antisense *Uchl1* levels with short hairpin RNA (shRNA) targeting its promoter region. MN9D cells constitutively expressing shRNA for antisense *Uchl1* did not show any changes in UCHL1 protein levels upon rapamycin treatment, whereas scramble control cells showed UCHL1 upregulation as in the parental line (Fig. 4b). Dephosphorylation of p70S6K and 4E-BP1 proved that rapamycin inhibited mTOR activity as expected. We then exploited the dominant-negative property of an antisense *Uchl1* mutant lacking the SINEB2 repeat element. Overexpression of antisense *Uchl1*(ΔSINEB2) inhibited the ability of full-length antisense *Uchl1* to increase protein levels (Supplementary Fig. 9). Upon rapamycin treatment, cells stably expressing antisense *Uchl1*(ΔSINEB2) did not show any UCHL1 protein induction despite dephosphorylation of mTOR targets (Fig. 4c). These complementary experiments prove that functional antisense expression is required for UCHL1 protein increase elicited by rapamycin.

Because antisense *Uchl1* transcript is enriched in the nucleus of dopaminergic neurons, we measured antisense *Uchl1* and *Uchl1* RNA content in the nucleus and cytoplasm of MN9D cells upon rapamycin treatment. As shown in Fig. 4d, rapamycin substantially increased antisense *Uchl1* concentration in the cytoplasmic fraction. This effect was confirmed by a concomitant decrease in its nuclear steady-state levels, and by the absence of any *de novo* transcription. The total content of primary and spliced transcripts remained constant (data not shown). *Uchl1* mRNA showed no change in subcellular distribution, *de novo* transcription or total cellular content. These data demonstrate that antisense *Uchl1* localization can be regulated by the mTOR pathway, and its cytoplasmic level correlates with the expression of UCHL1 protein.

We therefore monitored the association of *Uchl1* mRNA with polysomes to assess the role of translation in antisense *Uchl1*-mediated UCHL1 protein induction. Fractionated MN9D cell extracts were used to measure the recruitment of *Uchl1* mRNA on polysomes by

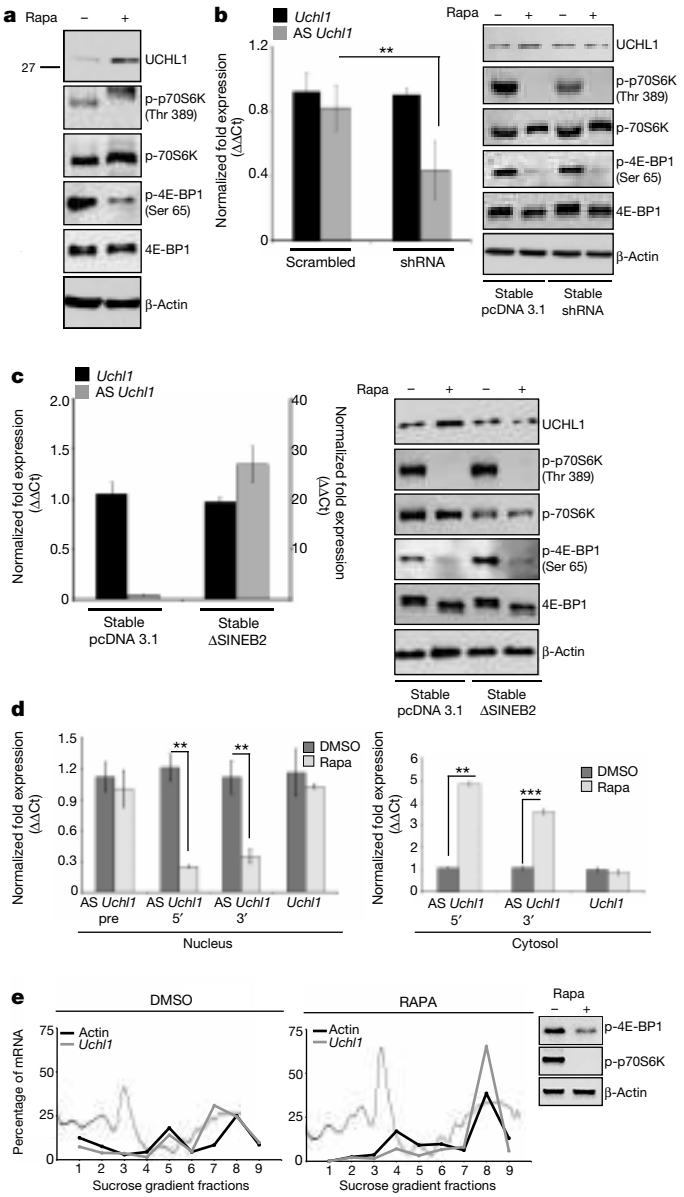

Figure 4 | Antisense *Uchl1* mediates UCHL1 protein induction by rapamycin. **a**, UCHL1 protein level is increased in rapamycin-treated MN9D cells. Rapamycin inhibition of mTOR pathway is verified with anti-p-p70S6K and anti-p-4E-BP1 antibodies. **b**, Silencing antisense *Uchl1* transcription (shRNA) in MN9D cells inhibits rapamycin-induced UCHL1 protein level. Left, mRNA levels; right, protein levels. **c**, Deletion of embedded SINEB2 (ΔSINEB2) is sufficient to inhibit rapamycin-induced UCHL1 protein upregulation. **d**, Antisense *Uchl1* translocates to the cytoplasm upon rapamycin treatment in MN9D cells. mRNA levels were measured with 5′ or 3′ primers. Data in **b**–**d** indicate mean ± s.d., $n \geq 3$. $^{**}P < 0.01$; $^{***}P < 0.005$. **e**, Rapamycin increases *Uchl1* mRNA in heavy polysomes; the absorbance profile is outlined in the background of each plot.

qRT–PCR and northern blotting (Fig. 4e and Supplementary Fig. 10). In basal conditions, *Uchl1* mRNA was associated with translating ribosomes. Rapamycin treatment induced a shift of *Uchl1* mRNA to heavier polysomes, consistent with an enhanced rate of translation initiation; this increase of *Uchl1* mRNA association to heavier polysomes did not occur in cells overexpressing the dominant-negative form of antisense *Uchl1* (Supplementary Fig. 11).

Antisense *Uchl1* is the representative member of a new functional class of lncRNAs that are part of S–AS pairs in the mammalian genome that require overlap at the 5′ end and the action of a SINEB2 repeat. This new function for SINEB2 sequences in the cytoplasm adds to their

well-established role in the nucleus as inhibitors of RNA polymerase II[16]. Stress-dependent nucleocytoplasmic shuttling of lncRNAs may be a common strategy to regulate translation, as CTN-RNA, another nuclear-retained lncRNA, was found to have a cryptic protein-coding sequence at its 3′ end when in the cytoplasm[21].

It is intriguing that this nuclear lncRNA-mediated mechanism for post-transcriptional control of gene expression is active when CAP-dependent translation is inhibited by rapamycin. This drug blocks mTORC1 kinase, which activates the eIF4F complex[19,22]. However, some mRNAs escape mTORC1 inhibition by being able to be recruited to ribosomes in an eIF4F-independent manner for presenting complex mRNA loops that function as internal ribosomal entry sites (IRES)[23]. Indeed, IRES-mediated translation is prominent in conditions of stress or growth factor inhibition and its alteration affects processes such as tumorigenesis[22,24]. In genetic and neurochemical models of Parkinson's disease, mTORC1 inhibition protects dopaminergic neurons from apoptosis[25,26].

Antisense lncRNA-mediated translation may be another mechanism to maintain synthesis of pro-survival proteins, such as UCHL1, that are involved in rapamycin neuroprotective function and more generally in cellular response to stress. This mechanism may represent the outcome of an evolutionary pressure on the genomic organization of anti-stress elements to favour gene-specific regulation of translation when CAP-dependent initiation is reduced. Finally, natural and synthetic antisense transcripts with embedded repetitive elements may represent molecular tools to increase translation of selected mRNAs, defining a potential new class of RNA therapeutics.

METHODS SUMMARY

5′ RACE for antisense *Uchl1* was performed with Gene Racer (Invitrogen). Double-fluorescence *in situ* hybridization of biotin- and digoxigenin-labelled probes was detected using fluorochrome-conjugated reagents. Images were captured with Confocal Laser Microscopy (LEICA). Expression of antisense *Uchl1* was performed on neuronal cells lines and dopaminergic neurons purified with LCM from TH-GFP mice. Cell lines were cultured under standard conditions. shRNA targeting the promoter of antisense *Uchl1* was cloned in pSUPERIOR.Neo.GFP vector (Oligo Engine). Polysomes were prepared by sucrose gradient and associated *Uchl1* mRNA was measured by qRT–PCR and northern blotting.

Full Methods and any associated references are available in the online version of the paper.

Received 3 December 2010; accepted 14 August 2012.
Published online 14 October 2012.

1. Birney, E. *et al.* Identification and analysis of functional elements in 1% of the human genome by the ENCODE pilot project. *Nature* **447,** 799–816 (2007).
2. The FANTOM Consortium. The transcriptional landscape of the mammalian genome. *Science* **309,** 1559–1563 (2005).
3. Kapranov, P., Willingham, A. T. & Gingeras, T. R. Genome-wide transcription and the implications for genomic organization. *Nature Rev. Genet.* **8,** 413–423 (2007).
4. Kapranov, P. *et al.* RNA maps reveal new RNA classes and a possible function for pervasive transcription. *Science* **316,** 1484–1488 (2007).
5. Beltran, M. *et al.* A natural antisense transcript regulates Zeb2/Sip1 gene expression during Snail1-induced epithelial-mesenchymal transition. *Genes Dev.* **22,** 756–769 (2008).
6. Ebralidze, A. K. *et al.* PU.1 expression is modulated by the balance of functional sense and antisense RNAs regulated by a shared cis-regulatory element. *Genes Dev.* **22,** 2085–2092 (2008).
7. Hastings, M. L., Ingle, H. A., Lazar, M. A. & Munroe, S. H. Post-transcriptional regulation of thyroid hormone receptor expression by cis-acting sequences and a naturally occurring antisense RNA. *J. Biol. Chem.* **275,** 11507–11513 (2000).
8. Huarte, M. *et al.* A large intergenic noncoding RNA induced by p53 mediates global gene repression in the p53 response. *Cell* **142,** 409–419 (2010).
9. Katayama, S. *et al.* Antisense transcription in the mammalian transcriptome. *Science* **309,** 1564–1566 (2005).
10. Spigoni, G., Gedressi, C. & Mallamaci, A. Regulation of Emx2 expression by antisense transcripts in murine cortico-cerebral precursors. *PLoS ONE* **5,** e8658 (2010).
11. Setsuie, R. & Wada, K. The functions of UCH-L1 and its relation to neurodegenerative diseases. *Neurochem. Int.* **51,** 105–111 (2007).
12. Liu, Y., Fallon, L., Lashuel, H. A., Liu, Z. & Lansbury, P. T. Jr. The UCH-L1 gene encodes two opposing enzymatic activities that affect α-synuclein degradation and Parkinson's disease susceptibility. *Cell* **111,** 209–218 (2002).
13. Barrachina, M. *et al.* Reduced ubiquitin C-terminal hydrolase-1 expression levels in dementia with Lewy bodies. *Neurobiol. Dis.* **22,** 265–273 (2006).
14. Barrachina, M. *et al.* Amyloid-β deposition in the cerebral cortex in dementia with Lewy bodies is accompanied by a relative increase in AβPP mRNA isoforms containing the Kunitz protease inhibitor. *Neurochem. Int.* **46,** 253–260 (2005).
15. Choi, J. *et al.* Oxidative modifications and down-regulation of ubiquitin carboxyl-terminal hydrolase L1 associated with idiopathic Parkinson's and Alzheimer's diseases. *J. Biol. Chem.* **279,** 13256–13264 (2004).
16. Nishihara, H., Smit, A. F. & Okada, N. Functional noncoding sequences derived from SINEs in the mammalian genome. *Genome Res.* **16,** 864–874 (2006).
17. Ponicsan, S. L., Kugel, J. F. & Goodrich, J. A. Genomic gems: SINE RNAs regulate mRNA production. *Curr. Opin. Genet. Dev.* **20,** 149–155 (2010).
18. Quentin, Y. Fusion of a free left Alu monomer and a free right Alu monomer at the origin of the Alu family in the primate genomes. *Nucleic Acids Res.* **20,** 487–493 (1992).
19. Andrei, M. A. *et al.* A role for eIF4E and eIF4E-transporter in targeting mRNPs to mammalian processing bodies. *RNA* **11,** 717–727 (2005).
20. Merrick, W. C. Eukaryotic protein synthesis: still a mystery. *J. Biol. Chem.* **285,** 21197–21201 (2010).
21. Prasanth, K. V. *et al.* Regulating gene expression through RNA nuclear retention. *Cell* **123,** 249–263 (2005).
22. Holcik, M. & Sonenberg, N. Translational control in stress and apoptosis. *Nature Rev. Mol. Cell Biol.* **6,** 318–327 (2005).
23. Gilbert, W. V. Alternative ways to think about cellular internal ribosome entry. *J. Biol. Chem.* **285,** 29033–29038 (2010).
24. Yoon, A. *et al.* Impaired control of IRES-mediated translation in X-linked dyskeratosis congenita. *Science* **312,** 902–906 (2006).
25. Malagelada, C., Jin, Z. H., Jackson-Lewis, V., Przedborski, S. & Greene, L. A. Rapamycin protects against neuron death in *in vitro* and *in vivo* models of Parkinson's disease. *J. Neurosci.* **30,** 1166–1175 (2010).
26. Santini, E., Heiman, M., Greengard, P., Valjent, E. & Fisone, G. Inhibition of mTOR signaling in Parkinson's disease prevents L-DOPA-induced dyskinesia. *Sci. Signal.* **2,** ra36 (2009).

Supplementary Information is available in the online version of the paper.

Acknowledgements We thank S.G. laboratory members for thought-provoking discussions and C. Leonesi for technical help. We thank F. Persichetti, A. Mallamaci, E. Calautti, S. Saoncella, A. Lunardi, D. De Pietri Tonelli, R. Sanges, M. E. MacDonald and T. Perlmann for support and discussions; and M. J. Zigmond and B. Joseph for sharing the MN9D cell line. This work was supported by the FP7 Dopaminet to S.G., E.S. and P.C., by The Giovanni Armenise-Harvard Foundation to S.G. and by the Compagnia di San Paolo to S.B.

Author Contributions C.C. designed and performed the experiments, and analysed the results; L.Ci. designed and performed the experiments, and analysed the results; M.B. designed and performed the experiments, and analysed the results; A.B. prepared polysomes; S.Z. designed the experiments, analysed the results and wrote the manuscript; S.F. carried out qRT–PCR on polysome fractions and the pulse labelling experiment; E.P. prepared polysomes and carried out northern blotting; I.F. analysed the results; L.Co. designed the experiments and analysed the results; C.S. analysed the data and discussed the results; A.R.R.F. performed bioinformatic analysis for the identification of SINEB2 and family members and designed ΔAlu and ΔSINEB2 mutants; P.C. provided reagents, experimental design and managing; S.B. designed polysome experiments, analysed the data and wrote the manuscript; E.S. performed bioinformatic analysis for the identification of S–AS pairs, designed experiments for the analysis of antisense *Uchl1* expression and analysed the results; S.G. designed the experiments, analysed the results and wrote the paper.

Author Information Reprints and permissions information is available at www.nature.com/reprints. The authors declare competing financial interests: details are available in the online version of the paper. Readers are welcome to comment on the online version of the paper. Correspondence and requests for materials should be addressed to S.G. (gustinci@sissa.it).

METHODS

Oligonucleotides. The complete list of oligonucleotides used for cloning and for quantitative real-time PCR experiments is included in Supplementary Information (Supplementary Fig. 12).

Plasmids. Full-length DNA sequence of antisense *Uchl1* was amplified via fusion PCR starting from RACE fragment and FANTOM clone 6430596G22 (GenBank AK078321.1) with forward mouse antisense *Uchl1* FL and reverse mouse antisense *Uchl1* FL primers.

Mouse *Uchl1* mRNA was subcloned from FANTOM clone 2900059O22 (GenBank AK013729.1) in the unique PmeI site of pcDNA3.1.

cDNA sequence of human antisense *UCHL1* was amplified from a sample of human brain total RNA (Clontech, 636530) with the primers human 5′F and human 3′R.

Oligonucleotides that target the sequence −14/+3 around the TSS of antisense *Uchl1* were annealed and cloned into pSUPERIOR.Neo.GFP vector (OligoEngine) in the BglII/XhoI site. Scrambled sequence was also cloned and used as control.

The antisense *Uchl1* 5′ deletion mutant (Δ5′) was generated by PCR using the oligonucleotides forward mouse antisense *Uchl1*(Δ5′) and reverse mouse antisense *Uchl1* FL. PCR fragment was cloned in the unique EcoRI site in pcDNA3.1.

The antisense *Uchl1* 3′ deletion mutant (Δ3′) was generated by PCR using the forward mouse antisense *Uchl1* FL and reverse mouse antisense *Uchl1*(Δ3′) primers and cloned in the unique EcoRI site in pcDNA3.1.

The antisense *Uchl1*(ΔAS) (ΔAlu + SINEB2) mutant was obtained by subsequent cloning of PCR fragment I (NheI–EcoRI site) and PCR fragment II (EcoRI–HindIII site) into pcDNA3.1. Primers forward mouse antisense *Uchl1* FL Nhe and reverse pre-SINE B2 EcoRI were used to generate fragment I; primers forward post-ALU EcoRI and reverse mouse antisense FL HindIII were used for PCR fragment II.

The antisense *Uchl1*(ΔA) (ΔAlu, 1000–1045) mutant was generated with a similar strategy to antisense *Uchl1*(ΔAS). Forward mouse antisense *Uchl1* FL NheI and reverse pre-ALU EcoRI were used for PCR fragment I; forward post-ALU and reverse mouse antisense FL HindIII for PCR fragment II.

The antisense *Uchl1*(ΔS) (ΔSINEB2, 764–934) mutant was obtained with a similar strategy to antisense *Uchl1*(ΔAS). Oligonucleotides forward mouse AS *Uchl1* FL NheI and reverse pre-SINE B2 EcoRI for fragment I; forward post-SINE B2 EcoRI and reverse mouse AS FL HindIII for fragment II.

For antisense *Uchl1*(ASf) (Alu + SINEB2 flipped), PCR fragment obtained with the primers forward SINEB2 inside and reverse Alu flip was cloned in the unique EcoRI site of antisense *Uchl1*(ΔAS).

For antisense *Uchl1*(Sf) (SINEB2 flipped), PCR fragment obtained with forward SINE B2 inside and reverse SINE flip oligonucleotides was cloned in the unique EcoRI site of antisense *Uchl1* ΔSINEB2.

For antisense *Uchl1*(73 bp), the method of 'annealing and primer extension' of two 3′-end overlapping oligonucleotides was used to generate the 73-bp antisense *Uchl1* overlap region. Annealed fragment was obtained with antisense *Uchl1* 73 bp forward and antisense *Uchl1* 73 bp reverse. Fragment was digested with XhoI and EcoRV and ligated into antisense *Uchl1* Δ5′ plasmid.

The antisense SCR 73-bp mutant was obtained with a similar strategy as antisense *Uchl1*(73 bp). The annealing extension was performed with oligonucleotides with scramble (SCR) sequence (antisense SCR forward and antisense SCR reverse).

Full-length mouse antisense *Uxt* was amplified by PCR starting from FANTOM clone 4833404H03 (GenBank AK029359.1) with specific primers (forward mouse antisense *Uxt* and reverse mouse antisense *Uxt*). PCR fragment was subcloned into pcDNA3.1 using XbaI and HindIII restriction enzymes.

The antisense GFP plasmid was generated with a similar strategy as antisense *Uchl1*(73 bp). Seventy-two base pairs corresponding to nucleotide −40/+32 with respect to the ATG of GFP sequence in pEGFP-C2 vector (Clontech) were chosen as target sequence for artificial antisense DNA generation. For annealing, the GFP antisense forward and GFP antisense reverse primers were used.

Cells. MN9D cells were obtained from M. J. Zigmond. Cells were seeded in 100-mm dishes in Dulbecco's modified Eagle's (DMEM) medium containing 10% fetal bovine serum (Invitrogen) supplemented with penicillin (50 units ml^{-1}) and streptomycin (50 units ml^{-1}). For experiments, cells were plated in poly-L-lysine (P2636, Sigma) coated dishes and grown overnight. Approximately 50% confluent cells were treated with 1 μM rapamycin (R0395, Sigma) or DMSO vehicle for 45 min.

For the establishment of stable cell lines (shRNA -15/+4, shRNA scrambled, pcDNA 3.1- and AS Uchl1ΔSINEB2), MN9D cells were seeded in 100-mm Petri dishes and transfected with Lipofectamine 2000 (Invitrogen) according to the manufacturer's instruction. Stable clones were selected by 500 μM neomycin (N1142, Sigma). HEK cells (Sigma) were cultured under standard condition in DMEM containing 10% fetal bovine serum supplemented with antibiotics. Transient transfections were done with Lipofectamine 2000 (Invitrogen). For all experiments, S and AS plasmids were transfected at 1:6 ratio.

Animal handling. All animal experiments were performed in accordance with European guidelines for animal care and following SISSA Ethical Committee permissions. Mice were housed and bred in SISSA/CBM non-SPF animal facility, with 12 h dark/light cycles and controlled temperature and humidity. Mice had *ad libitum* access to food and water. C57BL/6 male mice ($n = 5$), 8–10 weeks old, were used for *in situ* hybridization experiments. Laser capture microdissection (LCM) of dopaminergic neurons was performed on 8–10-week-old male TH-GFP/21-31 mice ($n = 3$). Intra-cardiac perfusions were done under total anaesthesia.

RACE and multiplex RT–PCR. The 5′ UTR of antisense *Uchl1* was amplified by RACE PCR (GeneRacer, Invitrogen) by MN9D total RNA and cloned into pGEM-T Easy vector (Promega).

qRT–PCR. Total RNA was extracted from cells and mouse tissue samples (adrenal gland, cerebellum, cortex, olfactory bulb, striatum, ventral midbrain, heart, colon, kidney, lung, lymph node, ovary, prostate, spleen, testis, uterus) using Trizol reagent (Invitrogen) according to the manufacturer's instruction. An RNA panel of 20 different normal human tissues (pools consist of at least three tissue donors with full documentation on age, sex, race, cause of death) was obtained from Ambion (AM6000). All RNA samples were subjected to DNase I treatment (Ambion). A total of 1 μg of RNA was subjected to retrotranscription using iScript cDNA synthesis kit (BioRad) and Real Time qRT–PCR was carried out using SYBR green fluorescence dye (2× iQ5 SYBR Green supermix, BioRad). TATA-binding protein (TBP) and RNA polymerase II (RPII) were used as housekeeping genes to normalize different mouse and human tissues as tested by the GeNorm program, version 3.5 (http://medgen.ugent.be/genorm/)[27]. GAPDH and β-actin were used as normalizing controls in all the other qRT–PCR experiments. The amplified transcripts were quantified using the comparative Ct method and the differences in gene expression were presented as normalized fold expression (ΔΔCt). All of the experiments were performed in duplicate. A heat map graphical representation of rescaled normalized fold expression ($\Delta\Delta Ct/\Delta\Delta Ct_{max}$) was obtained by using Matrix2png (http://www.bioinformatics.ubc.ca/matrix2png/). A list of oligonucleotides used for qRT–PCR experiments is in Supplementary Fig. 12.

LCM technology. For LCM, regions of midbrain from TH-GFP/21-31 mice were dissected and incubated in 1× Zincfix solution for 6 h. They were then cryoprotected in 30% sucrose solution at 4 °C overnight, embedded in Neg-50 section medium, snap-frozen and left to equilibrate in a cryostat chamber at −21 °C for 1 h before sectioning, as described earlier[28]. Cryostat 14 μm midbrain coronal sections were thaw-mounted on Superfrost plus glass slides (Mezzle-Glasser) and dopaminergic GFP^+ cells were gathered via LCM and collected in microfuge (PALM adhesive caps). RNA was immediately extracted using the Absolutely RNA Nanoprep kit (Stratagene), eluted in RNase/DNase free water (Ambion) and retro-transcribed.

Two-colour *in situ* hybridization. After perfusion with 4% formaldehyde, mouse brain was cryoprotected overnight in 30% sucrose. *In situ* hybridization was performed on cryostat slices (16 μm). Sense and antisense probes were generated by *in vitro* transcription from the cDNA encoding the distal 600 bp of mouse *Uchl1* cDNA and the last 1,000 bp of mouse antisense *Uchl1*. The probes for *Uchl1* and antisense *Uchl1* were labelled with digoxigenin (DIG labelling, Roche) and biotin (BIO-labelling mix, Roche), respectively. Incorporation of biotin and digoxigenin was checked via a northern blot assay. *In situ* hybridization was performed as described previously[29]. Slices were pre-treated with 3% hydrogen peroxide for 30 min. Hybridization was performed with probes at a concentration of 1 μg ml^{-1} (*Uchl1*) and 3 μg ml^{-1} (antisense *Uchl1*) at 60 °C for 16 h. For biotinylated RNA detection, streptavidin-HRP (Amersham Bioscience) was used (1:250) for 2 h in TNB buffer (Tris HCl pH 7.5 100 mM, NaCl 150 mM, 0.5% blocking reagent), and signals were visualized using the TSA Cy3 system (Perkin Elmer) after washing in TNT buffer (Tris HCl pH 7.5 100 mM, NaCl 150 mM, 0.05% Tween-20). *In situ* hybridization on DIG-labelled probe was performed with monoclonal anti-DIG antibody after TSA reaction. To combine RNA *in situ* hybridization with immunofluorescence, slices were incubated with anti-tyrosine hydroxylase (TH) antibody 1:1,000 (Chemicon). Signals were then detected with fluorescent dye-conjugated secondary antibody goat anti-rabbit 405 and goat anti-mouse 488. Sections were then washed, mounted with Vectashield (Vector lab) mounting medium and observed with a confocal microscope (Leica).

Western blot. Cells were lysed in SDS sample buffer 2×. Proteins were separated in 15% SDS– polyacrylamide gel and transferred to nitrocellulose membranes. Immunoblotting was performed with the following primary antibodies: anti-UCHL1 (3524 Cell Signaling), anti-UXT (11047-1-AP Proteintech Group), anti-p53 (1C12) monoclonal antibody (2524, Cell Signaling) and anti-β-actin (A5441, Sigma). For the mTOR pathway: anti-phospho-p70 S6 kinase (Thr 389) (9234), anti-phospho-4E-BP1 (Ser 65) (9451), anti-p70 S6 kinase (9202), anti-4E-BP1 (9452), anti-phospho-Akt (Ser 473) (3787) were all purchased from Cell Signaling. Signals were revealed after incubation with recommended secondary antibodies

conjugated with horseradish peroxidase by using enhanced chemiluminescence for UCHL1 (WBKLS0500 Immobilion Western Chemioluminescent HRP substrate) and ECL detection reagent (RPN2105, GE Healthcare).

Protein stability. MN9D cells were seeded in 12-well plates overnight and then exposed to 100 μg ml^{-1} protein synthesis inhibitor cycloheximide (CHX) for 15 min and rapamycin 1 μM or DMSO vehicle control for the following 45 min.

Cellular fractionation. Nucleo-cytoplasmic fractionation was performed using Nucleo-Cytoplasmic separation kit (Norgen) according to the manufacturer's instruction. RNA was eluted and treated with DNase I. The purity of the cytoplasmic fraction was confirmed by qRT–PCR on pre-ribosomal RNA.

Polysome profiles. Polysome profiles were obtained using sucrose density gradients. MN9D cells were treated with 1 μg ml^{-1} rapamycin for 35 min, then with 100 μg ml^{-1} cycloheximide for 10 min prior to lysis in 150 μl lysis buffer (50 mM Tris-HCl pH 7.5, 100 mM NaCl, 30 mM $MgCl_2$, 100 μg ml^{-1} cycloheximide, 0.1% NP-40, 40 U ml^{-1} RNasin, protease inhibitors cocktail). Whole-cell extracts were clarified at 4 °C for 10 min at 15,000*g*. The equivalent of 5–10 absorbance units at 254 nm of the clarified cell extract was layered onto 15–55% (w/v) sucrose gradient (50 mM Tris/acetate pH 7.5, 50 mM NH_4Cl, 12 mM $MgCl_2$ and 1 mM DTT) and centrifuged for 3 h 30 min at 39,000 r.p.m. in a Beckman SW41Ti rotor at 4 °C. The gradient was pumped out by upward displacement and absorbance at 254 nm was monitored using BioLogic LP software (Bio-Rad). One-millilitre fractions were collected, 1 ml Trizol reagent (Invitrogen) was added and RNA was extracted following the manufacturer's instructions. A fixed volume of each RNA sample was then retro-transcribed and the percentage of mRNA in each fraction was calculated as relative Ct value to total RNA.

Metabolic labelling. MN9D were used for analysis of translational rate. Cells were seeded at sub-confluency in 6-well plates, and rapamycin (1 μM) or DMSO stimulations were performed for 45 min. Cells were labelled with 5 μCi ml^{-1} of [^{35}S]methionine (Amersham Pharmacia Biotech) for 45 min. Cells were lysed in standard lysis buffer (Tris-HCl 20 mM, NaCl 20 mM, 0.5% Triton X-100) and centrifuged. Supernatants were trichloroacetic-acid-precipitated and filtered on glass fibre discs under vacuum. Discs were counted with scintillation fluid in a β-counter. Total proteins were measured with the standard BCA method. Rate of incorporation was expressed as CPM/total protein ratio (mean ± s.d.). Experiments were done in triplicate.

Pulse labelling and immunoprecipitation. To monitor *de novo* protein synthesis, HEK cells were transiently transfected with pEGFP plasmid (Clontech) in combination with antisense GFP or empty control vector. After 24 h, medium was replaced with methionine/cysteine-free DMEM for 1 h. Then, cells were labelled with 100 μCi ml^{-1} of [^{35}S]methionine/cysteine (EasyTag, Perkin-Elmer) for 1 h. Labelled cells were collected, lysed in RIPA buffer (150 mM NaCl, 50 mM Tris pH 8, 1 mM EDTA, 1% NP40, 0.5% deoxycholic acid and 0.1% SDS) and used for immunoprecipitation with anti-GFP antibody (Invitrogen) overnight. Immune complexes were isolated with protein G-sepharose beads (Amersham) and separated on 10% SDS–PAGE. Newly translated GFP was visualized by autoradiography. Densitometric analysis was performed on high-resolution images with Photoshop-CS5. Normalization was obtained relative to input.

Northern blot. Polysome fractions were digested with 100 μg ml^{-1} proteinase K in 1% SDS and 10 μg glycogen (Invitrogen) at 37 °C for 1 h. RNA was obtained by phenol/chloroform extraction and re-suspended in formaldehyde/formamide MOPS buffer. Samples were incubated for 5 min at 65 °C before being loaded into formaldehyde 1% agarose gel and run at 90 V for 4 h at 4 °C. RNA was transferred onto Amersham Hybond-XL nylon membranes and UV-crosslinked. A radio-labelled *Uchl1*-specific complementary RNA probe was transcribed from the same plasmid used for *in situ* hybridization, performing the reaction in the presence of 50 μCi of α-^{32}P-UTP (Perkin-Elmer). After treatment with DNase I (Ambion), the labelled riboprobe was purified on RNeasy columns (Qiagen). Membranes were pre-hybridized for 3 h at 65 °C with NorthernMax prehybridization/hybridization buffer (Ambion) supplemented with 50 μg ml^{-1} salmon sperm DNA (Invitrogen), and hybridized with UCHL1 riboprobe overnight at 65 °C in the same buffer. After extensive washes (most stringent conditions were 0.2× SSC/0.1% SDS at 65 °C), membranes were exposed to autoradiography at −80 °C with intensifying screens.

Bioinformatic analysis. For the identification of additional translational activator candidates, we searched for FANTOM3 full-length cDNAs that were non-coding RNAs and overlap the 5′ end of coding transcripts in a head-to-head configuration. The filtered set of 8,535 FANTOM3 ncRNA transcripts described previously[30] was used as our starting point. Genomic locations of these ncRNA transcripts and RefSeq[31] coding transcripts were extracted from the alignments in the UCSC Genome browser[32] to identify a set of 788 coding-sense–non-coding-antisense pairs. ncRNAs were then checked by RepeatMasker to identify SINEB2-related sequences (http://www.repeatmasker.org). This analysis reduced the number of pairs to 127 protein-coding transcripts with overlap at the 5′ end (60 with a sense strand version of the repeat, 53 with an antisense version and 14 with both sense and antisense versions).

Alignment of the SINEB2-related elements was then carried out using Clustalw (http://www.ebi.ac.uk/Tools/clustalw2/index.html). From this analysis the antisense overlapping transcripts with a repeat most similar to the one of antisense *Uchl1* as well as in the same orientation were chosen for experimental testing (antisense *Uxt*).

Statistical analysis. Statistical analyses were performed with paired two-tailed Student's *t*-test. Results are mean ($n \geq 3$) ± standard deviation (s.d.).

27. Vandesompele, J. *et al.* Accurate normalization of real-time quantitative RT-PCR data by geometric averaging of multiple internal control genes. *Genome Biol.* **3,** RESEARCH0034 (2002).
28. Biagioli, M. *et al.* Unexpected expression of α- and β-globin in mesencephalic dopaminergic neurons and glial cells. *Proc. Natl Acad. Sci. USA* **106,** 15454–15459 (2009).
29. Ishii, T., Omura, M. & Mombaerts, P. Protocols for two- and three-color fluorescent RNA *in situ* hybridization of the main and accessory olfactory epithelia in mouse. *J. Neurocytol.* **33,** 657–669 (2004).
30. Nordström, K. J. *et al.* Critical evaluation of the FANTOM3 non-coding RNA transcripts. *Genomics* **94,** 169–176 (2009).
31. Maglott, D. R., Katz, K. S., Sicotte, H. & Pruitt, K. D. NCBI's LocusLink and RefSeq. *Nucleic Acids Res.* **28,** 126–128 (2000).
32. Kent, W. J. *et al.* The human genome browser at UCSC. *Genome Res.* **12,** 996–1006 (2002).

doi:10.1038/nature11508

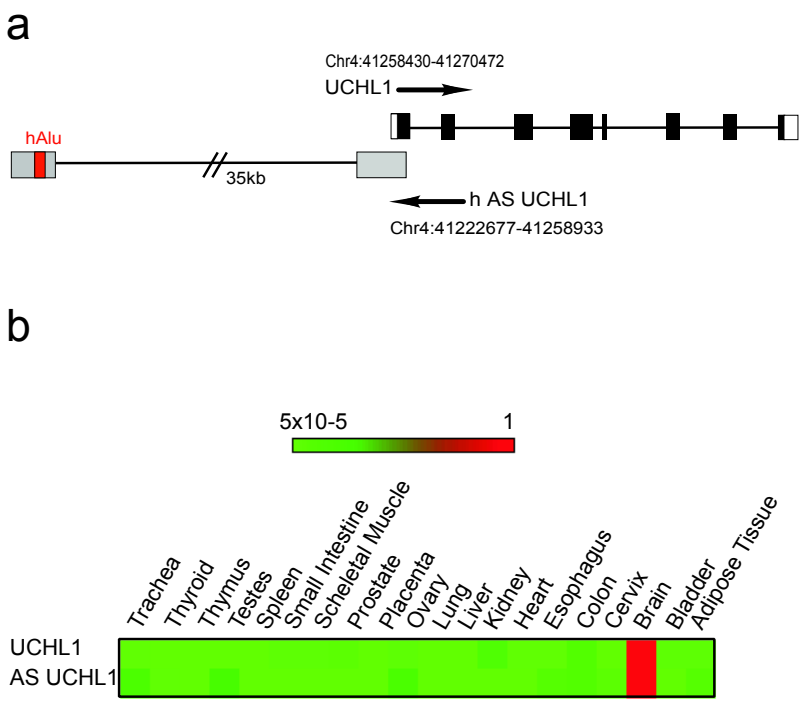

Supplementary Figure 1. Expression of antisense and sense UCHL1 in human tissues. a, Schematic diagram of human UCHL1/antisense (AS) UCHL1 genomic organization. UCHL1 exons are in black; 5' and 3' UTRs in white. AS UCHL1 exons are in grey; repetitive element (hAlu) in red. Introns are indicated as lines. **b,** Quantitative expression of UCHL1 and AS UCHL1 in human tissues. Heat map graphical representation of rescaled normalized fold expression (ΔΔCt/ΔΔCt MAX).

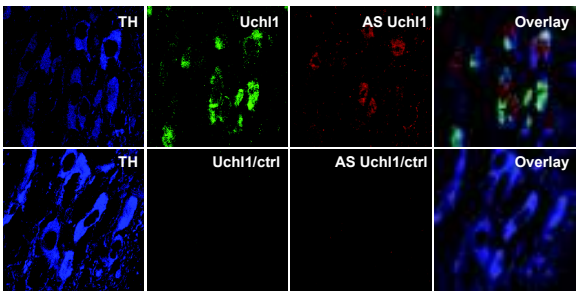

Supplementary Figure 2. Specificity of antisense Uchl1 expression in DA neurons of Substantia Nigra. Specificity of expression of Uchl1 sense (green) and antisense (AS) (red) transcripts (upper panels) as compared to control probes (Uchl1/ctrl and AS Uchl1/ctrl) (lower panels). DA neurons in Substantia Nigra are visualized by TH-staining in both panels (blue).

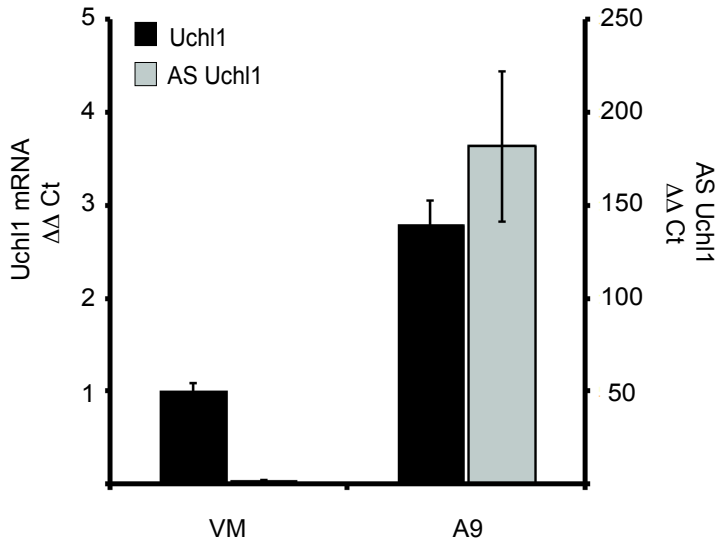

Supplementary Figure 3. Antisense Uchl1 is enriched in DA neurons. qRT-PCR starting from 300 LCM-isolated DA neurons from the Substantia Nigra of TH-GFP mice. Uchl1 and antisense (AS) Uchl1 were amplified with intron-spanning primers on three biological replica. ** $p<0.01$.

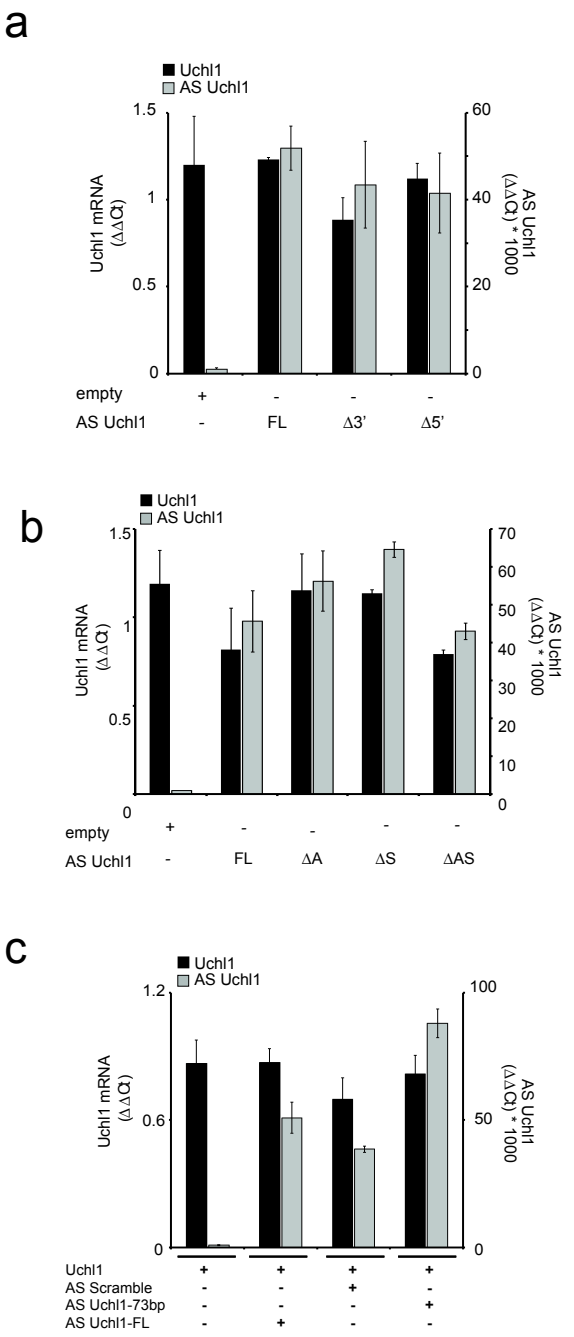

Supplementary Figure 4. Endogenous Uchl1 mRNA levels are not altered by overexpression of antisense Uchl1 mutants. a, qRT-PCR from MN9D cells transfected with Δ5' and Δ3' antisense (AS) Uchl1 mutants. Relative abundance of endogenous Uchl1 mRNA (left) and overexpressed deletion mutants (right) is shown. **b,** as in a) for ΔAlu (ΔA), ΔSINEB2(ΔS) and ΔAS mutants. **c,** as in a) for AS Uchl1-73bp. AS scramble and AS Uchl1-Full Length (FL) were used as negative and positive controls, respectively.

Riken Acc.	*AS to gene*	*NCBI Acc.*	*Orientation*	*Type*
AK019925	Ccdc44	NM_027346	RC	SINE/B2 #B3
AK029359	Uxt	NM_013840	RC	SINE/B2 #B3
AK032194	Nars2	NM_153591	RC	SINE/B2 #B3
AK032215	Nudt9	NM_028794	RC	SINE/B2 #B3
AK034331	n/a	NM_001012311	RC	SINE/B2 #B3
AK035015	Nrm	NM_134122	RC	SINE/B2 #B3
AK035406	Sv2b	NM_153579	RC	SINE/B2 #B3
AK041236	Ccdc88a	NM_176841	RC	SINE/B2 #B3
AK041654	Rcc	NM_133878	RC	SINE/B2 #B3
AK041742	Abhd11	NM_145215	RC	SINE/B2 #B3
AK042861	Wfdc5	NM_145369	RC	SINE/B2 #B3
AK044205	Rhod	NM_007485	RC	SINE/B2 #B3
AK045677	Eln	NM_007925	RC	SINE/B2 #B3
AK046828	n/a	NM_177006	RC	SINE/B2 #B3
AK047213	Uhmk1	NM_010633	RC	SINE/B2 #B3
AK048309	Epb4.9	NM_013514	RC	SINE/B2 #B3
AK053130	Rabgap1l	NM_001038621	RC	SINE/B2 #B3
AK054076	Gadd45a	NM_007836	RC	SINE/B2 #B3
AK078161	Nck1	NM_010878	RC	SINE/B2 #B3
AK078321	Uchl1	NM_011670	RC	SINE/B2 #B3
AK080749	Pgls	NM_025396	RC	SINE/B2 #B3
AK090347	3110005G23Rik	NM_028427	RC	SINE/B2 #B3
AK132441	A130022J15Rik	NM_175313	RC	SINE/B2 #B3
AK135599	Ednra	NM_010332	RC	SINE/B2 #B3
AK143014	Cdkn2aip	NM_172407	RC	SINE/B2 #B3
AK143784	Txnip	NM_001009935	RC	SINE/B2 #B3
AK145079	Gsk3b	NM_019827	RC	SINE/B2 #B3
AK149843	Cmtm6	NM_026036	RC	SINE/B2 #B3
AK163105	E4f1	NM_007893	RC	SINE/B2 #B3
AK165234	Dtx3	NM_030714	RC	SINE/B2 #B3
AK169421	n/a	NM_001110101	RC	SINE/B2 #B3

Supplementary Figure 5. Family of transcripts with embedded SINEB2. Family of FANTOM3 non-coding RNA clones that are antisense to protein coding genes and contain embedded SINEB2 in inverted orientation. In red, S/AS pairs tested in the manuscript.

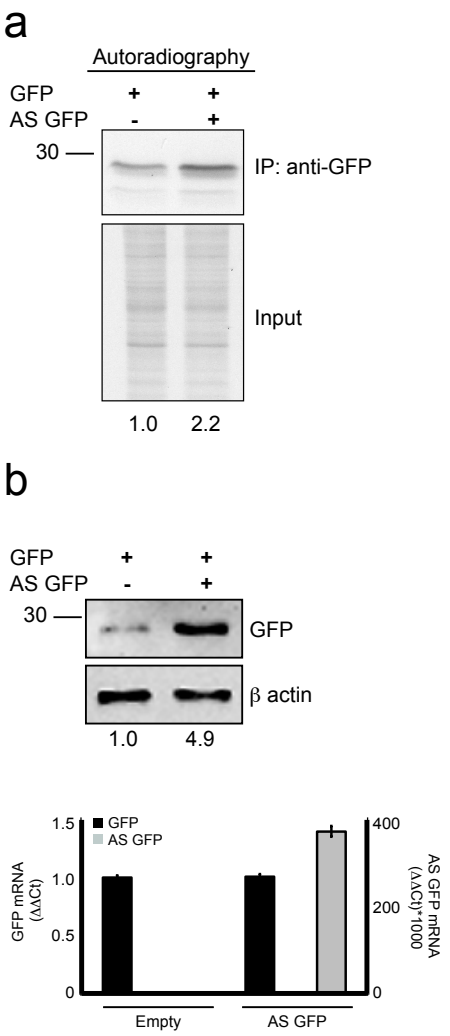

Supplementary Figure 6. Antisense GFP enhances GFP *de novo* **synthesis.** HEK cells were transfected with pEGFP plasmid and control vector (-) or antisense GFP (AS GFP), as indicated. Twenty-four hours after transfection cells were pulse-labeled with [35S]-Methionine/Cysteine for one hour. Labeled cells were harvested, lysed and immunoprecipitated with anti-GFP antibody. An aliquote of protein extract was used to monitor inputs. **a,** Autoradiography of IP and input. Bands of translated GFP were quantified relative to inputs. **b,** Expression of transfected constructs was analyzed in the same cells by western blotting to detect GFP protein (upper panel), and qRT-PCR to detect GFP and AS GFP transcripts (lower graph). For western analysis, actin served as a loading control. For qPCR, expression was normalized to actin, and mRNA levels in cells transfected with GFP plus empty vector was set to 1.

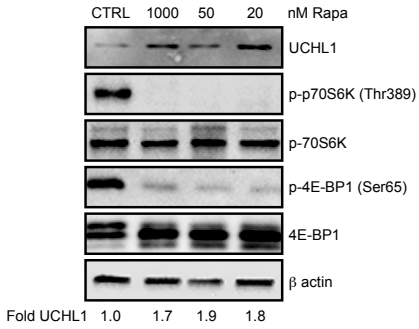

Supplementary Figure 7. Titration of rapamycin treatment on UCHL1 up-regulation. MN9D cells were treated with decreasing concentration of rapamycin (as indicated) for 45 minutes. Cell lysates were analyzed by western blot. Inhibition of mTOR was verified with anti-p-p70S6K (Thr389) and anti-p-4E-BP1 (Ser65) antibodies. Quantification of UCHL1 fold-induction is indicated.

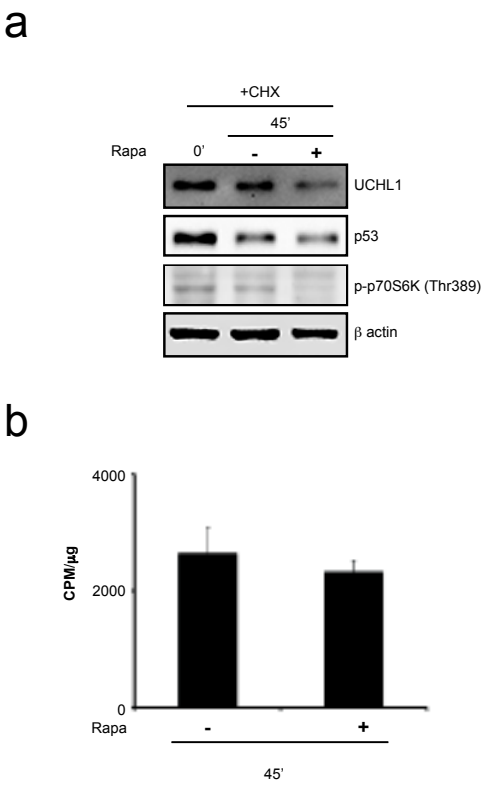

Supplementary Figure 8. Rapamycin treatment does not increase UCHL1 protein stabilization and global protein synthesis. a, UchL1 stability in MN9D cells treated with DMSO (CTRL) or with 1μM Rapamycin for 45 minutes, in the presence of 100μM Cyclohexamide (+CHX). p53 decay was used as positive control of CHX-dependent inhibition of translation. p-p70S6K (Thr389) was used as positive control for Rapamycin treatment. **b,** S35-Methyonine incorporation in MN9D cells treated with DMSO (-) or 1μM Rapamycin (+) for 45 minutes.

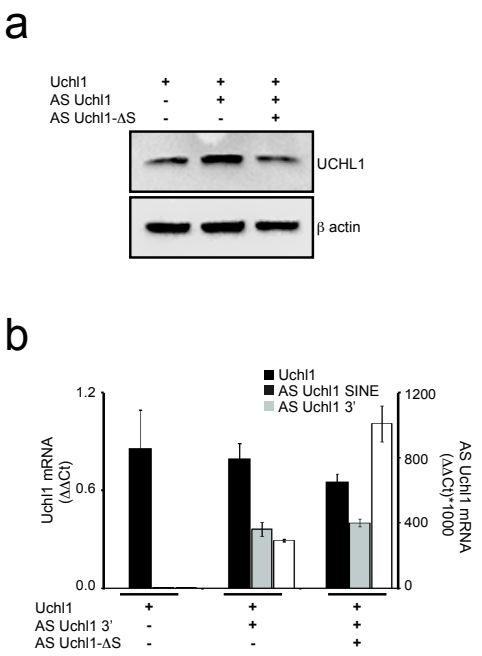

Supplementary Figure 9. Dominant-negative activity of antisense Uchl1-ΔSINEB2 (ΔS) over antisense Uchl1. a, Antisense (AS) Uchl1-ΔS acts as dominant-negative on AS Uchl1-mediated upregulation of UCHL1 protein levels in transfected HEK cells. **b,** No differences in Uchl1 mRNA levels upon AS Uchl1 or AS Uchl1-ΔS mutant expression.

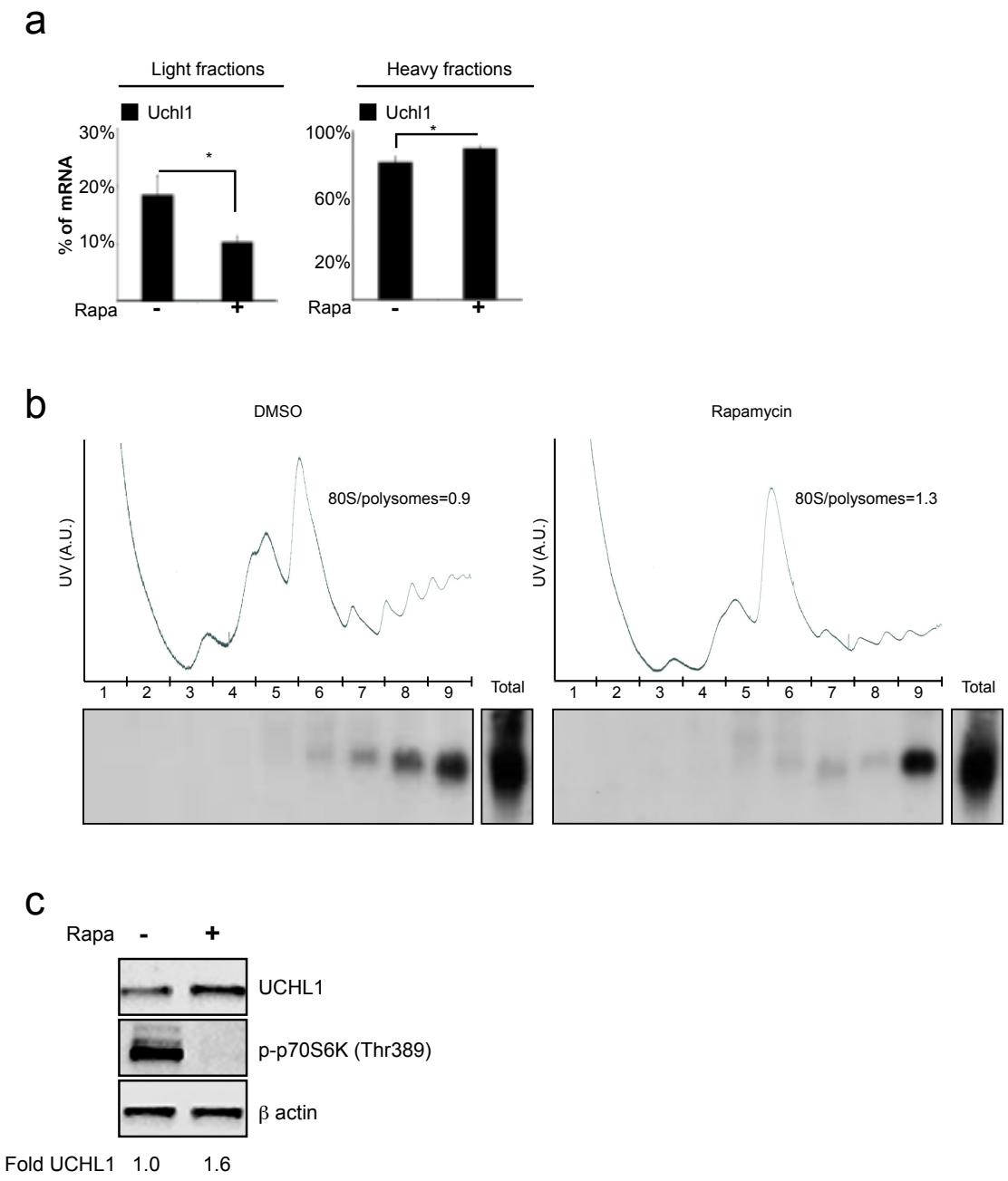

Supplementary Figure 10. Uchl1 mRNA increases association to heavy polysomes upon rapamycin treatment. MN9D pcDNA 3.1 stable control cells were treated with rapamycin (Rapa) or vehicle alone (DMSO). **a**, Uchl1 mRNA was measured in sucrose gradient fractions by qRT-PCR. Quantification of Uchl1 mRNA signals is obtained by the addition of the fractions corresponding to the light subpolysomal mRNPs and the heavy polysomes from three replica. Data indicate mean ± s.d. *p<0.05. **b**, RNA purified from 9 sucrose gradient fractions was used for Northern Blot analysis with radioactive riboprobes for Uchl1. **c**, Total protein lysates from the same preparation were analysed for UCHL1, p-p70S6K (Thr389) and beta-actin.

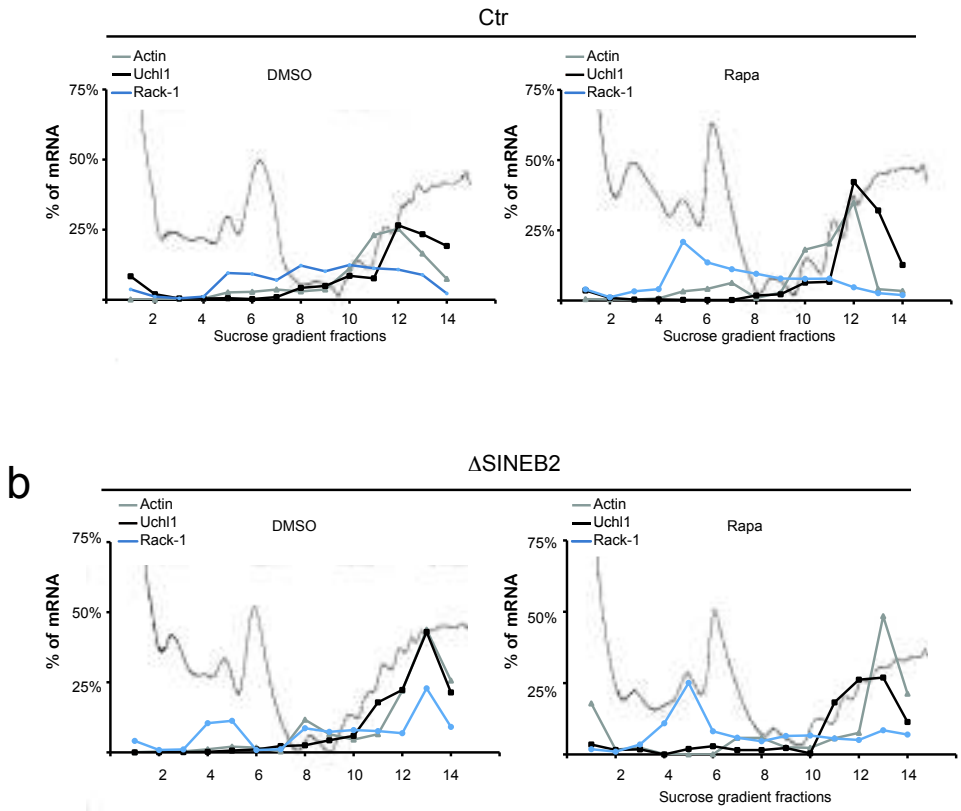

Supplementary Figure 11. Uchl1 mRNA association to heavy polysomes depends on a functional antisense Uchl1. qRT-PCR for **a,** MN9D pcDNA 3.1 stable control cells (Ctr) and **b,** stable antisense Uchl1 ΔSINEB2 mutant (ΔSINEB2) treated with rapamycin or vehicle alone (DMSO) was performed on RNAs purified from 14 sucrose gradient fractions. Association with each fraction is shown as linear plot of the percentage of RNA present in each fraction; the plot is superimposed on the absorbance profile of the gradient. Rack-1 is a TOP mRNA whose translation is specifically inhibited by rapamycin.

Cloning Oligo Name	**Sequence (5'->3')**
For mAS Uchl1 fl	ACAAAGCTCAGCCCACACGT
Rev mAS Uchl1fl	CATAGGAGTGTTTCATT
Human 5'F	AGATAATCTGGTGGTTGTGGAGAC
Human 3'R	CAGATGACATGCCAAAGAGATTAC
AS Uchl1 ShRNA	CGCGCAGTGACACAGCACA
For mAS Uchl1 Δ5'	CAGTGCTAGAGGAGGTCAGAAGAG
Rev mAS Uchl1 Δ3'	TGGCTTGTACCATTCTGTGC
For mAS Uchl1 fl Nhe	TATAGCTAGCACAAAGCTCAGCCCACACGT
Rev pre-SINE B2 EcoRI	GAGAGAATTCCAATGGATTCCATGT
For post-ALU EcoRI	GAGAGAATTCGATATAAGGAGAATCTG
Rev mAS fl HindIII	GCGCAAGCTTCATAGGGTTCATT
Rev pre-ALU EcoRI	GAGAGAATTCTTATAGTATGTGTTGTC
For post-ALU	GATATAAGGAGAATCTG
Rev pre-SINE B2 EcoRI	GAGAGAATTCCAATGGATTCCATGT
For post-SINE B2 EcoRI	GAGAGAATTCCTCCAGTCTCTTA
For SINE B2 inside	GAGAGTGCAGTGCTAGAGGAGG
Rev Alu flip	GAGACTCCCAGTCAGGCAATCC
Rev SINE flip	TATAGGAGCTAAAGAGATGGC
AS Uchl1 73bp F	GAGACTCGAGCTCGGGGTTAATCTCCATCGGCTTCAGCTGCATCTTCGCGGATGG
AS Uchl1 73bp R	ATATGATATCCGGCTCCTCGGGTTTGTGTCTGCAGGTGCCATCCGCGAAGATG
AS SCR F	ATATCTCGAGACATCACCCCAAGAAAAGCGGGAACGGTAGCTGGGTCTTGTTAAGATT
AS SCR R	GAGAGATATCCCTCGTTCCGATGGTTAAGACTCGGAATCTTAACAAGACCCAG
For mAS Uxt	TAGTCTCGCTGCAGTACG
Rev mAS Uxt	CATTATCTTCT
GFP AS F	ATATCTCGAGCCCGGTGAACAGCTCCTCGCCCTTGCTCACCATGGTGGCGACCGGTAGC
GFP AS R	GAGAGATATCTAGTGAACCGTCAGATCCGCTAGCGCTACCGGTCGCCACCATGGTGA
qRT-PCR Oligo Name	**Sequence (5'->3')**
mGapdh F	GCAGTGGCAAAGTGGAGATT
mGapdh R	GCAGAAGGGGCGGAGATGAT
mβ-actin F	CACACCCGCCACCAGTTC
mβ-actin R	CCCATTCCCACCATCACACC
mTBP S	TCAGTTCTGGAAAAATGGTGTG
mTBP AS	TGCTGCTAGTCTGGATTGTTCT
mRPII S	AATCCGCATCATGAACAGTG
mRPII AS	TCATCCATTTTATCCACCACCT
mAS Uchl1 F (Primer 3' F)	CTGGTGTGTATTATCTCTTATGC
mAS Uchl1 R (Primer 3' R)	CTCCCGAGTCTCTGTAGC
mAS Uchl1 SINE F	GGATATTGAGTTCCAAACACTGGT
mAS Uchl1 SINE R	TTCTCCTTATATCTCCCAGTCAGG
mAS Uchl1 overlap F (Primer 5' F)	GCACCTGCAGACACAAACC
mAS Uchl1 overlap R (Primer 5' R)	TCTCTCAGCTGCTGGAATCA
mUchl1 F	CCCCGAAGATAGAGCCAAG
mUchl1 R	ATGGTTCACTGGAAAGGG
mAS Uchl1 pre RNA F	CCATGCACCGCACAGAATG
mAS Uchl1 pre RNA R	GAAAGCTCCCTCAAATAGGC
mPre_ribosomal RNA F	TGTGGTGTCCAAGTGTTCATGC
mPre ribosomal RNA R	CGGAGCACCACATCGATCTAAG
mAS_Uxt F	CAACGTTGGGGATGACTTCT
mAS Uxt R	TCGATTCCCATTACCCACAT
mUxt F	TTGAGCGACTCCAGGAAACT
mUxt R	GAGTCCTGGTGAGGCTGTC
GFP F	GCCCGACAACCACTACCTGAG
GFP R	CGGCGGTCACGAACTCCAG
hUCHL1 S	GCCAATAATCAAGACAAAC
hUCHL1 AS	CATTCGTCCATCAAGTTC
hAS UCHL1 S	AAACCCATCCTTTCACCATCC
hAS UCHL1 AS	TTCCTATCTTCAGCCACATCAC
hTBP S 5'	TTCGGAGAGTTCTGGGATTGTA
hTBP AS 5'	TGGACTGTTCTTCACTCTTGGC
hRPII S 5'	GCACCACGTCCAATGACAT
hRPII AS 5'	GTGCGGCTGCTTCCATAA

Supplementary Figure 12. List of primers. Complete list of oligonucleotides used for cloning and quantitative PCR experiments.